In vivo electrophysiology in humans reveals neural codes for space and memory

Salman Ehtesham Qasim

Submitted in partial fulfillment of the
requirements for the degree of
Doctor of Philosophy
under the Executive Committee
of the Graduate School of Arts and Sciences

COLUMBIA UNIVERSITY

2021

Abstract

In vivo electrophysiology in humans reveals neural codes for space and memory

Salman Ehtesham Qasim

Memory serves an integral function in every aspect of human life. Losing that function can be a devastating consequence of disease, dementia, and trauma. In order to develop treatments or prophylactics for memory disorders we must identify the neural basis of memory. Animal research has made prominent strides studying the neural correlates of memory by examining the more easily observable and manipulable neural correlates of spatial context, since the brain regions necessary for declarative memory intersect profoundly with those needed for spatial navigation.

My research has two main goals. My first two studies, in Chapters 2 and 3, translate animal research relating the neural correlates of space to memory processes, and go beyond animal work to explore how internal features of experience such as goal states influence these conjunctive representations of space and memory. In Chapter 4, I expand my scope to examine how another internal feature, emotional context, affects the same brain regions on a network level to influence memory representations in the human brain. To perform these studies I recorded directly from the human brain in epilepsy patients performing a variety of memory tasks.

First, I measured single-neuron activity as subjects navigated a virtual environment, encountering various objects at unique locations. As subjects moved through the environments, they were instructed to recall the locations of specific objects they encountered—I identified neurons in the human entorhinal cortex, called "memory-trace cells", which selectively activated near the object-location that people were instructed to retrieve from memory. This is the first evidence that neurons in the brain can be tuned to the spatial context of an event for memory, and demonstrated a direct link between memory retrieval and the spatial tuning properties of neurons. For my second study, I examined whether spatially-tuned neurons in the MTL discharge at intervals organized by theta (2–10 Hz) oscillations (which represent network level brain-activity).

I identified a particular pattern that is prominent in rodents, called “phase precession”, during which spatially-tuned neurons spike slightly faster than the network oscillation, and which is theorized to hold great value throughout the brain for learning and memory. In addition to discovering this pattern for spatial sequences, I discovered that phase precession was also present during more abstract features of experience, like the specific goal a person was seeking. These findings suggest that principles of network-level brain activity for organizing spatial navigation may extend to humans, and to broader forms of cognition and memory. Finally, I examined the role of the amygdala in memory encoding during a verbal episodic memory task, finding that the emotional context of a word influenced the probability of its subsequent recall. By measuring the prevalence and coordination of brain oscillations in the amygdala-hippocampal circuit, I found that gamma oscillations (30–120 Hz) increased in both regions as a function of word arousal and encoding success, and connectivity within the amygdala-hippocampal circuit also showed significant theta-gamma coupling as a function of memory and high arousal. Furthermore, direct 50 Hz stimulation impaired memory for high arousal words. These findings suggest a causal relationship between gamma oscillations in the amygdala-hippocampal circuit for memory as a function of emotional context during encoding.

My work generalizes important neuronal principles from animal studies to humans (such as spatially-tuned neurons and phase precession), but also extends those findings more deeply to memory, and to internal/subjective aspects of memory that are difficult to directly measure in animals. Overall this work represents an important step towards understanding how the human brain enables declarative memory.

Table of Contents

List of Figures

List of Tables

Acknowledgements

Nothing I say here would be sufficient to capture how thankful I am to my parents. If anything useful or good comes out of my work, you deserve the credit for it. Some of that credit goes to my brother and sister, for their constant support.

Josh, thank you for being a great mentor for me since that moment in March, 2015, when I landed at O'Hare en route to my Columbia interview and discovered that every flight to NYC had been cancelled. We figured that out together and you met my sleep-deprived husk on the Amtrak from Baltimore almost 24 hours later, coffee and good vibes in hand. We have done a lot of science since then but that's what I remember most. I also want to thank Jonathan Miller, Elliot Smith, and Andrew Watrous for spending hours answering my dumb questions without ever making me feel dumb. My labmates deserve thanks for putting up with me - particularly Uma Mohan, who has had to put up with me the most.

None of this work would be possible if not for the patients who agreed to participate in this research during one of the most difficult times in their lives. In addition, I would like to thank the neurosurgeons who have been a driving force for so much of this work, the clinicians responsible for the care of these patients, the nurses and EEG technicians who helped us carry out our experiments, and the National Science Foundation for their generous financial support.

Finally, I want to thank Vino, and my friends, for making NYC feel like home, particularly in the midst of an unprecedented global pandemic. Vino, I could not have done this, or anything at all, really, if not for you. I know you will make fun of me for putting this in my thesis.

Dedication

For my family.

For Vino.

Chapter 1: Introduction

> Eighteen years have gone by, and still I can bring back every detail of that day in the meadow. Washed clean of summer's dust by days of gentle rain, the mountains wore a deep, brilliant green. The October breeze set white fronds of head-high grasses swaying. One long streak of cloud hung pasted across a dome of frozen blue.... Memory is a funny thing. When I was in the scene, I hardly paid it any mind. I never stopped to think of it as something that would make a lasting impression, certainly never imagined that eighteen years later I would recall it in such detail. I didn't give a damn about the scenery that day. I was thinking about myself. I was thinking about the beautiful girl walking next to me. I was thinking about the two of us together, and then about myself again. It was the age, that time of life when every sight, every feeling, every thought came back, like a boomerang, to me.
>
> *Norwegian Wood*
>
> *Haruki Murakami*

A fundamental aspect of human life is the ability to revisit experiences from earlier in our lives. This ability, called "episodic memory", and a memory for facts, called "semantic memory", make up the declarative memory systems that allow us to consciously engage with our past. Disorders that target memory, like Alzheimer's disease and other dementias, tragically disconnect us from that past, or from the knowledge we need to function in everyday life. In 2020, almost 6 million people are living with Alzheimer's in the U.S. alone; by 2050, this number is projected to increase to almost 14 million. The tragedy plays out across families as well—as of 2020, 16 million Americans are providing care to a family member or friend with Alzheimer's or other dementias [1]. Understanding how the human brain represents memories may enable us to prevent the degradation of these memories.

But memories, and particularly episodic memories, are complex. In the epigraph, for example, the narrator reflects on an important "scene" from his past. At minimum, his brain binds together information about what happened (a walk with a woman he loved), where it happened (in the meadows), when it happened (eighteen years ago), and orders the events in a sensible progression. Moreover, this particular experience is important to the narrator because of its emotional weight, which is evoked as clearly as any sensory detail. A memory like this requires that the brain query descriptive information in different domains, map the relational associations within each domain, bind information across domains, and organize all of this into ordinal sequences, all within the subjective framework of a person's thoughts, feelings, and motivations.

How does the brain encode and recall such complicated memories? Studies of people with different kinds of brain injuries have demonstrated a necessary role for the medial temporal lobe (MTL) in many of these individual functions, and in declarative memory as a whole. Studying the precise neural mechanisms in humans, however, is difficult because such experiments often rely on indirect or proxy techniques for estimating neural activity that may suffer from interpretability issues and poor spatial/temporal resolution. Studying these mechanisms in animals is also difficult, though for a different reason. While researchers can directly record from a rodent or monkey brain, it is often difficult to carefully assess an internal, cognitive process like declarative memory (and especially episodic memory), which is subject to internal contexts such as goals, intentions, and emotions, in animals.

Direct recordings of brain activity in animals have illuminated a potential path around this issue. Seminal work in rodents has revealed clear neural correlates of spatial context, at both the single-neuron and network level, in the MTL—the same brain region important for memory. Spatial context is a critical feature of experiences, and is crucial to revisiting experiences in memory [2]. Furthermore, spatial navigation requires complex sequence building and relational associations: the brain must represent individual positions, the relationship between positions, the binding of objects and boundaries to positions, and the arrangement of adjacent positions during movement [3]. This anatomical and conceptual convergence has led to the hypothesis that the MTL is

primarily responsible for representing episodes [4], and that the neural mechanisms of spatial representation may represent a specific (easily observable) instantiation of a general MTL relational framework for representing knowledge (semantic memory) and events (episodic memory) [5]. And so one approach to studying memory has relied on studying how the brain represents space. However, the neural correlates of space are not well established in humans (and other species), limiting the potential usefulness of this hypothesis. Furthermore, this line of research in animals inherits some of the inherent limitations in examining internal context in animals, with respect to the neural representations underlying space.

Here, I describe research exploring and extending this approach in the human brain, using direct, invasive brain recordings in humans performing memory tasks. In doing so, I not only provide evidence of the conjunction between spatial and mnemonic representations in the human brain, but extend these principles to explore how the subjective, internal features of memory, such as goals, intentions and emotions, influence these neuronal patterns of activity. The findings presented here thus represent new understanding about how the human brain represents memories in relation to decades of animal research and provide new foundations for examining memory beyond the domain of space.

1.1 Direct recording of human neuronal activity during behavior and cognition

First, I will describe the recording methodology my research uses to acquire signals from the human brain. For decades, neurophysiologists have directly recorded the electrical activity of individual neurons, or many thousands of neurons, in relation to experimental stimuli or behavior. Any consistent correlation between brain activity and this stimuli/behavior is theorized to represent a functional relationship—that the observed brain activity caused the behavior, or the stimuli elicited the observed brain activity [6]. In this way, scientists have long sought to understand how the brain enables our experience of the world.

Much of this research is performed in animals, thought it can be difficult to draw a straight line

from animal experience and physiology to humans [1]. However, this type of invasive brain recording is impossible to perform in healthy humans due to ethical concerns. We leveraged the rare ability to record directly from the human brain in epilepsy patients undergoing clinical neurosurgical treatment, as they performed memory tasks. I will briefly review the fundamental principles underlying in-vivo extracellular electrophysiology to emphasize the connection between the signals analyzed throughout my research and their biological relevance and genesis. Then, I will describe the application of these principles to human brain recordings in epilepsy patients.

1.1.1 Extracellular electrophysiology for measuring neural activity

Luigi Galvani first discovered that "animal electricity" was present in living tissue and could drive movement in a frog leg in the 1790s. This led to the idea that electrical current could drive important physiological processes [8]. Emil du Bois-Reymond discovered the action potential, the fundamental building block of neural electrophysiology, as the source of that phenomenon in the 1840s. The basic principle of electrophysiology relies on the movement of ions in physiological tissue. In the brain, ions are constantly shuttled through ion channels across the neuronal cell membrane, which helps to maintain a fairly static resting potential difference between the inside of the neuron and the extracellular space. During an action potential, an ionic gradient is established across the neuron's membrane. This ionic gradient drives the serial opening and closing of voltage-gated ion channels, triggering a rapid depolarization across the cell membrane [2]. This is an action potential, and can be measured extracellularly—the potential difference between depolarized and resting regions of the neuron induces current flow in the space around the cell membrane. This current flow may be measured using electrodes in the immediate vicinity of the cell membrane [10]. When action potentials propagate across an axon they triggers the release of chemical transmitters that can initiate action potentials in adjacent neurons across the synapse. In this way, action

[1] For example, research attempting to translate Alzheimer's treatments from animals to humans has a 99.6 % failure rate [7].

[2] Action potentials are vastly more complex than described here. Resting potentials may be determined by non-voltage dependant conductances. Heterogeneity in types of ion channels and voltage channels results in many different spiking patterns. Whether this impacts neural coding schemes is not clear [9]

potentials underlie the most dominant mode of communication between neurons, which directly implicates them in the behaviors and aspects of cognition that emerge from brain activity. Overall, detecting action potentials has become the most direct way to measure neuronal communication and computation, and to relate them to behavior.

The voltage fluctuations recorded by extracellular electrodes contain information about more than single-neuron action potentials. These electrodes can often be used to detect the extremely brief (3 ms), high amplitude transients indicative of action potentials, as well as the superimposed electrical activity of the local and distributed brain tissue (Fig. 1.1). This omnibus bio-potential is thought to come from many sources, such as fast and slow action potentials, intrinsic membrane resonance and potential oscillations, membrane hyperpolarization, gap junctions, and ephaptic coupling, but is mostly thought to depend on summed synaptic potentials representing the communication between neurons [11]. When this summed activity is recorded directly from deep brain structures it is referred to as the local field potential (LFP), as opposed to the surface of the cortex, where it is referred to as electrocorticography (ECoG). Action potentials (also referred to as "spikes") as well as LFP data can be parsed from the low and high frequency content of the overall voltage fluctuations recorded by small extracellular electrodes ($< 50\mu$mm), while larger electrodes are only capable of recording the macro-scale LFP/ECoG signal.

In addition, Hans Berger discovered, in 1928, that some form of this summed activity could be recorded from the scalp. As opposed to the invasive electroencephalographic (iEEG) techniques described above, this non-invasive technique is referred to as scalp electroencephalography (EEG) [13]. This method enabled researchers to non-invasively study how neural electrophysiology in humans related to human behavior and cognition.

1.1.2 Benefits of direct, extracellular electrophysiology

In addition to scalp EEG, researchers have discovered several other non-invasive methods for measuring brain-activity. These alternative methods include functional magnetic resonance imaging (fMRI), magnetoencephalography (MEG), and scalp EEG. fMRI measures the amount of oxy-

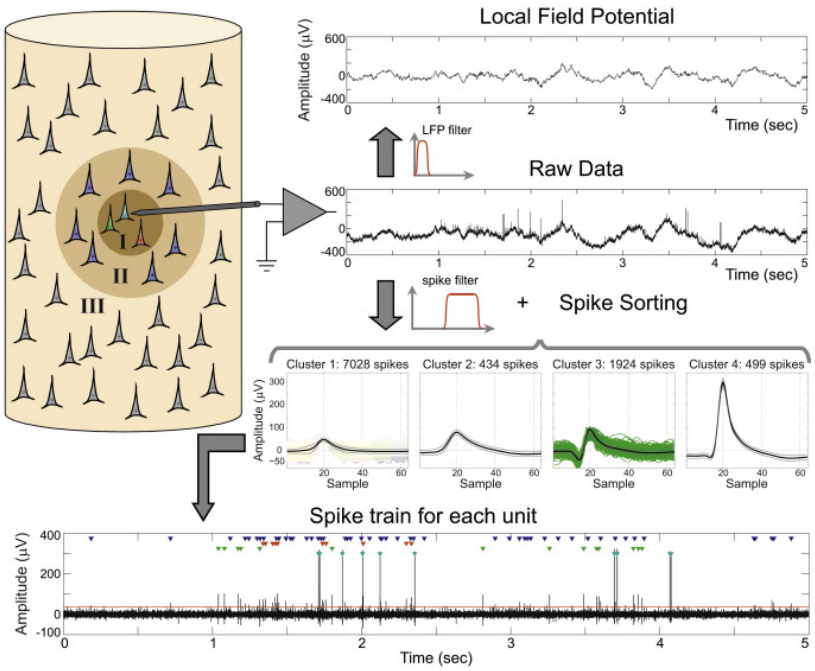

Figure 1.1: **Recording single-neuron action potentials and LFP using extracellular electrodes.** This schematic depicts the process of recording voltage fluctuations using extracellular electrodes, decomposing that signal into low-frequency (LFP) and high-frequency activity comprised of background noise (zone III), multi-unit activity (zone II) and single-unit activity (zone I). Note that single-unit activity can be recorded from multiple nearby neurons, and thus spike-sorting procedures must be applied assign spikes to the different neurons. The bottom most panel depicts the spike train with the occurrence of each putative spike marked. Reproduced from Rey et al., 2015 [12].

gen in the blood as a proxy signal for brain activity, while MEG measures the magnetic fields induced by electric currents in the brain. Scalp EEG, as described in the prior section, relies on detection of voltage differences by electrodes placed on the scalp. All three techniques are widely used to examine brain-wide patterns of activation, but are not as useful as direct, extracellular recordings for precise assessment of how brain activity relates to behavior. First, measuring single-unit action potentials and LFP directly from brain tissue provides among the best spatio-temporal resolution possible, as the signal is not smeared by the skull (scalp EEG), dependent on source localization of varying spatial resolution (MEG) [14], or based on slow dynamics (fMRI) [15]. This spatio-temporal resolution allows the closest correlation of brain activity to measurements of behavior and cognition. Second, single-unit action potentials in particular provide a direct measurement of neuronal activity, without the statistical methods required for fMRI and MEG, which

complicate interpretation and may lead to inflated false-positive rates [16]. By recording the activity of single neurons, or the summed activity of many synchronous neurons, researchers may attempt the most direct correlation of brain activity to behavior and cognition. However, directly recording action potentials and iEEG from humans is not common, as the only ethical context for invasively implanting electrodes in the human brain is for clinical purposes.

1.1.3 Brain recordings in epilepsy patients

In 1955, Ward and Thomas used glass micro-pipette electrodes to record action potentials in the brain of a living human for the first time. The person whose brain played host to this achievement was a patient with epilepsy; Ward and Thomas recorded this neuronal activity as they performed surgery to attempt to locate the brain region responsible for originating epileptic seizures. As prefaced in the prior section on non-invasive brain recording techniques, seizure loci often cannot be effectively localized using non-invasive techniques, requiring surgical intervention in serious cases [17].

The research presented here similarly leverages the rare opportunity to record neuronal data directly from the human brain, providing the closest possible correlate to *in-vivo* studies in animals. To do so, we utilize invasive neural recordings epilepsy patients who are implanted with electrodes on the surface of the cortex as well as in deeper brain structures during the course of surgical treatment for drug-resistant epilepsy. The electrodes enable clinicians to localize the patient's seizures for resection—for this, patients often must wait in a hospital for1–3 weeks with implanted electrodes. During this time, consenting patients perform various tasks while their neural data is simultaneously recorded. A majority of this process utilizes macro-electrodes which record LFPs. These electrodes record the activity of large populations of neurons from a $4mm^2$ area of the brain. In addition, these subjects were often implanted with microelectrodes in deep brain structures. These electrodes have a much smaller diameter (40μm) which extracellularly record the action potentials of individual neurons (Fig. 1.2A). Critically, safety studies have not reported increased complication rates in epilepsy patients due to these research microelectrode recordings, illustrating

the safety of these techniques for examining human neuronal activity in relation to behavior and cognition [18]. Examples of real-time, online single-neuron data collected from these microwires is depicted in Figure 1.2B.

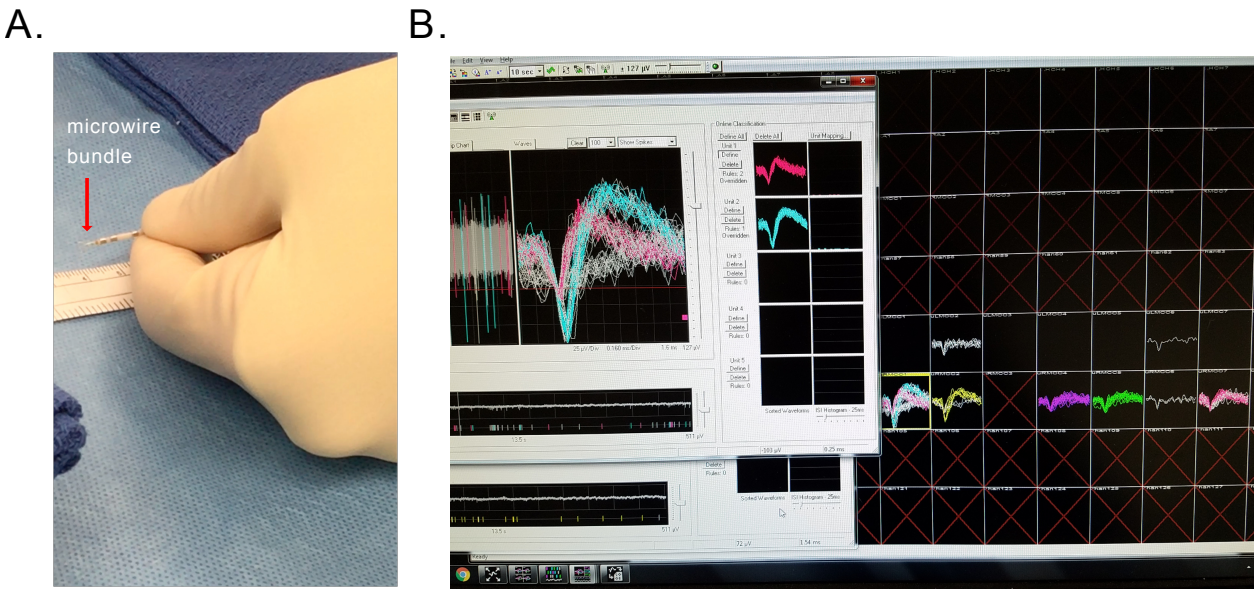

Figure 1.2: **Recording single-unit action potentials in an epilepsy patient performing a memory task.** A) Surgeon holding a Behnke-Fried micro-wire electrode after cutting them to approximately 3-5 mm prior to insertion. B) Real-time recording of single-unit action potentials in the Blackrock recording system software. Data were recorded from the hippocampus as the subject performed a memory task.

1.2 The medial temporal lobe systems for space and memory.

The MTL consists of the hippocampus (divided into the cornua ammonis 1-3, dentate gyrus, and subiculum) and the parahippocampal regions (parahippocampal cortex, perirhinal cortex, and entorhinal cortex) [19]. Many of these brain areas are fairly conserved (in terms of cytoarchitecture and connectivity) across many mammalian species, such as rodents, bats, non-human primates, and humans (Fig. 1.3A), with analogous regions identified across many other species such as birds, reptiles, and teleost fish [20]. Lesion studies, in which the MTL is selectively damaged/removed/inhibited, have found that this region is often required for spatial navigation and cognition, as well as certain types of memory. In addition, electrophysiological and imaging stud-

ies have characterized a plethora of single-neuron and network-level patterns of brain activity that correlate with spatial or memory function in many different species. In this section we will briefly synthesize across a subset of these studies to demonstrate the convergent roles of the MTL in spatial cognition and declarative memory in humans and other species.

1.2.1 Space

How does the brain keep track of space? The answer seems self-evident—it must have a map. This idea was given firmer, less tautologous shape in the 1940s when Edward Tolman observed that rats who had learned to wander a maze without food could expertly navigate the maze once food was finally present [21]. He thought this to be evidence that the rats had learned a "cognitive map" detailing the environmental structure and rat's place within it. This was not only an intuitive hypothesis, but one with potentially universal value, because a cognitive map might help us to "navigate" through more abstract, non-spatial domains such as semantics, time, or social relations. Several decades later, advances in electrode technology enabled researchers to directly record action potentials from outside the neuronal cell membrane while animals actively performed tasks. Using this technology, John O'Keefe and Jonathan Dostrovsky discovered that certain neurons in the rat hippocampus activated more when the rat moved through specific locations in the environment than other locations [22]. They called these cells "place cells", and their receptive fields "place fields", and theorized that neurons like these formed the basis for Tolman's cognitive map [23]. Indeed, place cells seemed to represent a neuronal correlate for one aspect of a cognitive map—where the animal is itself located (Fig. 1.3B). Since then, further advances in invasive recording technology, improved understanding of neuroanatomy, and careful behavioral experiments have enabled animal researchers to discover many neurons in the MTL that are responsive to different features of spatial context.

Chief among these was the discovery of grid cells in the entorhinal cortex [24]. Unlike place cells, grid cells are not simply active when a rat occupies a single location. Instead, grid cells have receptive fields that tiled the environment with a stereotyped hexagonal symmetry (Fig. 1.3B).

And while place cells are subject to alter their place field locations if an environment changes, grid fields tend to stay largely fixed in their orientation. As such, it is hypothesized that grid cells in the entorhinal cortex may represent the structure of the environment itself [25]. Additional spatially-tuned neurons include head direction cells, border cells, object cells, and a litany of vector-based cells that activate when the animal is moving in a particular direction with respect to different reference points. In this way, the hippocampal formation has been shown to host a variety of neurons defined by their responsiveness to variables an animal might need to represent their location in an environment, either egocentrically (first-person) or allocentrically (birds-eye view) [26].

In addition to the clear spatially-tuned responses of single neurons, the MTL in rodents is dominated by a low-frequency (theta: 5-10 Hz) local field potential (LFP), encompassing the summed activity of many thousands of neurons. This theta oscillation is so prominent in the rodent hippocampus that it has been linked to a very broad range of behaviors, but is most clearly correlated with spatial navigation [27]. The best example of this correlation was discovered by O'Keefe and Michael Recce in 1993, who observed that place cells spike slightly faster than the theta oscillation as the rodent runs the place field. This results in sequences of locations being encoded at different phases of theta oscillations [28]—a phase code for space that complements the rate code provided just by the spiking of individual neurons. Across an ensemble of place cells, this may result in many place cells firing in sequence in one cycle of a theta oscillation, thus compressing spatial trajectories into a brief timescale that is conducive to synaptic plasticity [29].

Thus, the MTL in rodents is home to both single-neuron and network-level correlates of spatial context. Critically, hippocampal lesions impair performance in spatial tasks that require the encoding of environmental structure or relationships between multiple environmental features but not in tasks that simply require the the animal to use a visual beacon for guidance [30, 31], suggesting that these neural correlates are functionally necessary for certain aspects of spatial cognition. Some of these neuronal correlates have been directly identified in some form in humans navigating virtual environments, using direct brain recordings as described in the prior section [32, 33, 34]; many have not. However, imaging studies in humans have shown consistent engagement of the MTL

during spatial navigation in virtual environments [35]. For example, fMRI studies have shown that hippocampal activity correlates with navigation accuracy, map-based navigation strategy use, and distance relationships [36, 37, 38, 39]. Recent work has even identified an fMRI signal [40] and LFP signal [41] thought to correlate with grid-like activity in the entorhinal cortex. These data suggest that spatial function in the MTL is relatively conserved in humans, though the precise nature of those spatial representations is largely unclear.

1.2.2 Memory

Declarative memory, also known as conscious memory, is hypothesized to consist of episodic memory and semantic memory [3]. Semantic memory is a memory for facts, while episodic memory is a memory for events. At minimum, episodic memory is thought to consist of key details of an event: what happened, where it happened, and when it happened. Tulving went further, suggesting that episodic memory also entails "mental time travel", a subjective re-experiencing of the event being recalled [43]. The MTL's importance to declarative memory was first hinted at by Vladimir Bekhterev, who reported MTL damage in an amnesic patient [44] [4]. In the next fifty years, a slightly clearer picture of of amnesic syndrome and hippocampal pathology began to emerge [45].

It was the cases of famous patients like H.M. and K.C., who both suffered from MTL damage and subsequent amnesia, that established a clear connection between the MTL and memory. H.M., arguably one of the most famous case studies in neuroscience, developed an anterograde amnesia that prevented him from forming semantic or episodic memories [49] (Fig. 1.3C). K.C. who was injured in a motorcycle crash, developed a severe retrograde amnesia. While K.C. could remember many factual details about his past, his memory for events was impaired—for example, he could remember that his brother had gotten married, and name all the people in a wedding photo, but could not remember his experience of attending that wedding [50]. Numerous studies of amnesiac patients have since demonstrated the necessity of the MTL for semantic and episodic memory

[3] An overview of the full taxonomy of memory systems is beyond the scope of this thesis. It is worth noting, however, that any recollection is likely to engage multiple types of memory processes [42].

[4] Bekhterev died mysteriously in 1927, though, and his work was suppressed by Joseph Stalin, leading to a large gap in the research associating MTL function with memory [44]

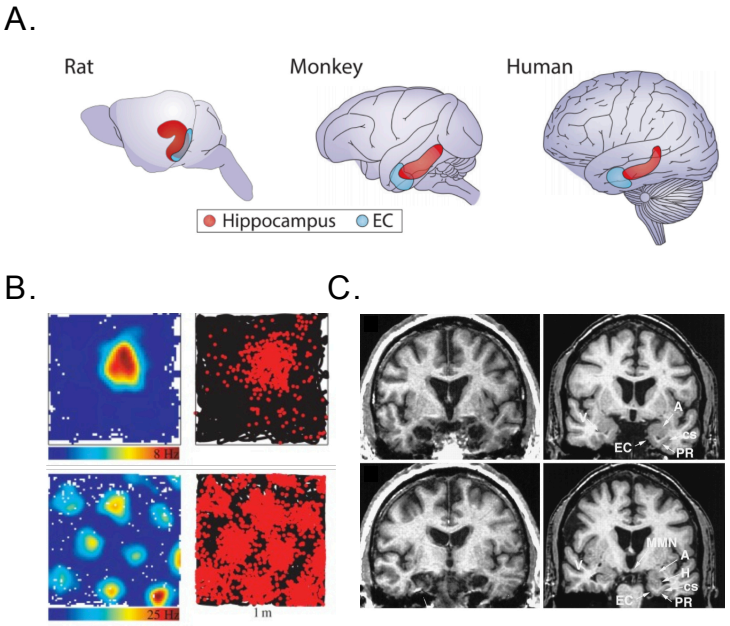

Figure 1.3: **The medial temporal lobe's involvement in space and memory.** A) Schematic of the largely conserved, though distinctly oriented, hippocampus (red), and entorhinal cortex (blue) in rodents, monkeys and humans. Reproduced from Strange et al., 2014 [46]. B) Heatmap and occupancy plot depicting the spiking activity of a hippocampal place cell (top) and entorhinal grid cell (bottom), recorded in rodents navigating around the square environment. Reproduced from Jeewajee et al., 2014 [47]. C) Magnetic resonance imaging (MRI) showing the medial temporal regions of patient H.M. (left), and a healthy 66 year old control (right), with white arrows denoting intact regions that are, in comparison, damaged in patient H.M. Reproduced from Corkin et al., 1997 ("Copyright 1997 Society for Neuroscience") [48].

processes, though with much heterogeneity, as these two seminal cases illustrate.

And unlike the neural correlates of space, the precise neurophysiology of declarative memory has not been well described. While spatial variables are easily observable external features, memory encoding and retrieval is largely an internal process with few external manifestations, particularly in animals [51]. To exacerbate this issue, while animal behavior may fulfill the minimum criteria of episodic memory (knowledge of what, when, and where), we may never know if animals undergo the subjective experience of reliving past events at all. Potential evidence for memory-related neuronal activity in animals has largely come from examining how neurons tuned to space may encode events by re-activating during memory retrieval [52, 53]. Other spatially tuned cells have shown evidence that they are modulated by remembered contexts [54], and the disruption of ensembles of spatial cells has been shown to disrupt memory [55]. The relationship between spatial

representation and memory function gained strong support in recent years on the basis of causal studies in rodents showing that optically/electrically manipulating spatially-tuned neurons and reward signals manipulate rodents' memory for reward locations [56]. In addition, researchers have recently discovered that certain cells in the MTL are sensitive to lengths of time elapsed during a delay period in which the animal had to maintain a memory [57, 58]. These time cells have been theorized to be involved in working memory, but may hold some relevance to episodic memory. Other time cells have also been found that are sensitive to the length and temporal boundaries of episodes [59]. In sum, animal researchers have demonstrated patterns of neural activation relating to the representation and reactivation of spatiotemporal context, but these observations have been some degrees removed from examining memory recall.

Research in humans, however, may more directly assay subjective experiences, and more directly cue research subjects to recall specific, separable memories, potentially allowing for more careful examination of the neuronal correlates of memory. The vast majority of such studies have used non-invasive techniques, such as fMRI to study how brain activity changes during memory tasks. Many of these paradigms utilize subsequent memory tests, in which brain activity for remembered stimuli is contrasted against brain activity for forgotten stimuli. Spaniol and colleagues [60] performed a meta-analysis of the fMRI literature studying episodic memory for word and picture stimuli [61, 62, 63, 64]. Consistent with prior work, they found consistent MTL activation during successful encoding and retrieval, suggesting a causal role for population level activity in these regions in memory processes [5]. Similarly, fMRI studies of autobiographical recall demonstrate similar activation when subjects recall real-world memories [65, 66]. MEG studies, too, have largely recapitulated these findings, while enabling researchers to more precisely attribute memory success to particular types of neuronal activity, such as theta oscillations [67].

On the other hand, there is limited work examining memory using direct brain recordings in humans. Paul Crandall pioneered the recording of single neuron activity in the human MTL in the 1960s [68]. Early studies by Eric Halgren et al. examined the activity of these neurons

[5]The precise brain regions implicated in imaging studies of memory show some heterogeneity, including a prominent role for cortical areas and variation as a function of objective vs. subjective recall [60].

during memory tasks and memory interviews and found little evidence for a direct relationship between single neuron firing and remembered items [69, 70]. However, they did find that MTL stimulation during stimulus presentation or recognition impaired memory. Studies examining the direct neuronal correlates of memory have increased in recent years, showing that neurons in the MTL that are active during stimulus presentation re-activate during memory [71, 72], or vary their phase-coding as a function of memory [73, 74]. The work I present in Chapters 2 and 3 build upon this sparse collection of research using human intracranial recordings to investigate memory.

1.3 Overview

In my first study (Chapter 2), I show that single neurons in the human entorhinal cortex represent a person's subjective memory for locations tied to specific events. In my second study (Chapter 3), I demonstrate that certain spatially tuned neurons in the human brain organize their sequential firing relative to concurrent brain rhythms, and that this neural code extends beyond space to specific goal-seeking episodes. Finally, I present evidence (Chapter 4) that the emotional features of a stimuli influences the hippocampal-amygdala circuit involved in memory for that stimuli. The first two studies not only replicate predominantly spatial findings from rodents, but generalize them to the domains of non-spatial cognition and memory, and the final study examines the role that internal, subjective features of an experience play on memory encoding and recall. Finally, I summarize the impact of these findings on our understanding of human spatial cognition and memory, and present directions for future research.

Chapter 2: Memory retrieval modulates spatial tuning of single neurons in the human entorhinal cortex

Salman E. Qasim, Jonathan Miller, Cory S. Inman, Robert E. Gross, Jon T. Willie, Bradley Lega, Jui-Jui Lin, Ashwini Sharan, Chengyuan Wu, Michael R. Sperling, Sameer A. Sheth, Guy M. McKhann, Elliot H. Smith, Catherine Schevon, Joel Stein, & Joshua Jacobs
Nature Neuroscience, 22: 2078–2086, 2019.

The medial temporal lobe (MTL) is critical for both spatial navigation and memory. While single neurons in the MTL activate to represent locations in the environment during navigation, it remains unclear how this spatial tuning relates to memory for events involving those locations. We examined memory-related changes in spatial tuning by recording single-neuron activity from neurosurgical patients performing a virtual-reality object–location memory task. We identified "memory-trace cells" whose activity was spatially tuned to the retrieved location of the specific object that subjects were cued to remember. Memory-trace cells in the entorhinal cortex (EC), in particular, encoded discriminable representations of different memories through a memory-specific rate code. These findings indicate that single neurons in the human EC change their spatial tuning to target relevant memories for retrieval.

2.1 Introduction

A key feature of memory is our ability to selectively recall particular experiences even if they occurred in a setting shared with other events. For example, if asked to recommend a tourist itinerary for a city you visited frequently, you can selectively recall distinct memories of locations from different trips to provide an answer. While lesion studies have demonstrated that many declarative memory processes depend on intact medial temporal lobe (MTL) structures, such as

the hippocampus and entorhinal cortex (EC) [75, 76], it is not clear how neuronal activity in these regions enables us to target a particular memory for retrieval among related experiences.

We examined how the brain represents distinct memories through the lens of spatial cognition, relying on the fact that the brain uses similar circuits and mechanisms to support both spatial and memory processes [77, 5]. The discoveries of place cells in the hippocampus [22] and grid cells in the EC [24] demonstrated that neurons in these memory-critical regions [76] also exhibit spatial tuning. Previous work proposed that spatially tuned cells remap their firing patterns across different environments, so events that occur in different environments are associated with different spatial maps [78, 79]. Recent work has extended this idea that different contexts are associated with different spatial maps by showing that the activity of spatially tuned cells may be modulated by changes to internal, top-down processes such as an animal's behavioral state, attention, or goal [80, 55, 81]. In this way, different patterns of spatially modulated neuronal activity may index different behavioral and cognitive contexts, and these distinct neural representations may aid in the retrieval of distinct memories.

The EC is a viable candidate for linking memory retrieval to spatial representation [82], as it features a variety of spatially tuned cells [24, 33], plays a role in memory maintenance and retrieval [83, 84], and integrates diverse sensory and cognitive information about an experience in service of memory [85, 25]. Recent work has begun to link memory processes with spatial firing patterns in the EC, such as the identification of "object-trace" cells in the rodent EC whose spatial tuning was determined by the locations previously occupied by objects [53], the finding of reduced grid-cell representations in patients at risk for Alzheimer's disease [86], and the discovery that remembered reward locations influence grid-cell field locations [87].

Building off this work, we hypothesized that single neurons in the MTL, and particularly in the EC, would exhibit spatial tuning modulated by past experiences. Such separable neuronal representations may, in turn, enable top-down, targeted memory retrieval of those past experiences. To test this hypothesis, we analyzed the activity of single neurons from the MTL of human epilepsy patients as they performed a cued spatial-memory task in which they learned and

subsequently recalled object locations while moving through a virtual environment. A key feature of this task is that subjects were provided a cue on each trial denoting the specific object location to retrieve, while the environment remained unchanged—this enabled us to assess how top-down, targeted memory retrieval might engage distinct spatial representations in the brain. As a result, we observed single neurons in the EC and cingulate whose spatial tuning varied as a function of the particular cue provided for memory retrieval. Specifically, the activity of these cells tracked the patients' subjective memory for the current cued object location, hence we refer to them as "memory-trace" cells. Furthermore, the firing of EC memory-trace cells showed a memory-specific rate code that distinguished which object–location memory had been cued for retrieval. This memory-specific rate code was robust, emerging both when subjects were near the cued objects' location, as well as when subjects were provided with a retrieval cue but did not move through the environment. These findings illustrate how spatially tuned neurons in the EC support our ability to use top-down cues to selectively target relevant memories for retrieval.

2.2 Methods

2.2.1 Task.

Nineteen patients with drug-resistant epilepsy performed 31 sessions of a spatial-memory task at their bedside with a laptop computer and handheld controller. This study was approved by the Institutional Review Boards of Columbia University, Columbia University Medical Center, Emory University, University of Texas Southwestern, and Thomas Jefferson University. All subjects provided written consent agreeing to participation in this experiment. In this virtual reality (VR) memory task, subjects are moved from the beginning to the end of a linear track on each trial. The track is 68 VR-units long, which corresponds to approximately 231 meters when converted using the height of the virtual avatar relative to the environment and track length. The ground was textured to mimic asphalt and the track was surrounded by stone walls (Fig. 2.1A). On each trial subjects are placed at the beginning of the track and shown text cues instructing them to press a button on the game controller when they reach the location of a specified object ("instruction pe-

riod"). Immediately after receiving this cue, subjects press a button on a game controller to move to the "hold period," in which they are held stationary at the entrance to the track for 4 seconds. Next, the "movement period" begins automatically, in which subjects are moved forward along the track. Subjects are moved passively for 56 of 64 trials and on other, randomly selected trials, control movements with a handheld controller (Supplementary Fig. S2.1A). Individual trials consisted of either encoding or retrieval trials (see Fig. 2.1A). The first two times that subjects encounter a particular object are encoding trials, in which the object is visible during movement so the subjects can learn its location. On subsequent retrieval trials, the object is invisible and subjects are instructed to recall its location by pressing the controller button when they believe they are at the correct location. To measure task performance, we compute the distance error (DE) on each trial, defined as the distance between the subject's response location and the actual location of the object. Subjects encode and retrieve a total of 4 unique object–location associations (16 trials of each) over the course of a session, with each object located at a different randomly selected location (Fig. 2.1B). Objects' temporal order and spatial order were randomly associated, such that the each object would be randomly be assigned to locations 1-4 independent of the temporal order of that object (i.e. the 1st object in the session could be presented in the 4th location).

In addition to pressing a button to indicate their memory for the object location, subjects are told to press a button as they enter the "stopping zone" at the end of the track, which is visually delineated by a red floor coloring at the end of the track. Pressing the button in this region ends the movement period, and subjects are then shown a fixation cross for 5 seconds ("fixation period"). Finally, during the "feedback" period at the end of each trial, subjects receive points corresponding to how close to the correct location they pressed the button during movement. Only one object was ever present on the track at any given time. The task was split into two blocks so that subjects would only be cued to retrieve from either the 1st or 2nd object in the first block vs. the 3rd or 4th object for the second block. After learning the location of an object during the encoding trials, subjects were cued with that object for at least two consecutive trials before potentially being cued with the other object for that block (see Supplementary Fig. S2.1A).

A distinctive feature of our task is that during movement periods subjects are moved passively while their speed is automatically changed in a seemingly random fashion. These uncontrolled speed changes encourage subjects to attend continuously to their current VR location because they cannot accurately predict future positions by integrating their past velocity. Within each third of the track, subjects are moved at a constant speed, which is randomly chosen from the range of 2 to 12 VR units per second. The areas where speed changes occur is indicated in the schematic shown in Figure 2.1B. When speed changes occur, acceleration occurs gradually over the course of one second to avoid a jarring transition.

2.2.2 Data recording.

The subjects in our study were epilepsy patients who had Behnke–Fried microelectrodes surgically implanted in the course of clinical seizure mapping [88] at four hospital sites: Emory University Hospital (Atlanta, GA), UT Southwestern Medical Center (Dallas, TX), Thomas Jefferson University Hospital (Philadelphia, PA), and Columbia University Medical Center (New York, NY). Microwire implantation and data acquisition largely followed previously reported procedures [33] and were approved by an Institutional Review Board (IRB) at all participating institutions, and informed consent was obtained from all participants. The depth electrodes feature 9 platinum–iridium microwires (40 μm) extending from the electrode tip and were implanted in target regions selected for clinical purposes. We recorded microwire data at 30 kHz using either the Cheetah (Neuralynx, Tucson, AZ) or NeuroPort (Blackrock Microsystems, Salt Lake City, UT) recording systems. Data collection and analysis were not performed blind to the conditions of the experiments. We used Combinato [89] for spike detection and sorting. We excluded neurons that had a mean firing rate below 0.2 Hz or above 15 Hz (potential interneurons). Manual sorting identified single- vs. multi-unit activity vs. noise on the basis of previously determined criteria [90, 91].

Microelectrode bundle localization followed a similar process as described previously [92]. We determined the anatomic location of each implanted microwire electrode bundle using a combination of pre-implantation magnetic resonance imaging (MRI) and post-implantation computed

tomography (CT) scans (Supplementary Fig. S2.2). First, we performed automated whole brain and medial temporal lobe anatomic segmentation on T1-weighted (whole brain coverage, 3D acquisition, 1mm isotropic resolution) and T2-weighted (temporal lobe coverage, coronal turbo spin echo acquisition, $0.4 \times 0.4 \times 2$ mm resolution) MRI [93, 94] . A post-implantation CT scan was then co-registered to the MRI scans and a neuroradiologist identified the positions of electrode contacts and microwire bundles based on the source images and processed data [95].

2.2.3 Statistical analysis.

No statistical methods were used to pre-determine sample sizes but our sample sizes are similar to those reported in previous publications [96, 33]. For all omnibus testing (ANOVA) described in this study, we used a non-parametric permutation method to generate a large number of permutations where observations are permuted within each block. This enabled us to determine critical statistics and p-values (permutation adjusted) against empirically derived null distributions. Firing rate was z-scored within each session, omitting manual movement trials. Because overall z-scored firing rates may be subject to bias from stimulus-induced increases in firing rate, we computed the z-score after removing the spatial bin with the highest firing rate on each trial or spatial bins with $z > 3.29$ (exceeding the 99.9th percentile of the normal distribution).

2.2.4 Identifying place cells and memory-trace cells.

To examine how neuronal activity varied with location in the virtual environment, we binned the virtual track into 40 bins, referred to as "VR-bins" (equivalent to 1.7 VR-units) enabling us to measure neuronal firing rates in this binned space. For each cell, we counted the spikes in each spatial bin and divided this quantity by the time spent in that bin to yield a firing rate estimate. We smoothed this firing rate estimate on the single-trial level using a Gaussian kernel with a width of 8 VR-bins (± 4 VR-bins). We excluded the bins in which subjects spent less than 100 ms over the course of the entire task. This excluded several bins in the stopping zone, because the movement period ended as soon as subjects pressed the button in the stopping zone. We did not analyze data

from the manual movement trials for this study.

We used a two-way repeated-measure ANOVA to examine the effects of subject location (1-40 VR-bins), object retrieval cue (1, 2, 3, 4), and their interaction, on the binned firing rate of each cell. After using the ANOVA to screen cell responses, we defined indvidual spatial firing fields as contiguous bins in which firing rate exceeded a baseline threshold [97, 32, 98, 99]. We determined this baseline threshold independently for each cell, using non-parametric permutation testing to build empirical estimates of the threshold by circularly shifting the firing rate estimates 500 times, re-binning the firing rate, and selecting the 95th percentile of the permuted distribution of firing rates.

We defined place cells as those cells that showed a significant main effect of location on firing rate via the ANOVA, and that also had a spatial firing field (its “place field") greater than 5% the size of the track. Additionally, we performed an ANCOVA to confirm the main effect of position in the ANOVA, with position serving as a main factor while speed and time were covariates [100]. This analysis used a 3-s window surrounding the response, as anticipatory motor responses occur within 1 s of a movement [101]. We only considered a neuron to be a place cell if its firing was significantly modulated by subject location even after factoring time and speed in as covariates in the ANCOVA. Additionally, six cells showed a main effect of object cue on firing rate. These cells were excluded from analyses. We defined memory-trace cells as those cells whose firing rate showed an interaction between subject location and object cue in the ANOVA and that showed a significant spatial firing field (its “trace field") for at least one cue. A trace field for a particular object cue was considered unique if the peak location, where firing rate was maximal, did not overlap with that of any other trace field for that cell. Because all subsequent analyses relied on this characterization of place and memory-trace cells, we conducted a suite of control analyses to ensure that the proportions of cells categorized as such was robust to: dependence between task sessions for individual patients, recordings from seizure-onset zones [102], changes in bin-size for spatial firing-rate estimates, and the statistical assumptions of our omnibus testing. These analyses and their results are summarized in Supplementary Table 2.

2.2.5 Correlation between encoding and retrieval firing rates.

We computed the correlation between the spatial firing patterns of each memory-trace cell between retrieval and encoding trials to establish if memory-trace cells fire in the same locations during these phases at different firing rates ("congruent") or whether they exhibited completely different firing patterns during these two phases ("incongruent"). Specifically, we limited this analysis to the blocks of trials in which the subject viewed a cue for which a memory-trace cell had a trace field, as these cells had trace fields for 1–4 of the cues. We assessed significance using a permutation procedure, comparing the actual correlation coefficient to the coefficient computed by applying the same procedure to randomly shuffled firing rate vectors. We then tested the significance of the proportion of cue-conditions showing congruent spatial firing between encoding and retrieval trace fields against the proportion showing incongruent spatial firing.

2.2.6 Effects of attention during encoding trials.

We examined the possibility that memory-trace cell activity during retrieval trials was driven by changes in attention [103] compared to encoding. In the encoding trials of the task, the object is visible. We therefore reasoned that subjects' performance on these trials—as measured by the subject's distance to the object at the moment of button press—would provide a useful metric for how closely the subject was attending to their location in space. Though it was not possible to ensure that attention is perfectly matched between encoding and retrieval trials, this assay allowed us to examine the putative effect of attention on neural activity independently of memory retrieval. We therefore split encoding trials into low- and high-attention groups, based on whether the distance error between the button press and the visible object was greater or less than 1.5 VR bins (determined via mean split). We performed a two-way ANOVA assessing how memory-trace cell activity during encoding was modulated by the location of the trace field relative to the response (pre or post) and the attention level on that trial (low or high).

2.2.7 Task period firing rate comparisons.

In order to compare the magnitude of pre- vs. post- response firing rate changes to firing rates during different task periods, we computed the "response period" firing rate by normalizing the activity in the 10 VR-bins preceding the response by the 10 VR-bins following the response. This also helped ensure that correlations computed between task periods and the response period (see Fig. 2.6) were not confounded by trial-wide increases in baseline firing rate. We used robust linear regression to examine the correlation between hold and response period activity (Fig. 2.6B, C). This approach minimizes the effect of outliers using iteratively re-weighted least squares with a bisquare weighting function [104].

To further verify that some other aspect of our chosen response period was not leading to artifactual correlation, we computed the correlation between the hold period firing rate and a matched "control period". The control period was computed identically to the response period, but we used the regions of the track that did not overlap with the response period. In this way, the control period was of equal length to the response period, and the neural activity during this control period did not overlap with the neural activity during the response period in order to control for the effect of the response on firing rate.

2.2.8 Cross-decoding analysis.

We used a multivariate cross-decoding framework to test whether memory-trace cell activity reflected information about each object–location memory across different retrieval contexts. This framework is schematized in Supplementary Figure S2.13. To assess cross-decoding performance, we pooled the memory-trace cells recorded across all patients and sessions and constructed two pseudopopulations: EC memory-trace cells and non-entorhinal memory-trace cells. Pseudopopulation decoding has been used to describe the common neural dynamics of functionally similar subsets of cells without the inherent noise correlations shared by neurons recorded in the same session [96]. For each decoder, we used a k-nearest neighbors algorithm using a one-vs.-all paradigm for multi–class decoding of the remembered item from the recorded neuronal activity. Firing rates

were binned by task period and normalized. As detailed in the previous section, on each trial we computed the "response period" firing rate by normalizing the activity in the 10 VR-bins preceding the response by the 10 VR-bins following the response (Supplementary Fig. S2.13). We computed the response period firing rate for every trial, regardless of response accuracy. We also used a similar method to compute a matched "control period", which was based on the 20 VR-bins that were not used to compute the response period activity.

For cross-decoding, each separate decoder was trained to predict the currently cued object–location memory from the normalized firing rates of the population of memory-trace cells for each of the task periods. Each model was then tested on activity from a different period. In addition to our cross-decoding framework, we trained and tested decoders on the same periods' activity—these decoders were trained using leave-one-out cross validation to assess performance (Supplementary Fig. S2.13). We assessed significant decoding accuracy using a binomial test. Chance-level decoding accuracy was 25%, as verified by shuffling all labels and re-assessing the decoding performance across the 1000 random permutations.

2.3 Results

We recorded from 299 neurons in the EC, hippocampus, amygdala, and cingulate cortex of 19 neurosurgical patients who performed an object–location memory task (Fig. 2.1A, Supplementary Figs. S2.1, S2.2). In this task, subjects were instructed to learn the locations of different objects along a virtual linear track and then to recall the locations after the objects were removed. The task consisted of separate encoding and retrieval trials, which followed the same general structure, except that objects were visible on the track during encoding and absent during retrieval trials. Each trial began with an "instruction period," in which subjects viewed the name of the cued object for that trial. The "hold period" followed, during which subjects remained stationary at the entrance to the track for 4 seconds. Next was the "movement period", in which the subject was moved automatically down the track at randomly varying speeds. During encoding trials, the object was present on the track, enabling the subject to press a button as they reached the object's

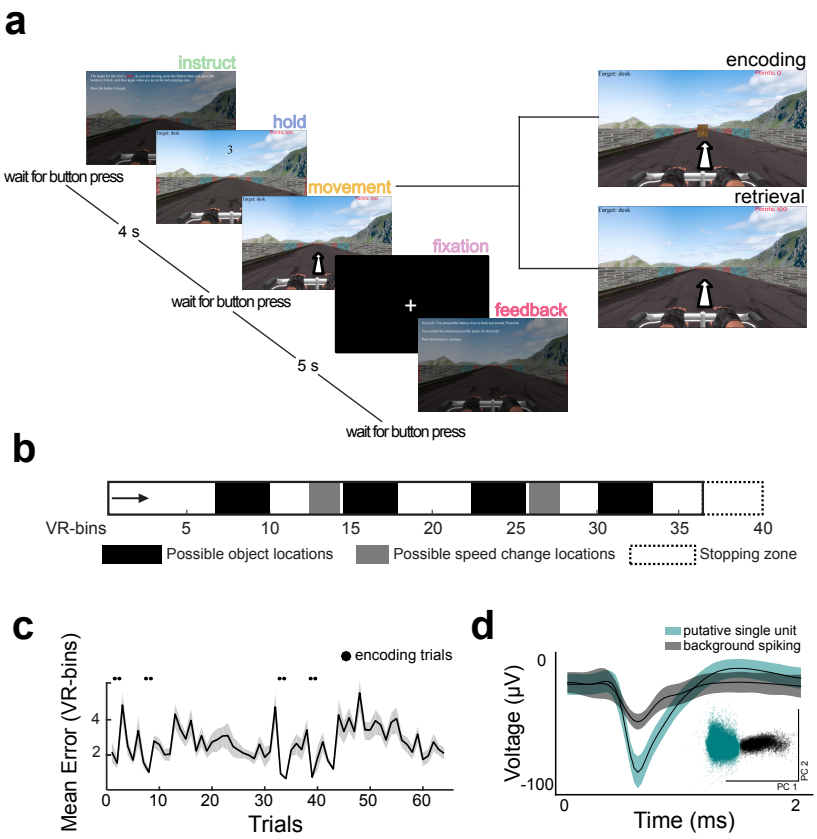

Figure 2.1: **Task overview.** A) Timeline of the object–location memory task. Inset indicates that movement periods either consist of encoding or retrieval epochs. B) An overhead map of the environment. Arrow represents the starting point of each trial. C) Mean response error on retrieval trials, averaged over all task sessions (n = 19 patients and 31 total sessions). Shading indicates SEM. D) Example putative single-unit waveform and example sub-threshold background spiking. Solid lines indicate mean waveform, shading indicates SEM. Inset shows separation of waveform principal components, whereby one cluster represents the putative single-unit waveform and the other represents the background spiking.

visible location (Fig. 2.1B). During retrieval trials, the object was absent and the subject pressed a button at the location where they remembered the cued object being present. Subjects generally showed high accuracy during retrieval trials, pressing the button within 2.8 virtual units (VR-bins) of the correct location, or 7% of the track length, on average (Fig. 2.1C).

We examined how the activity of individual neurons (see Fig. 2.1D for example) represented the subjects' spatial location in the task by computing each neuron's firing rate as a function of their position along the track during retrieval trials. To assess the modulation of neuronal activity, we used a two-way repeated-measure ANOVA to identify neurons whose activity during retrieval

trials varied as a function of the subject's location ($1 - 40$ spatial bins), the retrieval cue ($1 - 4$ possible cues), and their interaction, determining significance using a permutation procedure. As we describe below, this analysis revealed two groups of neurons with distinct firing patterns (Fig. 2.2). We found neurons with firing rates that varied as a function of only subject location, similar to conventional place cells [22, 32]. We also found neurons that we refer to as memory-trace cells, which exhibited a distinctive type of response. The spatial tuning of memory-trace cells shifted along the track depending on the retrieval cue that the subject had viewed at the beginning of each trial.

2.3.1 Place cells activate in fixed locations, independent of memory retrieval demands.

We identified place cells as those that showed a significant main effect of location on firing rate, and had at least one place field (Fig. 2.3; see *Methods*). A significant number of cells (50 of 299, $p = 8.78 \times 10^{-14}$, binomial test vs. 5% chance) fulfilled our criteria as place cells. Most place fields were smaller than 10% of the track length and none covered more than 40% of the track (Fig. 2.3C).

We found significant numbers of place cells in the EC, hippocampus, and cingulate (Fig. 2.3D; all $p < 10^{-4}$, binomial test vs. 5% chance). To examine the possibility that these findings were the result of neuronal responses to time [105] or speed [106], we used an ANCOVA to test if these cells' location-related modulation persisted after including speed and time as covariates [100]. 90% of place cells continued to show significant spatial coding after accounting for potential effects of time or speed, indicating that their activity primarily reflected the subject's spatial location.

2.3.2 Spatial tuning of memory-trace cells shifts according to the retrieval cue.

In contrast to place cells, Figure 2.2B depicts the activity of two example EC memory-trace cells, whose spatial tuning shifted depending on the particular object–location cue that the subjects viewed at the beginning of each trial. We identified memory-trace cells systematically as those cells that showed significantly increased firing in contiguous spatial bins for at least one cue, which we

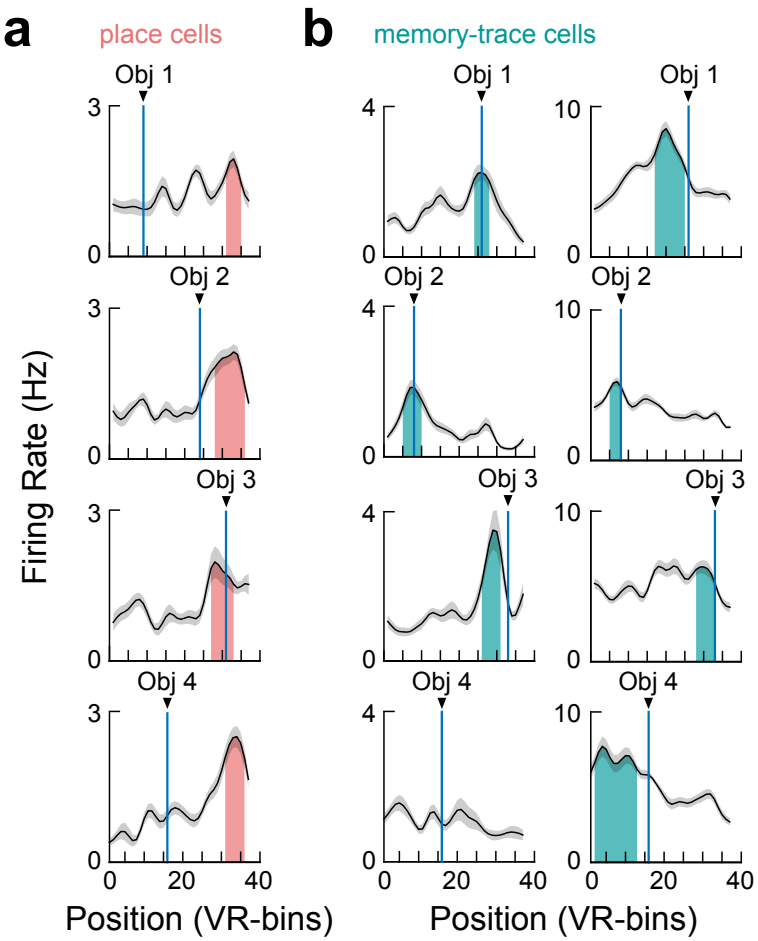

Figure 2.2: **Examples of place and memory-trace cells.** A) The mean firing rate (black lines, n = 12 trials per block) of an example hippocampal place cell. Individual plots show this cell's activity for trial blocks with different cue objects. Vertical blue lines indicate object locations. Grey shading indicates standard error (n = 12 trials). Colored region indicates place fields determined by finding contiguous bins with elevated firing rates (see *Methods*). B) The activity of two EC memory-trace cells. Note that in contrast to the place cells in panel *A*, these cells' firing fields (shaded regions) shift depending on the retrieval cue.

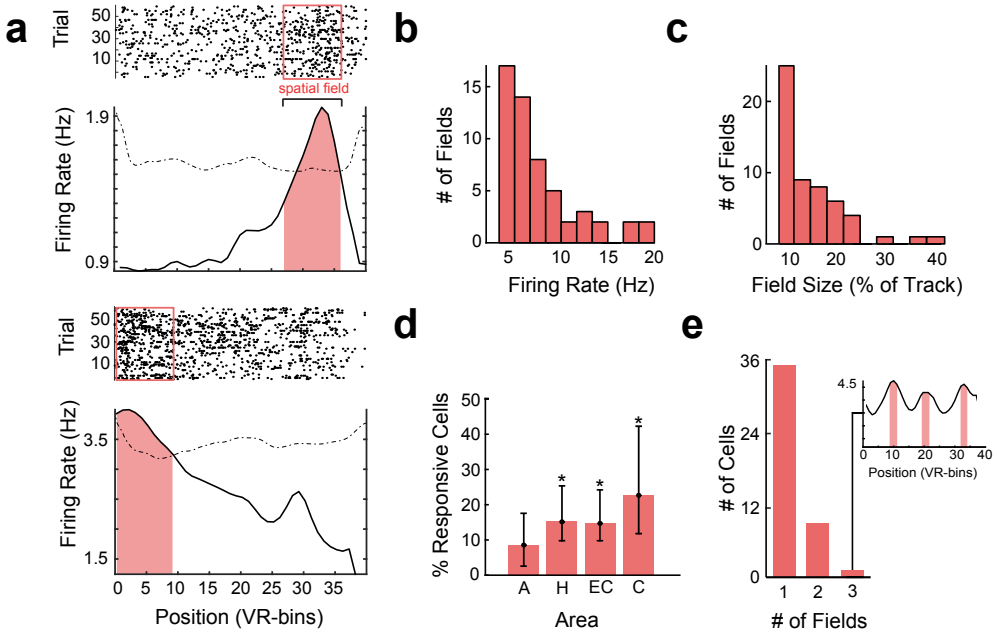

Figure 2.3: **Place cell activity.** A) Raster plot and mean firing rate for two example place cells recorded from the hippocampus. Box and shading indicate place fields. Dotted line represents the threshold for identifying place fields, assessed non-parametrically (see *Methods*). B) Distribution of mean firing rates among place fields. C) Distribution of field sizes across all place cells, expressed as a percentage of the track. D) Proportion of place cells recorded in each brain area. A = amygdala (n = 5 cells), H = hippocampus (n = 16 cells), EC = entorhinal cortex (n = 18 cells), C = cingulate (n = 6 cells). Asterisks indicate significant proportions (p's$< 10^{-4}$, two-sided binomial test vs. 5% chance). Bars indicate the 95% confidence interval from a binomial test. E) Number of responsive cells with more than one spatial field. Inset shows an example cell from the cingulate that showed three spatial fields.

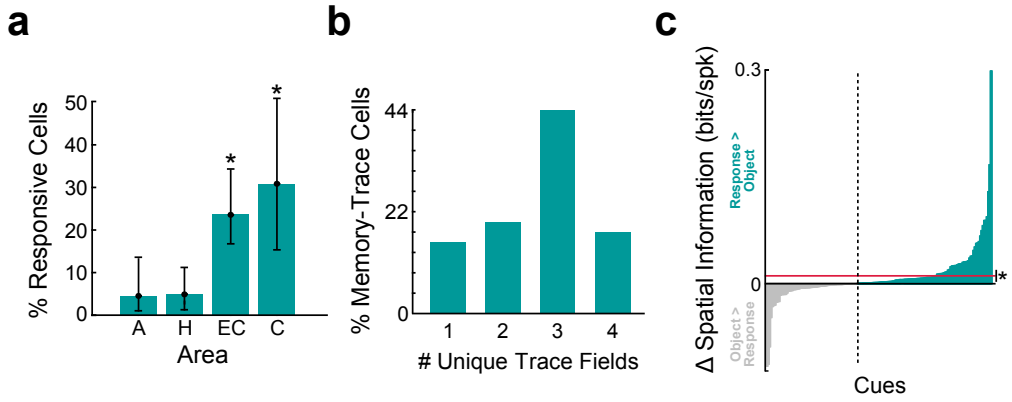

Figure 2.4: **Trace-fields shift according to subjects' memory for cued object locations.** A) Distribution of memory-trace cells across brain areas. A = amygdala (n = 3 cells), H = hippocampus (n = 5 cells), EC = entorhinal cortex (n = 27 cells), C = cingulate (n = 8 cells). Asterisks indicate significant proportions (p's$< 10^{-5}$, two-sided binomial test vs. 5% chance). B) Distribution of the counts of unique trace fields exhibited by memory-trace cells. C) Difference in spatial information for each memory-trace cell's firing rate for each cue (n = 168 across all memory-trace cells), when aligned relative to response location vs. object location. Asterisk denotes a significant paired difference (mean = 0.01 bits/spike, sign-rank test $z = 3.4$, $p = 0.0007$).

refer to as "trace fields" (see *Methods*), and whose spatial firing pattern significantly shifted across different cues (determined via a location × cue interaction in the ANOVA). Overall, a significant number of cells (43 of 299; $p = 6.37 \times 10^{-10}$, binomial test vs. 5% chance) fulfilled these criteria for memory-trace cells (Supplementary Figs. S2.3, S2.4). These cells were found primarily in the entorhinal and cingulate cortices (Fig. 2.4A; p's$< 10^{-5}$, binomial tests vs. 5% chance). We observed at least one memory-trace cell in 15 of 19 subjects (Supplementary Table 1); 12 of 19 subjects exhibited both place and memory-trace cells.

Individual memory-trace cells exhibited a unique trace field for anywhere between one and four cues (Fig. 2.4B, see Supplementary Fig. S2.4), distinguishing them from "cue-association" cells[107] which only responded to a single association. Specifically, the firing of many memory-trace cells shifted to represent multiple locations over the course of a session, often appearing to fire near the location of the object cued for each trial.

To determine if memory-trace cell activity reflected underlying memory retrieval processes, we next examined whether the spatial tuning of these neurons was more strongly anchored to the response location—where the subject believed the object to be—rather than the object's true loca-

tion [108]. If this were the case then re-aligning memory-trace cell firing relative to the response location would yield a stronger pattern of spatially modulated firing compared to the pattern observed when re-aligning firing rate relative to the object location. We tested this by quantifying the spatial information[109], a measure of the specificity of the spatial tuning, in both the response- and object-aligned configurations for each of the four cues. Spatial information was significantly greater in the response-aligned configuration compared to the object-aligned configuration (Fig. 2.4C, sign-rank test, $z = 3.4, p = 0.0007$), suggesting that memory-trace cell firing represents subjects' location relative to the location targeted for memory retrieval.

2.3.3 Memory-trace cell activity tracks subjective memory for cued object locations during retrieval.

Having determined that memory-trace cells were more strongly spatially tuned in response-aligned configurations,we next assessed in more detail where these cells fired in relation to the spatial location of subjects' responses. As shown in Figure 2.5A, trace fields clustered in the spatial bins immediately preceding the response location, appearing on average 2.5 VR-bins before the response location ($t(125) = -2.09, p = 0.038$). This accumulation of trace fields prior to the response suggested that trace-field activity signaled the relevance of a location for upcoming memory retrieval [110]. Furthermore, trace fields appeared significantly closer to subjects' response locations than the true object location on a given trial ($t(1495) = 1.79, p = 0.037$). To confirm this preference for locations preceding the response, we computed the grand average of memory-trace cell firing rates in the spatial locations surrounding the response (Fig. 2.5B). This confirmed that memory-trace cells generally increased their firing as subjects approached the response location, and then decreased following the response (paired t-test pre- vs. post- firing rate, t(1986)=3.99, $p = 6.73 \times 10^{-25}$; Supplementary Fig. S2.5). The broad peak and gradual decline in average firing rate across memory-trace cells depicted in Figure 2.5B reflects the heterogeneity of trace-field offsets relative to the response location (Fig. 2.5A), as opposed to all trace fields appearing at the same offset.

To further test if memory-trace cell activity tracks subjective memory we analyzed the memory-trace cell firing rate on retrieval trials where subjects made large errors (16.8 % of trials)—these trials enabled us to dissociate subjects' response location and the actual object location. By comparing the response- and object-aligned firing rates during these trials, we found that these cells' firing peaked significantly closer to the response location than the actual object location (Fig. 2.5C; $t(333) = 2.13$, $p = 0.033$). These results further support the notion that memory-trace cell spatial tuning is anchored to subjects' retrieval of a cued object's location from memory.

Because cells in the MTL have shown evidence of coding for time [105], we considered the possibility that memory-trace cells were firing at specific timepoints, rather than spatial offsets, relative to the response (Supplementary Fig. S2.6). We thus performed an analysis comparing the degree to which individual memory-trace cell activity was predicted as a function of distance or time relative to the response. This analysis revealed that the firing rates of memory-trace cells were more strongly predicted by the spatial rather than temporal offset($t(42) = 2.35$, $p = 0.024$), supporting the notion that memory-trace cell activity represents the distance to upcoming recalled locations.

We next sought to better understand the type of distance-to-memory information represented by memory-trace cells. We examined whether memory-trace cell firing fields appeared at fixed offsets from the response location, as might be expected from a general distance code for relevant locations [81], or if they appeared at cue-specific distances, as might be expected in a form of goal-oriented remapping [55]. We conducted an analysis of trace-field offset consistency across cues (Supplementary Fig. S2.7), and found that a significant number of memory-trace cells had trace fields at reliably fixed offsets across cues (5/37 cells with > 1 trace field, $p = 0.036$, binomial test vs. 5% chance) while a different subset of cells that were equally prevalent (5/37 cells) showed significantly variable offsets across cues.

To further determine if the activity of memory-trace cells specifically relates to memory retrieval, we examined their firing patterns on encoding trials where the cued object was visible. Comparing neural activity between encoding and retrieval trials—which were perceptually identi-

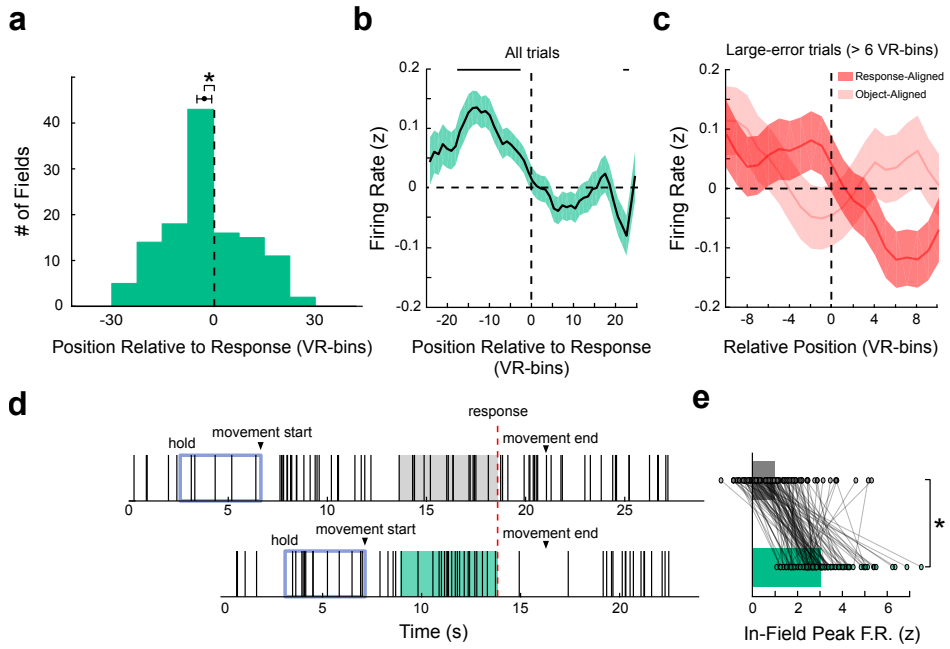

Figure 2.5: **Memory-trace cells track subjective memory during retrieval** A) Distribution of trace-field locations (n = 126 trace fields across 43 memory-trace cells) relative to response location (indicated by black dashed line). Asterisk indicates mean field location significantly precedes response location ($t(125) = -2.09, p = 0.038$, two-sided t test). B) Mean firing rate during retrieval trials (z-scored) of all memory-trace cells (black line, n = 1990 trials) aligned to response location. Shading indicates SEM. Horizontal lines indicate spatial bins that are significantly different from baseline (p's$<$ 0.05, two-sided t test, FDR-corrected). C) Mean firing rate (z-scored) of all memory-trace cells during large-error trials (solid lines, n = 334 trials) , aligned to response location (dark red), or object location (light red). Shading indicates SEM. D) Example spike trains from a single EC memory-trace cell during an example encoding (top) and retrieval (bottom) trial for the same cued location. Vertical lines denote spike times. Responses were aligned and shaded (5 seconds pre-response) to qualitatively illustrate difference in spiking between trial types. E) Population data showing greater memory-trace cell peak firing rate in-field (z-scored) during retrieval than encoding trials, as visualized by the example in panel D ($t(125) = 12.92, p = 8.95 \times 10^{-25}$, two-sided t test). Circles denote individual trace fields (n = 126).

cal aside from the visible object—specifically enabled us to identify features of memory-trace cell responses that related to memory retrieval, while controlling for other factors that differed across trials, such as object identity [85], goal locations [111, 81], and motor planning [101]. Overall, we found that when a subject was located in a memory-trace cell's firing field, there was increased activity on retrieval trials compared to encoding ($t(125) = 12.9, p = 8.9 \times 10^{-24}$; Figs. 2.5D,E). To assess whether memory-trace cells simply fired in the same locations during encoding trials but with lower firing rates, we computed the spatial correlation between the memory-trace cell firing patterns during retrieval and encoding (*see Methods*, Supplementary Fig. S2.8). Memory-trace cell spatial firing patterns were largely uncorrelated between encoding and retrieval ($\chi^2(1) = 149.35$, $p < 2.2 \times 10^{-16}$), meaning that the spatial tuning we observed during retrieval was not present at lower firing rates during encoding. In contrast, place cells exhibited significantly more stable spatial tuning between encoding and retrieval trials than memory-trace cells (Supplementary Fig. S2.9; Mann-Whitney U-test, z = 5.25, $p = 1.48 \times 10^{-7}$). These results indicate that during encoding memory-trace cells either shift spatial tuning or are simply inactive, supporting the idea that the memory-trace cell spatial tuning we observed uniquely supports memory retrieval. Furthermore, we found no effect of low versus high measures of attention on memory-trace cell activity (*see Methods*; $F_{(1,639)} = 0.16$ & 0.48; p's> 0.05, permutation-adjusted), indicating that attention likely did not explain the encoding–retrieval differences. This is consistent with findings indicating that attentional mechanisms do not fundamentally differ between encoding and retrieval [112].

In sum, memory-trace cell spatial tuning was predominantly modulated by subjects' response location specifically during cued memory retrieval. This pattern was robust even when subjects' responses were inaccurate, suggesting that memory-trace cells tracked subjects' internal representation of the cued object's location.

2.3.4 Activity of memory-trace cells in EC separably and robustly represents different memories.

Although the above analyses showed that the activity of memory-trace cells tracks retrieved locations in the environment, it remained unclear whether these cells support memory representa-

tions more generally, beyond moving through the relevant environment. This question is important to answer because it could help explain how we are able to remotely recall events from outside the environment in which they occurred. We investigated this question by analyzing memory-trace cell activity during the hold period of our task, which follows the subjects' initial viewing of the retrieval cue during the instruction period. We hypothesized that during the hold period subjects would exhibit similar neural representations of the current memory retrieval cue as when moving through the target location in the environment. We therefore asked if the same patterns of neuronal activity associated with retrieval of particular memories during movement also emerged during the hold period. Overall, memory-trace cell firing rates were significantly elevated during the hold period of retrieval trials (Fig. 2.6A; $F_{(4,10075)} = 2.88$, $p = 0.021$, post-hoc t-tests, p's< 0.05, FDR-corrected). This effect was not seen during encoding trials, or by non-trace cells (Supplementary Fig. S2.10). This indicates that memory-trace cells were generally engaged during the hold period, even though subjects were still, rather than moving through the environment.

We hypothesized that the mean firing rate of memory-trace cells during the hold period would be correlated with their activity when subjects remembered the location during movement. Finding such a pattern would indicate that memory-trace cell representations for retrieved locations generalized beyond memory retrieval during movement, supporting the potential utility of trace-cell representations for retrieval across multiple contexts. To facilitate comparison of memory-trace-cell firing rates across the hold period and the response location, we first characterized the changes in firing rate in the spatial bins surrounding the response location (Fig. 2.5B), which we called the "response period". We measured the magnitude of the response-modulated changes in memory-trace cell activity by normalizing each cell's pre-response firing rate by its post-response firing rate, thus accounting for background activity of each neuron. This also helped ensure that correlations computed between a trial's hold and response periods would not be confounded by overall trial-wide increases in baseline firing rate. For each cell, we then computed the correlation across trials between the firing rates during the hold and response periods (Fig. 2.6B). We compared this measure to the correlation in firing rate between the hold period and a matched "control period",

which was computed similarly to the response period using regions of the track that did not overlap with the response period. We found that memory-trace-cell firing was positively correlated between the hold and response periods, and not between the hold and control periods (Fig. 2.6C, Supplementary Fig. S2.11A), indicating that a consistent pattern of neuronal activity for individual cues was present during the hold and response periods (see Fig. 2.6D and Supplementary Fig. S2.11B for examples). Firing rate during these periods was not correlated with task performance (Supplementary Fig. S2.12).

We next used a multivariate cross-decoding analysis [113] to more fully characterize how the neural representations of specific memories that emerged during the response period were recapitulated across various task periods (see *Methods*; Supplementary Fig. S2.13). Here we trained separate decoders to predict the currently cued object location memory from the normalized firing rates of the population of memory-trace cells for each task period. We then tested each model's decoding performance on activity from the response period. In this analysis, if we were to observe that a model trained on one period demonstrated elevated decoding performance when tested on memory-trace-cell firing during the response period, then it would indicate that the neural representations of specific memories were similar between these two periods.

The results of this analysis indicated that the firing rates of EC memory-trace cells, specifically, represented individual memory cues similarly between the hold and response periods. For EC memory-trace cells, when comparing test performance in the response period for various training models, only the model trained on the hold period showed significantly elevated accuracy (Fig. 2.7A; $p = 0.0043$, binomial test vs. 25% chance). This pattern was not present for memory-trace cells outside the EC (Fig. 2.7B). Additionally, we observed significant decoding from EC memory-trace cells when we both trained and tested models on the response period using 10-fold cross-validation (white bar, Fig. 2.7A; $p = 0.029$, binomial test), which confirms the reliability of these patterns.

To characterize the patterns of memory-related neural activity across the task more fully, we also performed a complete cross-decoding analysis, in which we compared the performance of

training and testing models across all pairs of task periods (Supplementary Fig. S2.14C). In particular, we did not find significant cross-decoding for data from the control period. This indicates that EC memory-trace cells do not represent the currently cued memory when the subject is far from the target location. Furthermore, to test if these patterns were robust, we also individually applied this cross-decoding analysis to the first and second halves of each session. Decoding performance did not differ between both halves (all p's$>$ 0.05, chi-square test), suggesting our findings were consistent throughout the session. Overall, these results demonstrate that EC memory-trace cells exhibit a distinctive firing-rate code for individual memory cues that is consistent both during the hold period as well as when the subject moves through the associated target location.

2.4 Discussion

A crucial aspect of human memory is our ability to actively target and differentiate past experiences. Here we show that the activity of EC memory-trace cells selectively represents and differentiates between memories from a single environment. Critically, memory-trace cells represent information about locations that subjects had been cued to remember, illustrating how top-down memory demands influence the brain's representation of space. Our observations suggest that memory-trace cell activity represents object locations you are trying to remember. The activity of EC memory-trace cells, specifically, was predictive of the cued memory both during the stationary hold period as well as when subjects moved through retrieved locations, suggesting these cells support a generalizable and robust memory-specific representation. Our findings thus indicate that, in addition to the fixed metric for space provided by grid cells [24, 33], the human EC also contains neurons that support a flexible spatial code modulated by top-down memory demands. Below, we discuss how memory-trace cells relate to previous single-cell findings in the hippocampus and EC relevant to space and memory, and how they help explain the broader role of the EC in the brain's memory network.

Place cells in the hippocampus are thought to represent a map of the current environment, and evidence shows that these representations remap in response to changes to the environment [114,

115]. This led to the hypothesis that different environmental contexts induce orthogonal spatial representations in these cells, which are used to index different maps for past experiences [78, 79]. The phenomenon of “goal-oriented" remapping, in which place fields change location and/or accumulate near goal locations without changes to local cues or spatial context, demonstrates that top-down influence and goal-driven behavior can modulate spatial firing [80, 55]. A significant proportion of memory-trace cells exhibited firing fields at different offsets from the response location depending on the cue being retrieved, demonstrating a potential link to goal-oriented remapping and suggesting that the link between remapping and memory-trace cell activity should be further investigated. Furthermore, distal CA1 place cells — which receive direct EC input — show partial remapping based on the presence and location of objects in the environment [116], raising the possibility that EC memory-trace cells also influence or interact with hippocampal remapping. Future work should investigate the relationship between our findings and remapping, and how these phenomena interact in service of memory.

The fact that memory-trace cell activity tracked the current cued memory indicates that subjects' top-down memory retrieval states influenced the firing of these cells. Related work has found cells that represent goal-related spatial information in the hippocampal formation of rodents and bats [97, 111, 81]. The key distinction between memory-trace cells and these other cell types is that memory-trace cells do not significantly activate when objects, the putative goal, are visible in the environment. As such, memory-trace cell activity likely is more specifically related to memory retrieval processes, rather than goal coding in general. Interestingly, some specific properties of memory-trace cells recapitulate elements of these goal-coding cells. Specifically, goal cells in rodent subiculum also fire in locations preceding rewards[81], and goal representations in bats [111] are also maintained even when the goal is occluded. Additionally, some memory-trace cells exhibited firing fields at fixed offsets from the response location independent of the cue, providing a potential link to hippocampal goal-vector coding. Future work that more extensively measures memory-trace cell activity during navigation to visible goals may characterize their similarity to the goal cells found in the hippocampal formation.

Our finding that memory-trace cells in the EC, in particular, exhibited consistently decodable representations of individual object–location memories extends prior work documenting the EC's role in the representation of object features and context in rodents and non-human primates [117, 85]. Specifically, our findings bear significant resemblance to "object-trace cells" discovered in rodent EC [53] and cingulate [118]. Rodent object-trace cells activated in locations where animals had previously encountered objects and could represent a non-specific, putative trace of all the objects that the rodent had encountered in the environment. However, human memory-trace cells had two crucial additional features that were not observed in rodents. The activity of memory-trace cells specifically tracked the location subjects recalled, indicating that subjects' top-down memory target modulated their spatial tuning, rather than showing increased activity for all previous object–locations as in rodent object-trace cells. Additionally, memory-trace cells exhibited a memory-specific rate code even when subjects were not moving through the environment.

This prevalence of memory-trace cells in the EC may advance our understanding of the functional role of the entorhinal region in memory. Recent work using neuromodulation has demonstrated a causal role for the EC in human spatial and episodic memory [92, 119]. Additionally, the EC is thought to be an early staging ground for the onset of Alzheimer's disease [120, 121], with evidence suggesting that the spread of Alzheimer's pathology begins in the EC [122] and that entorhinal tau is directly linked to memory decline in old age [123]. Given these lines of research, one possibility is that the memory-trace cells we identified are affected by stimulation or lesion of the EC, resulting in these subsequent effects on memory. Indeed, recent work has shown that mice expressing tau pathology in EC showed concomitant spatial memory deficits and major loss of cells in EC layers II and III, providing evidence of a potential link between loss of memory-related cells in the EC (such as memory-trace cells) and memory deficits [124].

Additionally, recent work in humans has shown that the activity of grid cells is degraded in people at risk for Alzheimer's [86], and is correlated with spatial memory performance [125, 41]. It is possible that grid cells and memory-trace cells both contribute to EC memory circuits, and the relationship between them may be important to understanding how spatial and memory processes

interact in the EC. Indeed, two recent studies in rodents discovered that grid cell maps shift to represent remembered reward locations, suggesting the influence of task-relevant variables on the structure of entorhinal spatial maps [87, 126]. Our findings build upon this work by demonstrating a specific way in which top-down processes may interact with flexible spatial representations to index events for memory retrieval in the EC.

In addition, a notable feature of our results is that we found significant proportions of memory-trace cells in cingulate cortex in addition to the EC. Our previous work identified grid-like single neuron activity in the cingulate cortex of humans, in addition to the EC [33], complementing related findings from fMRI showing grid representations outside of the EC [125]. The co-localization of memory-trace cells and grid cells suggests that these cells represent a common memory network that involves both EC and cingulate cortex. Going forward, further exploration of the relationship between memory-trace cells and grid cells may provide insight into the neural mechanisms underlying spatial and mnemonic function across regions.

In conclusion, we demonstrate the existence of memory-trace cells that flexibly change their spatial tuning to distinguish individual memories during retrieval. EC memory-trace cells exhibited consistent activity across the hold and response periods of our task, allowing us to decode cued memories and indicating that EC representations persist beyond purely spatial or navigational settings. This supports the notion that the EC is important for general relational and contextual memory representations [85, 25]. Looking forward, although our results focus on how memory modulates spatial tuning to distinguish subjective memory representations, other emerging lines of work now show that the EC maps non-spatial features of experience [127, 128]. Our findings may therefore enable new lines of investigation in various species of how entorhinal neuronal representations of space and other domains are modulated by top-down demands in service of memory and other high-level cognitive processes.

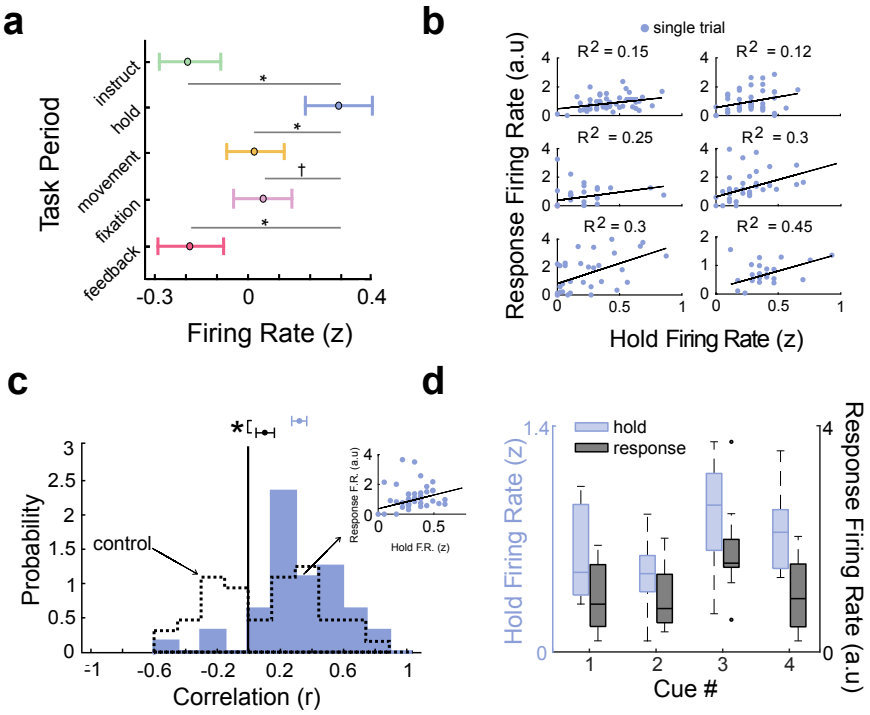

Figure 2.6: **Memory-trace cell activity is correlated between the hold period and response period.** A) Mean normalized (z-scored) firing rate (circles) across all memory-trace cells by task period ($n = 1990$ trials). Error bars indicate SEM. Asterisks indicate $p < 0.05$ (FDR corrected two-sided t tests); † indicates $p < 0.1$. B) Relation between firing rates between hold- and response periods for six example memory-trace cells. Black line denotes the robust linear regression fit. "A.u" denotes arbitrary units, indicating that the response period activity is defined by a ratio (of pre- vs. post- response firing rate).Each plot depicts 48 retrieval trials, with the exception of the middle-left and bottom-right plots which show truncated sessions of 24 trials. C) Distribution of Pearson correlation coefficients for memory-trace cell firing rates between hold and response periods ($n = 43$ cells). Inset shows one example cell's correlation. Circles indicate mean, and error bars indicate SEM. Dotted line denotes control distribution (see *Methods*). Asterisk indicates significant difference ($t(42) = 2.99$, $p = 0.0046$, two-sided t test). D) Mean normalized firing rate (solid lines) during hold and response periods for each object cue, for an example EC memory-trace cell. Circles indicate single-trial activity, error bars indicate SEM ($n = 12$ trials).

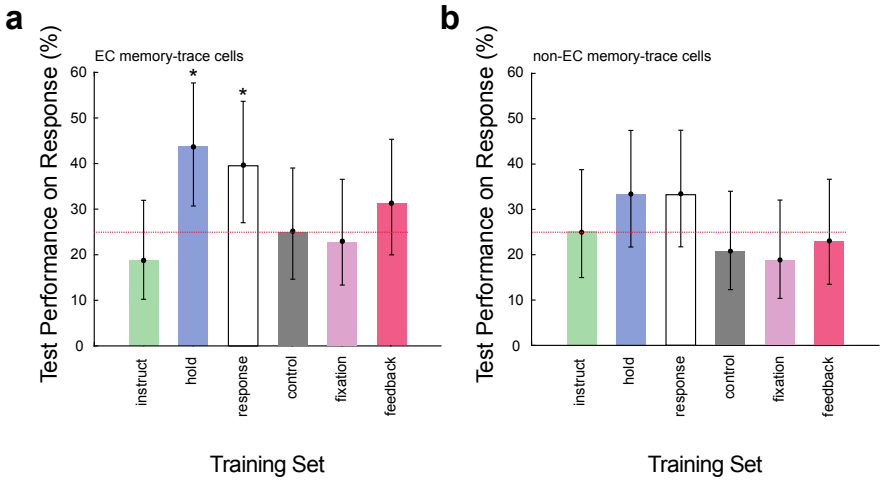

Figure 2.7: **EC memory-trace cell activity predicts cued memory across hold and response periods.** A) Results of memory-decoding analysis for entorhinal cortex memory-trace cells (n = 27). Individual bars distinguish models that were trained on different task periods, with all models tested on activity during the response period using trial-level cross validation. Black circles denote percentage, and error bars indicate SEM. Asterisks indicate above-chance decoding accuracy (p's< 0.05, two-sided binomial tests). B) Test performance for decoders based on non-entorhinal cortex memory-trace cell firing (n = 16), with training on each of the task periods and testing on the response period.

2.5 Supplementary Material

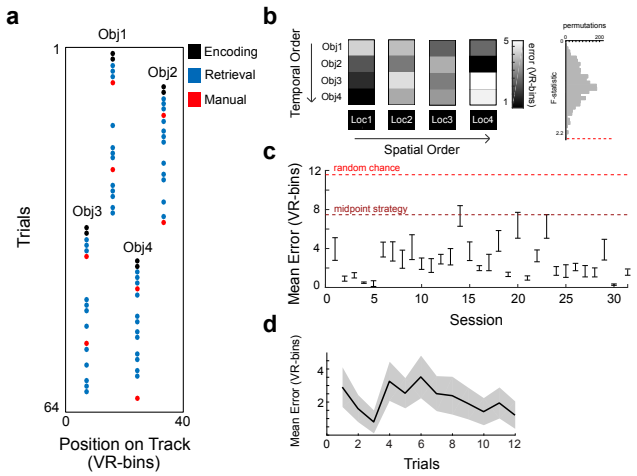

Figure S2.1: **Trial structure and behavioral performance.** A) The first two trials for each object cue were encoding trials (black), followed by retrieval trials (passive movement, blue; manual movement, red). B) Left: Error plotted as a function of both temporal order and spatial order of objects. Darker colors indicate lower error. Columns represent effect of spatial order, rows represent effect of temporal order, individual bins represent interaction between specific spatial and temporal ordering on shuffled error from ANOVA. Right: Analysis of effects of temporal and spatial order. We found a significant interaction ($F_{(9,\ 1385)} = 2.25$, $p < 10^{-3}$, permutation-adjusted) such that certain combinations of spatial and temporal order led to differences in performance. Red dotted line indicates true test statistic and the histogram indicates the distribution of permuted interaction test statistics for effects of temporal and spatial order on shuffled error. C) Mean error for each session ($n = 48$ trials for 28 full sessions, 24 for 3 truncated sessions). Error bars indicate SEM, and center of bars indicates mean. Red dotted lines indicate the error levels expected by chance, following strategies where the subjects respond randomly (light red) and where the subject always responds at the midpoint of the environment (dark red). D) Mean error across the 12 retrieval trials (blue dots in panel *A*) comprising each object–cue block, averaged over subjects ($n = 118$ trial blocks over 31 sessions). Shading indicates SEM. Note that subjects learned the object–location association quickly (first two trials), only to show increased errors beginning after trial 3 upon the introduction of another object location to hold in memory.

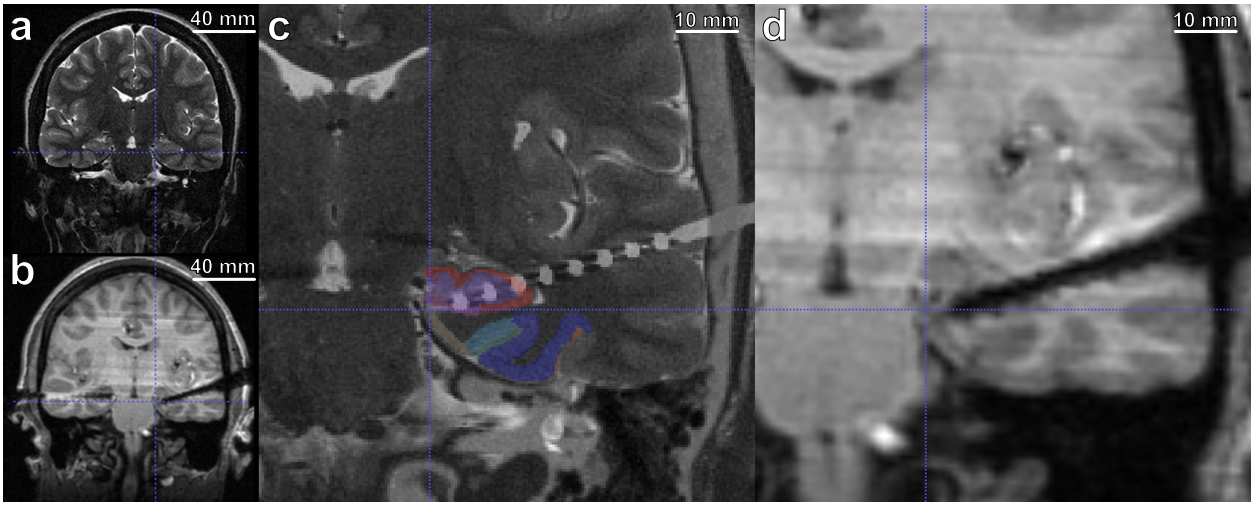

Figure S2.2: **Approach to localization of microelectrodes.** A) Pre-implantation coronal T2-weighted MRI scan from one subject. B) Co-registered post-implantation T1-weighted MRI scan. C) Coronal T2 scan overlaid with software segementation of medial-temporal subregions and the post-implantation CT to show macroelectrodes. Blue crosshairs indicates the location of the microwires. Coloring scheme for the MTL segmentation: EC (tan), BA35 (light blue), BA36 (dark blue), subiculum (pink), dentate gyrus (purple), CA1 (red). D) Post-implantation 3D T1-weighted MRI showing the confirmed location of the micro-electrode from panel C (blue crosshairs) in EC.

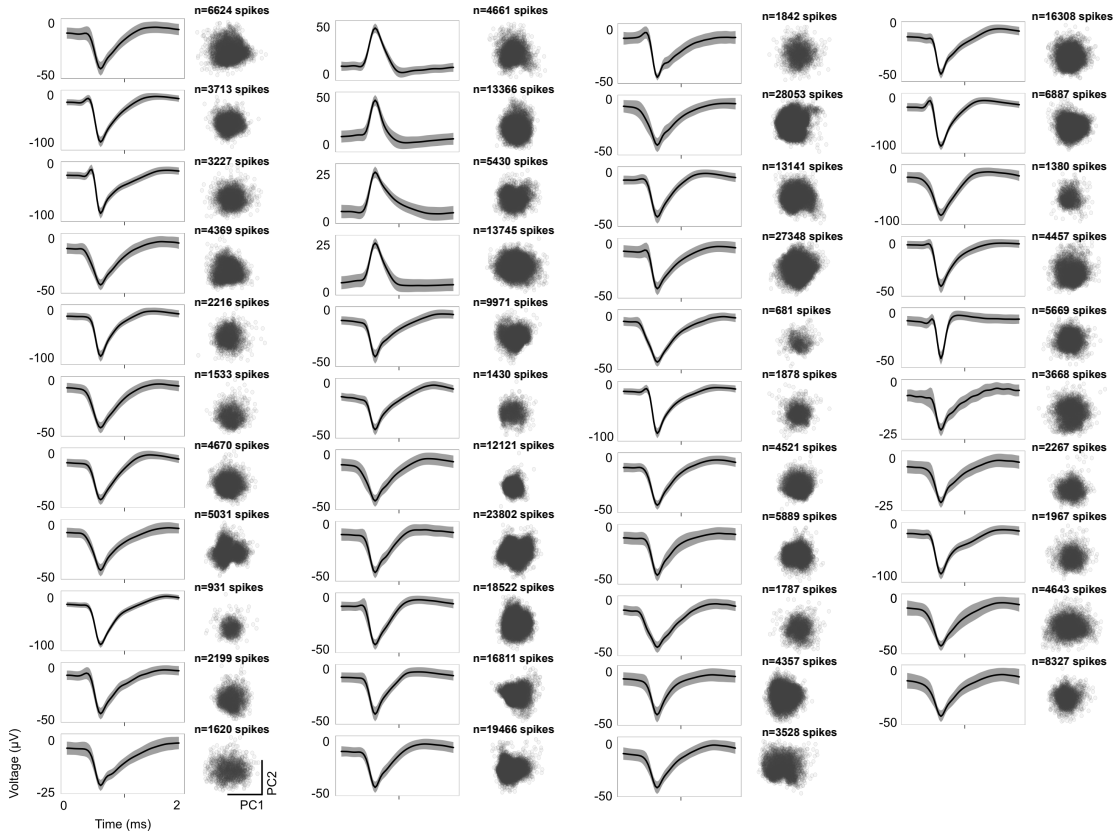

Figure S2.3: **Memory-trace cell waveforms.** Each pair of plots depicts putative single-unit waveforms and their first two PCA components. Left panel: Mean single-unit waveform. Cells with positive polarity waveforms were recorded using the Neuralynx Cheetah system (see *Methods*). Shading indicates SEM. Right: Single clusters depicting first two principal components of each putative single-unit waveform.

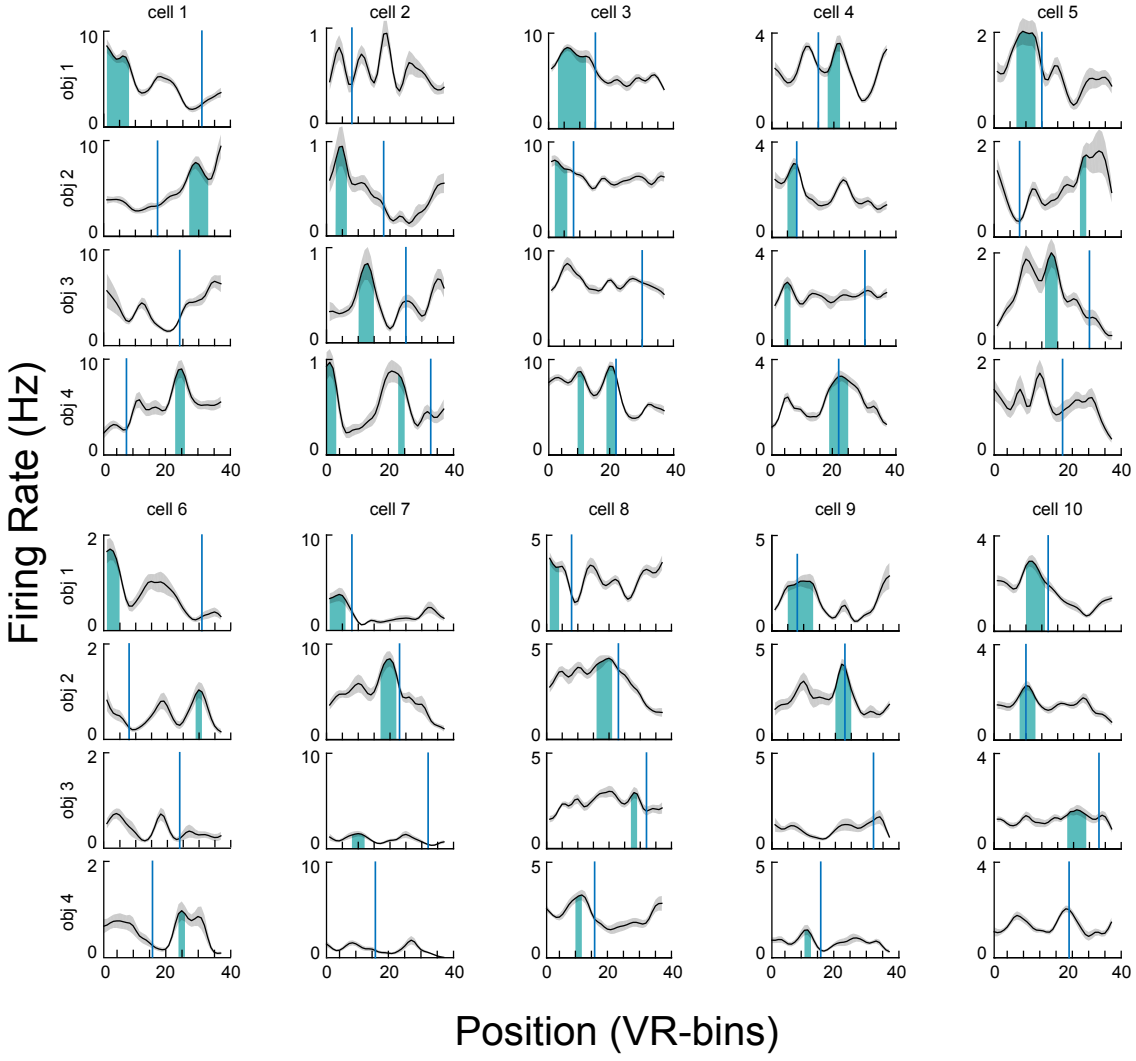

Figure S2.4: **Examples of memory-trace cell activity during retrieval trials.** Plots illustrate mean firing rates of memory-trace cells for each object cue, as in Fig. 2B. Vertical blue lines indicate the location of the cued object, which was not visible to the subject during retrieval. Teal shading regions indicate spatial fields, identified as contiguous bins exceeding a non-parametrically determined threshold (see *Methods*). Grey shading indicates standard error (n = 12 trials). Regions: cells 1–2 = amygdala, cells 3–5 = EC, cell 6 = cingulate, cells 7–9 = EC, cell 10 = hippocampus.

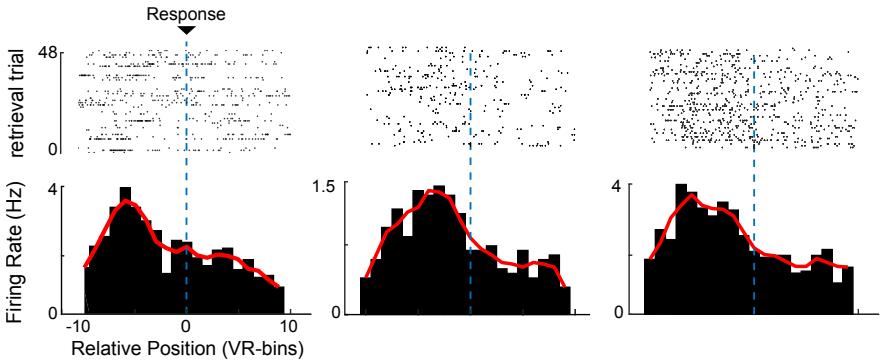

Figure S2.5: **Memory-trace cell spiking relative to response location.** Raster plot of spiking activity and corresponding peristimulus histogram (PSTH) for three example EC memory-trace cells, aligned relative to response location (indicated by blue dotted line). Red line indicates smoothed (moving-average) PSTH.

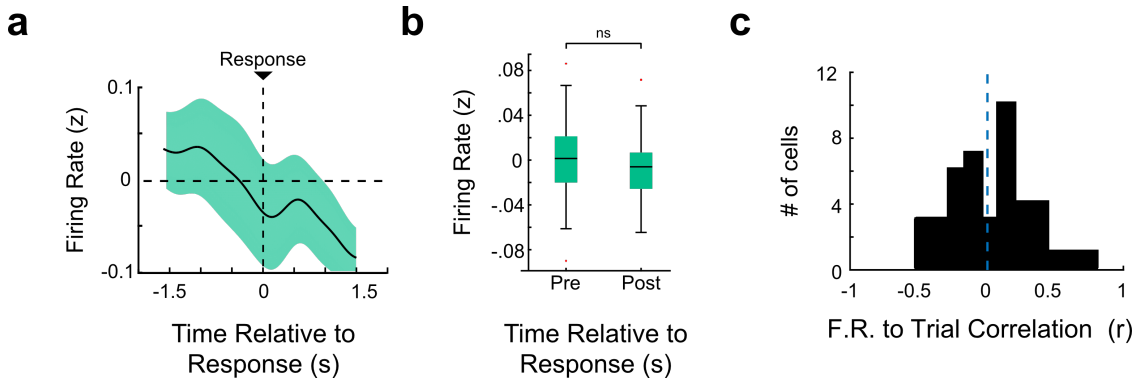

Figure S2.6: **Memory-trace cell activity and time.** A) Mean firing rate (z-scored) of all memory-trace cells aligned to response time (black line, $n = 1990$ trials). This analysis used a 3-s window surrounding the response, as anticipatory motor responses occur within 1 s of a movement. Shading indicates SEM. Here, no bins showed significant difference from baseline, in contrast to our earlier analyses that showed significnat differences when we aligned neuronal activity as a function of spatial distance to the response (cf. Fig. 5B). This indicates that memory-trace cell activity likely does not reflect a time-locked anticipatory signal for the subjects' motor action, the button press. B) Memory-trace cell firing rate ($n = 43$) averaged in fixed time bins in the 3-s window from panel A (1.5-s pre- and 1.5-s post-response). Center line indicates median, box limits indicate interquartile range (IQR), whiskers indicate 1.5×IQR from first and third quartiles. Red dots denote outliers. Label "ns" indicates $p > 0.05$ ($t(42) = 1.39$, $p = 0.17$ two-sided paired t test), which supports the result from Panel A that showed no significant difference between mean firing rates when binning by time. C) Histogram of Pearson's correlation coefficients testing the relation between memory-trace-cell firing rate and trial number within each session. This distribution did not significantly differ from zero ($t(42) = 0.74$, $p = 0.46$, two-sided t test), indicating that memory-trace-cell activity did not trend systematically over the course of a session.

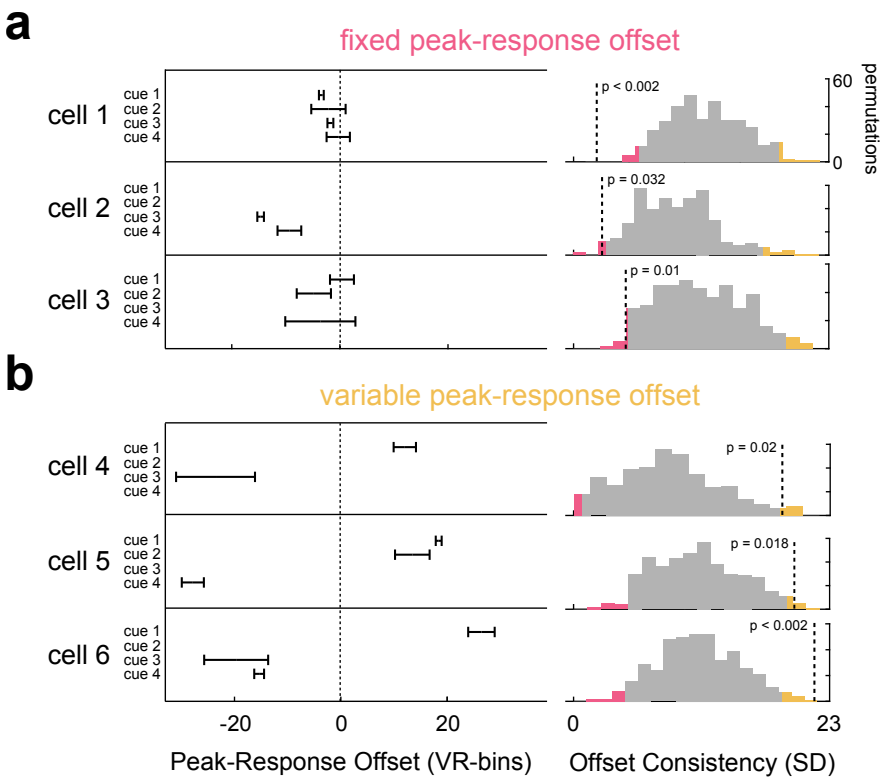

Figure S2.7: **Example memory-trace cells that activated at consistent (Panel A) and variable offsets (B) across cues.** A) Three example cells that activated at consistent offsets relative to cues. Left: The offsets between trace-field peaks and response location for different cues. Note that each cell had a trace-field for between one and four of the cues. Right: Analysis of offset consistency, parameterized by the standard deviation (SD) of peak-response offsets across cues. Histogram depicts distribution of SD measured from randomly shuffled data for each cell; black dotted line depicts true SD. Gray bins denote the center 95th percentile of permuted values. p value for each cell is labeled on the corresponding histogram relative to the shuffled data. This analysis was performed by identifying, for each cell, the peak-response offsets, or the distance between the trace-field peak and the response location, for all cues ($n = 48 trials$ for 28 full sessions, 24 for 3 truncated sessions). We then computed the standard deviation (SD) of these offsets for each cell. A cell that activated at consistent offsets would show a small SD and, inversely, a cell that activated at variable offsets would have a large SD. To determine if a cell's SD value was *significantly* low or high, we compared the cell's actual SD with the distribution of SD values from a permutation procedure that was separately performed for each cell. We generated 500 surrogate values for each cell in a manner that matched the original data by following these steps: 1) determined which cues (1–4) the cell exhibited a field for, 2) generated a surrogate cell which had fields for the same cues by randomly selecting trace-fields for those cues from other memory-trace cells, 3) computed the standard deviation across the surrogate cell's peak-response offsets, 4) and repeated 500 times. This permutation method enabled us to control for inherent properties of the task environment or cue position that might bias trace-field position and focus our analyses on cell-specific effects related to the variability of peak-response distances. B) Same as A but for three example memory-trace cells that showed significant offset variability.

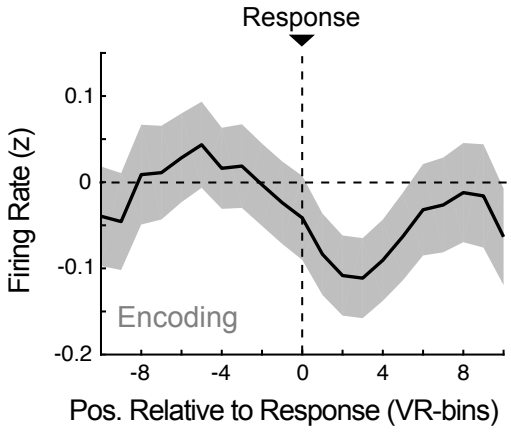

Figure S2.8: **Memory trace cell activity during encoding is not suppressed *prior* to the object location.** Mean firing rate (z-scored) of all memory-trace cells (black line, n = 322 trials) aligned to response location (as in Fig. 5B) for encoding trials. Shading indicates SEM. No bins show significant difference from baseline. This analysis enabled us to examine an alternate explanation for the encoding-retrieval difference we found in memory-trace cell firing rates. Namely, the possibility that memory-trace cells suppress firing rates during encoding trials when an object is visible on the track, similar to either "mismatch cells" in hippocampus or odor-selective suppressive cells in EC. Suppression is typically characterized by a decrease in firing prior to stimulus followed by a rebound. This plot shows that memory-trace cells did not show the pattern seen in mismatch cells.

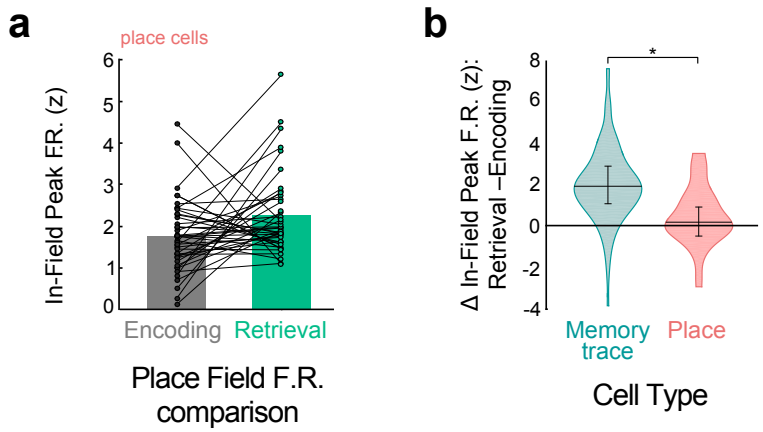

Figure S2.9: **Place cell firing during encoding trials.** A) Comparison of place cells' peak firing rate in field (z-scored) between encoding and retrieval trials, analogous to (Fig. 5E). Circles denote individual fields. Since place cells seemed to show a slight increase in peak in-field firing rate during retrieval trials, we asked how encoding-retrieval differences compared between place cells and memory-trace cells. We thus computed a two-way ANOVA measuring whether in-field firing rate varied as a function of trial type (retrieval vs. encoding), and/or cell type (place cell vs. memory-trace cell). For place cells, we used only the first 12 retrieval trials to match the number of trials used to assess trace fields. We found a significant interaction ($F_{(1,335)} = 24.04$, $p = 0.036$, permutation-adjusted), indicating that the increased firing rate we observed for memory trace cells during retrieval was significantly greater than for place cells. B) Change in in-field peak firing between encoding and retrieval trials for memory-trace and place cells (n's= 43, 45, respectively). Horizontal line indicates the medians of the violin plots, tips indicate minima/maxima, and error bars indicate interquartile range (IQR). We used a post-hoc test to directly compare the change between retrieval and encoding in-field firing for place cells and memory-trace cells, and found that place cells exhibited significantly more stable firing fields between retrieval and encoding than memory-trace cells. Asterisk indicates significance from two-sided Mann–Whitney U-test ($z = 5.25$, $p = 1.48 \times 10^{-7}$).

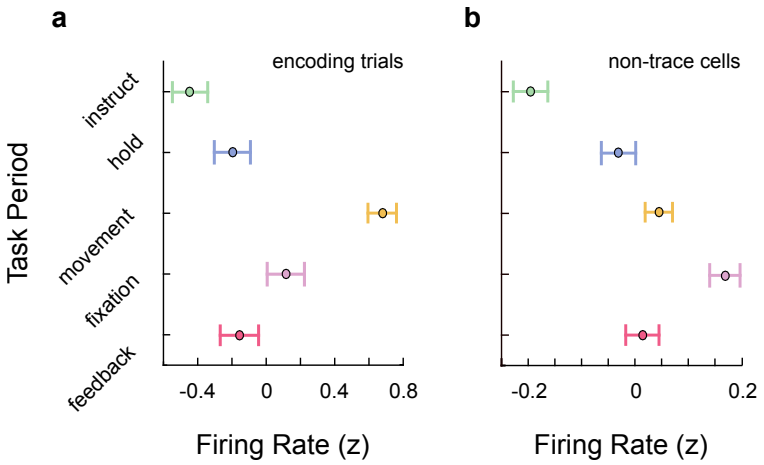

Figure S2.10: **Analysis of firing rate during encoding trials across task periods.** A) Mean firing rate for all memory-trace cells during encoding trials (z-scored) by task period (n = 332 trials). Error bars denote SEM. B) Mean firing rate for non-trace cells during retrieval trials by task period (n = 8472 trials). Error bars denote SEM.

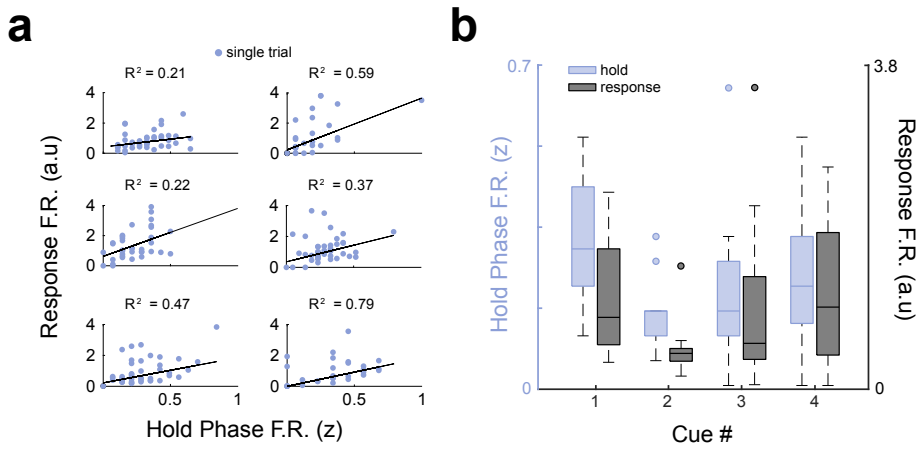

Figure S2.11: **Additional examples of memory-trace cell activity during hold and response periods during retrieval trials.** A) Scatter plots illustrate the relationship between normalized firing rates in the hold and response periods for six representative memory-trace cells across all trials. Line shows the fit from a robust linear regression (similar to Fig. 6B). Each plot depicts 48 retrieval trials, with the exception of the top- and bottom- plots on the right, which show truncated sessions of 24 trials. B) Mean normalized firing rate (solid lines) of a representative EC memory-trace cell during the hold and response periods, averaged across all trials for each cue object (similar to Fig. 6D). Circles indicate single-trial activity, error bars indicate SEM (n = 12 trials).

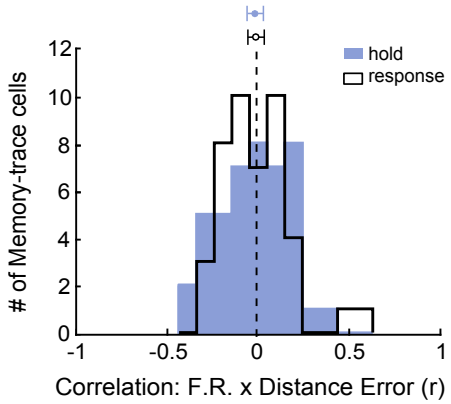

Figure S2.12: **Analysis of the Pearson's correlation between memory-trace firing rate and distance error during hold and response intervals.** Histograms of correlation coefficients between firing rate and distance error for both hold (blue) and response (white) periods (n = 43 cells). Black dotted line denotes correlation coefficient of zero. Circles indicate mean, error bars indicate SEM. Both distributions of correlation coefficients are not different from zero (t(42) = 0.73, 0.45, p's= 0.47, 0.66, two-sided t test), indicating that trial-by-trial memory-trace cell firing rates during both hold and response periods are unrelated to the distance error on that trial.

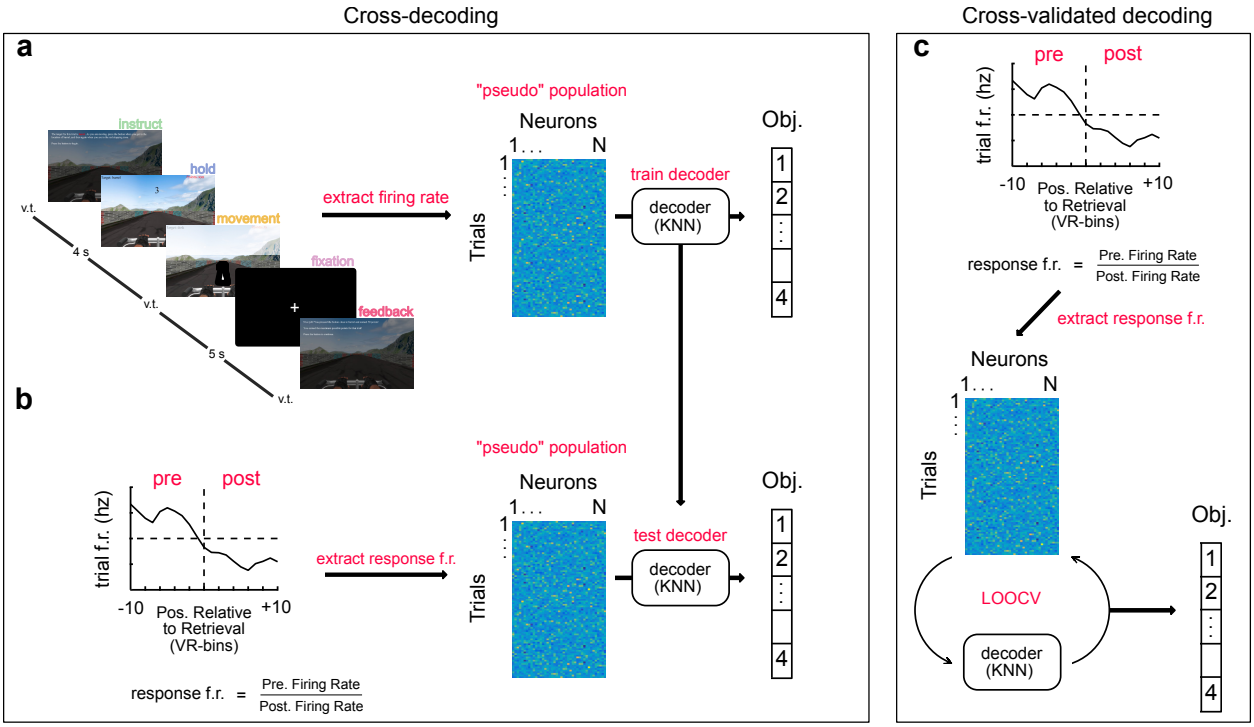

Figure S2.13: **Illustration of the multivariate decoding procedure.** A) Paradigm for cross-decoder training. Pseudopopulations of neural activity were constructed by extracting the activity of cells during the different periods of interest. Decoders were trained on this data using a k-nearest-neighbor (KNN) framework to predict the object cue for each trial. B) Paradigm for cross-decoder testing. Response period activity for each trial was computed by normalizing the pre-response firing rate by the post-response firing rate. This measure was extracted for each trial and used as the test set for the decoders trained on each task period. C) Paradigm for cross-validated decoding. We also trained and tested a decoder using just the response period activity. In order to ensure we had separate train–test data, we used leave-one-out cross-validation (LOOCV). The same feature extraction and decoding framework was applied across both task periods.

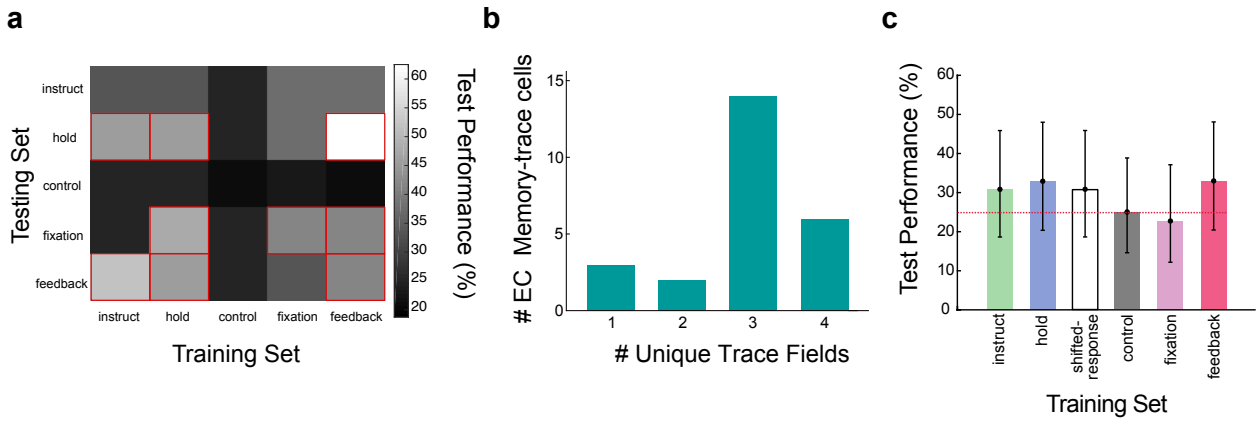

Figure S2.14: **EC memory-trace cell decoding.** A) Matrix of cross-validated decoding accuracy for all train–test combinations of task phases using firing rates from EC memory-trace cells. On-diagonal entries indicate within-condition decoding and off-diagonal entries indicate cross-decoding. Notably, all cross-decoding that tested on the control period performed below significance (chance level at 25%), indicating that the results in Fig. 7A were not an artifact of how we defined the response period. It is also worth noting that training on the feedback period firing rate and testing on the hold period led to the best decoding, overall. B) Distribution of the counts of unique trace fields exhibited by memory-trace cells in the EC only. Because EC memory-trace cells primarily had 3+ unique trace-fields, it indicated that our decoding results were driven by dissociable firing rates across different spatial fields rather than being explained by cells with only 1 trace field. C) Results of a control decoding analysis for EC memory-trace cells, using a "shifted" response period closer to non-cued objects (n = 27). Individual bars distinguish models that were trained on different task periods, with all models tested on activity during the response period using trial-level cross validation. Black circles denote percentage, and error bars indicate SEM. Red dotted line denotes chance (25%). We hypothesized that integrating alternate object locations into our decoding would lessen the distinction between different object–location trials and weaken the decoding results. To test this, we defined a "shifted" response period by computing the firing-rate ratio using a post-response location 6 VR-bins further down the track than the post-response bins used for the original response period —a location that should be closer to a different object location than the current cued object. No cross-decoding yielded significant decoding using the shifted response period, indicating that the spatial bins around the response location were the most informative in decoding the cued object held in memory.

Subject #	# Sessions	Age	Gender	Diagnosis	# Amygdala units	# Hippocampal units	# Entorhinal units	# Cingulate units	# memory-trace cells
R1008	1	55	F	R anterior temporal	0 of (6)	0 of (6)	0 of (0)	0 of (0)	0
R1027	1	48	M	Bi orbitofrontal, R temporal, R insula	1 of (15)	0 of (1)	0 of (0)	0 of (0)	1
R1030	4	23	M	L medial temporal	1 of (21)	0 of (1)	0 of (0)	0 of (0)	1
R1092	3	44	M	Bi medial temporal	0 of (0)	0 of (17)	0 of (0)	0 of (0)	0
R1139	2	19	M	R temporal	0 of (0)	0 of (0)	0 of (0)	2 of (10)	2
R1152	1	20	F	L mesial temporal	0 of (0)	0 of (2)	0 of (0)	5 of (14)	5
R1182	1	40	M	L insula	0 of (0)	0 of (0)	1 of (4)	1 of (3)	2
R1219	1	38	F	L hippocampal head	0 of (0)	0 of (6)	3 of (14)	0 of (0)	3
R1278	3	22	F	R parietal	0 of (0)	0 of (0)	18 of (65)	0 of (0)	18
U0048	1	40	M	L temporal	0 of (10)	1 of (2)	0 of (0)	0 of (0)	1
R1268	1	32	F	R middle temporal gyrus	0 of (0)	0 of (2)	0 of (0)	0 of (0)	0
R1241	1	52	M	Bi medial temporal	1 of (10)	0 of (0)	0 of (0)	0 of (0)	1
R1297	1	24	M	Heterotopia left temporal neocortex	0 of (0)	0 of (3)	0 of (0)	0 of (0)	0
R1299	1	43	M	L hippocampus	0 of (0)	1 of (12)	0 of (0)	0 of (0)	1
R1315	2	22	M	L anterior hippocampus	0 of (0)	0 of (12)	0 of (0)	0 of (0)	0
U0001	1	21	M	R anterior temporal	0 of (0)	1 of (19)	0 of (0)	0 of (0)	1
R1354	2	27	M	L hippocampus	0 of (0)	2 of (14)	0 of (0)	0 of (0)	2
R1362	3	47	M	L amygdala/hippocampus	0 of (0)	0 of (0)	4 of (26)	0 of (0)	4
R1414	1	31	F	R mesial temporal	0 of (0)	0 of (0)	1 of (4)	0 of (0)	1

Table 2.1: **Contribution of subjects and sessions to total cell counts:** Table indicates the total number of memory-trace cells and total cells for each patient, by brain region. The right-most column indicates the number of memory-trace cells observed on unique recording channels across sessions of the task. L: Left, R: Right, Bi: Bilateral.

Control Analysis	% Place Cells	% Memory-trace cells	χ^2 (df=1): Place	χ^2 (df=1): Memory-trace
Original	*15.1% (45/299)*	*14.4% (43/299)*	*NA*	*NA*
One session per patient	15.6% (31/199)	17.1% (34/199)	0.026	0.668
Omit SOZ	15.9% (32/201)	16.9% (34/201)	0.070	0. 593
30 spatial bins	13.0% (39/299)	15.4% (46/299)	0.499	0.119
50 spatial bins	10.4% (31/299)	17.4% (52/299)	2.954	1.014
GLM	11.0% (33/299)	20.4% (61/299)	2.123	**3.771**

Table 2.2: **Statistical outcomes from control analyses:** Each row of the table indicates the outcome of a different control analysis. SOZ = Seizure onset zone. All χ^2 test values indicate comparisons between original percentages and control percentages. Bold text denotes significance. *Row 1:* The results of the original analysis. *Row 2:* Results of analysis controlling for the dependence of multiple sessions per subject. Several patients contributed multiple sessions of the task, with each session analyzed independently. However, in order to ensure that patients contributing multiple sessions to this study were not confounding our results (Supp. Table 1), we ran control analyses utilizing only the first session recorded from each patient. This controlled for any confounding effect of multiple sessions. *Row 3:* Results of analysis controlling for electrodes in epileptic regions. The subject cohort examined in this study has drug-resistent epilepsy. Prior research has supported past work in epileptic cohorts through use of scalp EEG or fMRI. Still, it is important to consider whether electrophysiology research in the epileptic brain is reflective of healthy brain. 31% of the single-units we analyzed were recorded on microwires localized to clinically determined ictal onset zones. To more rigorously control for any confounding effect of epileptic activity, we re-ran all analyses excluding all neurons recorded from these clinically defined ictal onset zones. Our main findings remained unchanged with respect to the proportion of place cells and memory-trace cells. *Rows 4-5:* Results of analysis controlling for spatial binning of firing rate. In order to assess the spatial binning on our results, we calculated the results of our main analyses using 30 and 50 equal sized spatial bins, rather than 40 bins as in our main analyses. The number of place cells and memory-trace cells identified by the ANOVA did not vary significantly as a function of the number of bins. *Row 6:* Results of analysis controlling for ANOVA screening. For our ANOVA analyses, we used a non-parametric permutation method to generate a large number of permutations where observations are permuted within each block. This meant we did not assess significance using a parametric F-test (which is the aspect of the ANOVA generally sensitive to non-normality in the residuals)—rather, we determined our critical statistic against empirically derived null distributions from our permutation testing. Still, to ensure the validity of our statistical categorization of cell responses, we re-did our analysis using a generalized linear model utilizing a Poisson distribution. Setting a rigorous threshold of $p < 0.001$, we found that 61 cells showed a significant interaction (Memory-trace), and 33 showed a main effect of location (Place). Therefore, it is unlikely that our primary finding emerged from the specific analysis used to characterize cell responses, and in fact found more memory-trace cells using this modified approach ($p = 0.0521$).

Chapter 3: Phase precession in the human hippocampus and entorhinal cortex

Salman E. Qasim, Itzhak Fried, & Joshua Jacobs
bioRxiv, 2020. doi: https://doi.org/10.1101/2020.09.06.285320.

Knowing where we are, where we have been, and where we are going is critical to many behaviors, including navigation and memory. One potential neuronal mechanism underlying this ability is phase precession, in which spatially tuned neurons represent sequences of positions by activating at progressively earlier phases of local network theta oscillations. Phase precession may be a general neural pattern for representing sequential events for learning and memory. However, phase precession has never been observed in humans. By recording human single-neuron activity during spatial navigation, we show that spatially tuned neurons in the human hippocampus and entorhinal cortex exhibit phase precession. Furthermore, beyond the neural representation of locations, we show evidence for phase precession related to specific goal-states. Our findings thus extend theta phase precession to humans and suggest that this phenomenon has a broad functional role for the neural representation of both spatial and non-spatial information.

3.1 Introduction

Our brain's ability to link related experiences is critical to everyday life, and to our memory for past experiences. One crucial example is spatial navigation, which requires awareness of individual locations and the association between multiple locations, such as those on the same path. Similarly, episodic memory requires the encoding of individual events and the association between sequential events. The hippocampal formation is important for both spatial cognition and episodic memory [75, 23, 30, 129]. Therefore, neural activity in this region might play a key role in linking sequential

locations and events.

Specifically, theories of how the brain represents sequential experiences rely on the idea that the timing of neuronal spiking is critical for learning associations [130, 131, 132, 133, 134, 135]. Spike timing, in turn, is thought to be coordinated across networks by fluctuations in the large-scale network activity that can be estimated via the local field potential (LFP) [136, 137, 138, 139, 140, 11]. This suggests that a coordinated relationship between network oscillations and single-neuron spiking may play a mechanistic role in complex behaviors or aspects of cognition, such as memory [141, 73], that require the association of sequential events. A prominent potential mechanism for the binding and compressing of sequential events is hippocampal phase precession, extensively observed in rodents, during which active neurons rhythmically spike in coordination with the local theta frequency (5–10 Hz) oscillation. Phase precession is readily observable in many hippocampal place cells [28] and entorhinal grid cells [24, 142]. Because these neurons spike slightly faster than the theta oscillation as the rodent runs through specific locations, phase precession results in sequences of locations being encoded at different phases of theta oscillations. As such, phase precession may compress spatial trajectories on the scale of behavior into the brief timescale of the theta cycle that is conducive to synaptic plasticity [143, 144, 29].

There is evidence that phase precession's utility for binding and compressing sequential events may be used by the brain to represent non-spatial features of experience as well. While phase precession is often described in hippocampal place cells or entorhinal grid cells, it has also been observed in a diverse range of brain areas such as ventral striatum [145], subiculum [146], basal forebrain [147], and medial prefrontal cortex [148]. Critically, a slew of recent work has directly observed phase precession independent of location within a place or grid field, encoding elapsed time during REM sleep [149], wheel-running [57], jumping [150], fixation [151], presentation of task-relevant stimuli [128, 152, 153], and task epoch [147]. The widespread prevalence of phase precession suggests that this phenomenon has a more general role beyond representing the current spatial location, and that it could be relevant for building neural representations in many regions to support diverse aspects of cognition, learning, and memory.

Despite its prevalence in rodents, and the many theories suggesting a fundamental role for phase precession in neural coding [28, 154, 155, 156], phase precession has not been observed in humans. To examine this issue, we analyzed simultaneous single-neuron and LFP activity from neurosurgical patients as they performed a virtual spatial memory task and examined the patterns of spike–LFP interaction. Here, we describe spatial phase precession in humans analogous to that observed in navigating rodents. We also describe evidence for phase precession related to the coding of non-spatial variables, in which neurons transiently spike faster than the theta oscillation during trajectories to specific goals. Overall, our findings extend precession to humans and demonstrate its potential use for encoding both spatial and non-spatial features of experience.

3.2 Methods

3.2.1 Data recording and participants.

The thirteen participants in our study were epilepsy patients who had Behnke–Fried microelectrodes [88] (Ad-Tech Medical) surgically implanted in the course of clinical seizure mapping at the University of California, Los Angeles. The Medical Institutional Review Board at the University of California-Los Angeles approved this study (IRB 10–000973), and patients provided informed consent to participate in research. Microwire signals were recorded at 28–32 kHz, and we used Combinato for spike detection and sorting [89]. Manual sorting identified single- versus multi-unit activity versus noise on the basis of previously determined criteria [90, 91]. The local field potential for each neuron was recorded from the local microelectrodes and was downsampled to 250 Hz for spectral analysis. For comparison with rodent data we used a publicly available dataset (CRCNS hc-2, hc-3) [157, 158, 159].

3.2.2 Task.

This behavioral task is described in several previous studies [160, 72, 161]. Subjects first learned the navigational controls during a 4-delivery training session in a large, wide-open arena. After the practice session, subjects performed the main task, in which they were instructed to

drive passengers to one of 6 goal stores in the virtual environment. Upon arrival, on-screen text displayed the name of the next randomly selected destination store. The task was self-paced in order to accommodate patient testing needs and therefore subjects performed at ceiling. The size of the virtual environment was 10×10 VR units, the width of the road was 2.5 VR units, and the obstructed area in the center of the road was 5×5 VR units. During navigation, subjects had a 60° field of view, a maximum forward speed of 1.25 VR units/s, a maximum backward speed was 0.5 VR units/s, and maximum angular velocity of 40°/s. To encourage subjects to take the shortest route to each destination, subjects received 50 points for each successful delivery and had one point deducted for each second that they spent navigating. Points were constantly displayed on-screen. Patients performed an average of 73 ± 11 deliveries in each session. To assess performance on this task, we measured subjects' excess path length (EPL) on each trajectory, defined as ratio of the actual path length to the ideal path length. We computed ideal path length on each trial using the A-star search algorithm to identify the most computationally efficient path between goals in the environment [162].

3.2.3 Statistical analysis and software.

All statistical analyses were carried out in Python, primarily using the SciPy [163] and statsmodels [164] libraries. For comparisons between two groups, we primarily utilized the Wilcoxon rank-sum test unless otherwise specified. For omnibus testing, we used ANOVAs, determining the p-value by comparing the real test-statistic to those from empirically derived null distributions generated by shuffling the true data. All figures were made using the Matplotlib [165] and Seaborn libraries.

3.2.4 Characterizing place-cell activity.

To assess how neuronal activity related to the subject's virtual spatial location, first, we binned the environment into a 10×10 spatial grid. We computed the firing rate map for each neuron by dividing the number of spikes by the amount of time spent in each spatial bin. We then used an

ANOVA to assess whether the interaction of X and Y spatial bin (and thus 2D position) significantly modulated firing rate. To assess the significance of the ANOVA we circularly shuffled the firing rate and generated 500 surrogate test-statistics, and used this null distribution to determine the shuffle-corrected p-value of the ANOVA using the real data. These p-values were then FDR-corrected for multiple comparisons between the three movement types (CW, CCW, bi-directional).

Only neurons with critical statistics exceeding 99% of the shuffled data ($p < 0.01$) were considered to be spatially modulated. We considered spatially-modulated neurons to be analogous to place- and grid- cells, because the firing rate in at least one spatial bin deviated significantly from the others. We identified the spatial bin with the highest firing rate (analogous to the center of a place- or grid- field). We only included a spatial bin if the person passed through it at least 3 times, and occuped it for at least 4 seconds.

3.2.5 Spectral analysis of LFP and spike time.

To assess the prevalence and frequency of theta oscillations in the human and rodent LFP, we computed the continuous Morlet wavelet transform (wave number 6) at 20 logarithmically spaced frequencies between 1 and 32 Hz. Then, to identify theta-like oscillations, we utilized an iterative algorithm to subtract the aperiodic background and fit a Gaussian to putative peaks [166]. For this fitting procedure, we restricted the maximum number of peaks to 2, and the maximum peak width to 4 Hz. We only assessed the peak height (parameterized as the height of the Gaussian's peak relative to the aperiodic background) and the peak frequency (parameterized as the center frequency at which the Gaussian reaches its peak) for the largest peak in the PSD. To assess the prevalence and frequency of theta oscillations in human and rodent spiking, we computed the autocorrelation of spike times, and performed a fast Fourier transform (FFT), yielding the PSD of the spike train.

3.2.6 Phase estimation.

We estimated the instantaneous phase of LFPs in the theta frequency range. Theta oscillations in human hippocampal formation are often bursty and non-stationary, and vary from low (2–5 Hz) to high (5–10 Hz) frequencies [167, 168, 169]—similar patterns are observed in bats [170] and non-human primates [171, 172]. In order to analyze fluctuations in the LFP analogous to rodent theta, we estimated 2–10 Hz phase by identifying peaks, troughs, and midpoints in the lowpass-filtered LFP, and linearly interpolated between these points. This phase-interpolation method has been used previously to effectively estimate theta phase in bats [173], as well as in rodents [174], [175]. To ensure that phase estimates were not based on an unreliable low amplitude signal, we computed the instantaneous power of the LFP and discarded those time-points in which the power fell below a 25th percentile threshold [173].

3.2.7 Spatial phase precession.

To identify phase precession in this dataset, for each spatially modulated cell we first identified every trajectory through the cell's peak firing location. Following the methods used in some recent studies for measuring phase precession [176, 47, 173], first for each such trajectory, we identified the spike closest to the center of the bin as the center spike (our reference point for the center of the bin on each trajectory) [176, 47, 173]. We limited our analysis to spikes in close spatial proximity to the center of the peak firing bin. To do so, we only analyzed the 11 closest spikes to the center of the peak firing bin. To ensure that these 11 spikes did not occur too distant from the peak firing bin, we set a diameter threshold of 40% of the environmental width, meaning that we did not analyze spikes that occurred further than 2 VR-units from the center of the peak firing bin. We re-ran our analyses while varying the inclusion criterion for the number of spikes (9, 11, & 13) and the radius (40% & 60%) and found that the parameters we selected did not significantly affect the proportion of cells exhibiting spatial phase precession ($\chi^2 = 5.25$, $p = 0.5$, chi-squared test).

We next tested for phase precession using circular statistics. Specifically, for each cell we measured the relation between spike phase and the subject's position by computing the circular–

linear correlation coefficient [177]. To assess statistical significance, we used a shuffling procedure. For each cell we computed a surrogate distribution for this correlation coefficient by assigning random phases to each spike from the distribution of all the spike phases for that neuron, and re-computing the correlation 500 times. This null distribution effectively scrambled the relationship between spike position and spike phase and controlled for any effect of spurious phase estimates. A circular-linear correlation was considered significant only if it exceeded the 95^{th} percentile of this surrogate distribution.

3.2.8 Control analyses for spatial phase precession.

We performed two control analyses for alternative explanations for the spatial phase precession we observed. The first analysis tested whether the peak firing bin, our analogue to the place-field center, was important to observing precession. To do so, we selected control locations for each cell and assessed the strength and prevalence in these control bins. Control bins were chosen as to not overlap with the peak firing bin (at least 30 % of the map width away) and also had to be traversed a minimum of 3 times with a minimum firing rate of 0.5 Hz. Furthermore, because we only analyzed the 11 spikes in the immediate vicinity of the peak firing bin, control bins matched the peak firing bin in sample size of spikes per trajectory, ensuring that effects were not confounded by firing rate differences.

Another possible alternative explanation for our findings is that the phase precession we observed here is actually encoding time to peak firing, independent of spatial position, with particular spike phases occurring at specific time-intervals within any epoch of elevated firing rate [178, 179]. To control for this possibility, we identified epochs of elevated firing rate in the time domain without any information about position, which we refer to as “firing rate motifs" [178, 179]. We identified the spike that occurred closest in time to the peak firing of each motif field, and used the 11 spikes in the immediate temporal vicinity (within 2 seconds before or after) to compute a circular-linear correlation between spike phase and spike time relative to the motif field peak, matching our spatial phase precession analysis.

3.2.9 Non-spatial phase precession

To measure non-spatial phase precession without reference to place fields, we compared the spiking frequency of each neuron to the frequency of the local LFP, with relatively faster rhythmic spiking classified as phase precession [180, 157]. However, detecting oscillations in spike times alone is difficult in humans (Supplementary Fig. S3.1B) and bats [173], potentially due to the transient, non-stationary nature of theta observed in these species [167, 173]. Instead, we applied a method introduced by Mizuseki et al. [157] which measures spiking frequency relative to the ongoing LFP. This is a particularly useful method when the ongoing LFP is non-stationary but may still be an important reference “clock" for neuronal spiking. To perform this procedure, we computed the autocorrelation histogram of each neuron based on the timescale determined by the phase of the reference LFP, rather than the conventional method of using absolute time. We computed this autocorrelation using 60-bins with window-length of 4 cycles [173]. We then computed the Fourier transform of the autocorrelation histogram to yield the power spectral density (PSD) of the frequency of spiking relative to the LFP. Here, a peak relative frequency greater than 1.0 indicates that the cell is oscillating at a faster frequency than the reference LFP. We excluded neurons that exhibited both a peak near 1.0 as and significant phase-locking ($p < 0.05$, Rayleigh test) to ensure that we did not mistakenly identify phase-locked neurons [160] as exhibiting phase precession. To measure the strength of this effect we measured the amplitude of the PSD, normalized by the total amplitude across all other relative frequencies [146], which we refer to as the “modulation index" (MI) (Fig. 3.4A).

In order to ensure that our results did not arise from poor phase estimates due to low LFP amplitude, we discarded spikes that occurred during the lowest 25^{th} percentile of LFP power in the oscillation of interest [146, 173]. In order to ensure that low spike counts did not confound our estimates we only analyzed cells with more than 100 valid spike-phase estimates for the autocorrelogram. We compared the modulation index to the null distribution of modulation indices for the peak frequency generated by circularly-shuffling the phases within each cycle of theta. This rigorous, within-cell shuffling ensured that cross-cycle dynamics (such as precession) were disrupted

while maintaining slower and more rapid spiking dynamics [146, 173]. The modulation index was considered significant if it exceeded the 95th percentile of this surrogate distribution. Finally, we excluded cells that exhibited significant phase-locking during the entire session (Rayleigh test) in order to ensure that peaks close to 1.0 did not result from phase-locked spiking.

3.2.10 Goal-state phase precession

To measure goal-state phase precession, we separately applied our analysis of non-spatial precession to spiking during each of the six goal trials. We only included neurons for which we observed at least 100 spikes per goal, to allow us to analyze non-spatial precession for each goal. We established two tests to characterize significant goal-state phase precession. First, just as we did with session-wide non-spatial precession, the magnitude of detected phase precession (as indicated by a peak in the spike-phase spectra exceeding 1.0) had to be greater than the 95th percentile of the shuffled distribution. Because we conducted this test for all six goals separately, we used the False Discovery Rate procedure [181] to correct the resulting p-values for multiple corrections across goals. If a goal exhibited significant non-spatial precession, we then compared the goal-specific modulation index to a surrogate distribution of modulation indices generated by selecting 500 random spike-trains from across the entire session. Each null spike-train was generated to match the number of spikes recorded during the significant goal to ensure that firing rate differences did not account for our results. A significant p-value indicated goal-state precession that was significantly stronger for the goal in question than for the session as a whole.

3.3 Results

3.3.1 Spatial phase precession in hippocampus and entorhinal cortex during navigation.

We analyzed recordings of neuronal spiking from 1,074 neurons in the hippocampus, entorhinal cortex, parahippocampal gyrus, anterior cingulate cortex, and amygdala of 13 neurosurgical patients undergoing clinical treatment for drug-resistant epilepsy. During recordings, subjects performed a goal-directed navigation task in a 2D virtual environment on a laptop computer [72] (see

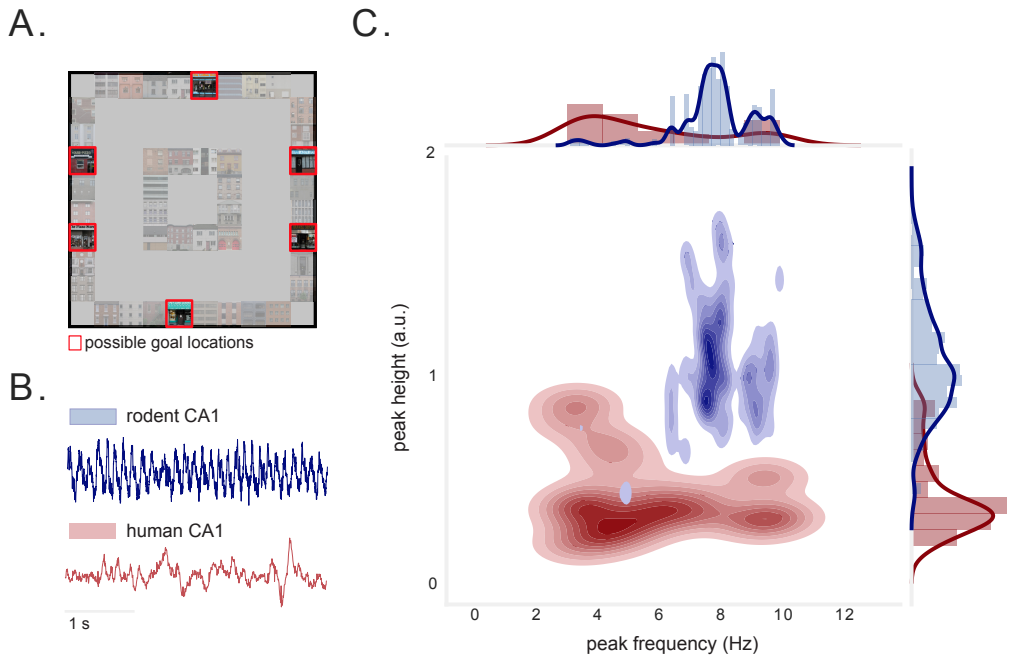

Figure 3.1: **Virtual environment and hippocampal theta oscillations during task.** A) Overhead view of task environment. Red squares denote locations of possible goal locations. B) Examples of raw LFP data from rodent (publicly available dataset [159]) and human hippocampus. C) Joint distribution of peak frequency and peak height of LFP power spectral density (PSD) from rodent (blue) and human (red) hippocampus. Rodent hippocampal recordings exhibit highly stereotyped peaks. Human hippocampal recordings exhibit significantly smaller peak heights, and peaks are at significantly lower frequencies (p's$< 2 \times 10^{-34}$, Wilcoxon rank-sum tests).

Methods). The virtual environment contained six goal stores surrounding the perimeter of a square track, with the center of the environment obstructed by buildings. Subjects were able to travel around the track in either clockwise or counterclockwise directions (Fig. 3.1A).

Given our interest in phase coding, we first characterized the prevalence of theta oscillations in the human hippocampus and compared their properties to those seen in rodents, leveraging a publicly-available dataset [157]. Compared to rodents, human hippocampal theta spanned a significantly broader range of frequencies ($p < 4 \times 10^{-4}$, Levene test), with significantly smaller, lower-frequency peaks in the power spectrum (p's$< 3 \times 10^{-8}$, Wilcoxon rank-sum tests; Figs. 3.1B-C, SS3.1A). Because human theta appears to span both low and high frequencies [169], we assessed phase precession with respect to oscillations at a broad range of LFP theta frequencies (2–10 Hz) (Fig. 3.1C). To assess phase precession we first identified each neuron whose firing was modulated

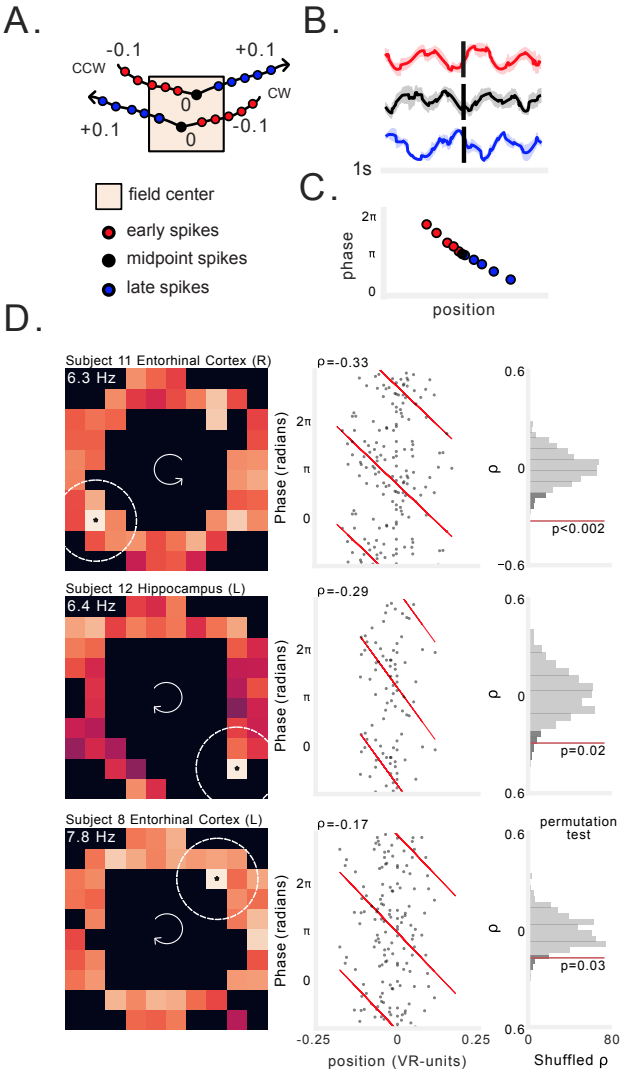

Figure 3.2: **Examples of spatial phase precession in human hippocampus and entorhinal cortex.** A) Schematic illustrating our method for selecting spikes near peak firing bin (*see Methods*). For each spatially modulated neuron we analyzed phase precession using spikes that occurred early (red), at the midpoint (black), and late (blue) in trajectories through the center of the firing field. B) Spike-triggered average (STA) LFP (reconstructed from phase) for early, midpoint, and late trajectory spikes from one neuron. C) Schematic of spike phase as a function of distance from center spike during a trajectory through the field, showing phase precession as a negative progression of phase-by-position. D) Three examples of spatial phase precession. Each row shows an individual neuron. Left: firing rate heat map. Text label indicates average firing rate in peak firing bin, which is noted with an asterisk. Brighter colors denote higher firing rates. Dotted lines indicate maximum radius around field in which spiking was assessed. Arrows in the center of the heatmap indicate the movement direction. Middle: spike phase as a function of location relative to the field center. Spike phases are duplicated vertically to enable visualization of circular-linear regression (red). Rho indicates circular-linear regression coefficient. Right: statistical assessment of circular-linear regression rho using surrogate distribution of circular-linear regression rho values generated by permutation of spike phases. Red line indicates value of real data. Dark gray shading indicates 95^{th} percentile of surrogate distribution.

by the subject's position in the virtual environment. We labelled the clockwise (CW) and counter-clockwise (CCW) movement periods and then used a shuffle-corrected ANOVA to identify 292 spatially modulated neurons that fired significantly more when subjects moved through particular locations during one or both of these movement conditions [182], after correcting for multiple comparisons (see *Methods*). Because phase precession in rodents is most predominant near the place-field center [183] and on short trajectories [184], we tested for phase precession during short trajectories through the field center, defined as the peak firing location for each neuron (Fig. 3.2A).

We observed that some of the spatially tuned neurons showed spiking at progressively earlier phases of the theta oscillation during individual trajectories through their firing field (Supplementary Fig. S3.2). To assess if this was a consistent pattern across trajectories, we leveraged the fact that during phase precession, spikes at later positions in the trajectory should occur at earlier phases, manifesting as a negative correlation between spike-phase and position [28]. In this way, spiking at different phases of the LFP would correspond to different relative positions along the path to a neuron's firing field center (Fig. 3.2B,C). We tested for this pattern by measuring the correlation [177] between spike-phase and position using circular statistics [185] and a shuffle-based permutation procedure (see *Methods*).

By performing this procedure across all of the spatially-tuned neurons we identified, we report the first evidence of phase precession in humans. Figure 3.2D shows three examples of single neurons recorded in the hippocampus and entorhinal cortex that exhibited significant phase precession during navigation at particular spatial locations (see Supplementary Fig. S3.3 for additional examples). Each of these neurons increased their firing in a specific region of the environment (Fig. 3.2D, left). As a person approached the center of that region, the neuron initially spiked at late phases of the 2–10 Hz LFP, but as they continued their trajectory through the center and past it, spikes occurred at progressively earlier phases (Fig. 3.2D, middle). This change in spike phases between early positions and late positions is characterized by significant negative phase–position correlations (Fig. 3.2D, right).

After testing the spatially-tuned neurons in our dataset for phase precession with our permuta-

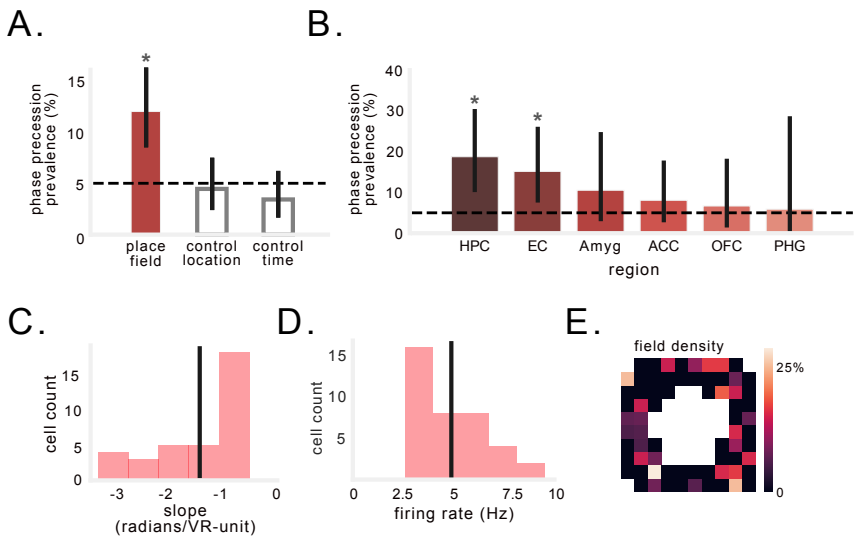

Figure 3.3: **Prevalence and characteristics of spatial phase precession in humans.** A) Percentage of spatially modulated neurons that exhibit phase precession during trajectories through the firing field (filled bar). Grey bars show control analyses of precession relative to alternative locations, or as a function of time, not position, during spiking episodes (see Supplementary Fig. S3.4). Black dotted line denotes chance. Solid black line indicates 95% binomial confidence interval. Asterisk indicates significant proportion of spatially modulated cells exhibiting phase precession during trajectories through the firing field ($p < 3 \times 10^{-6}$, binomial test). B) Percentage of spatially modulated cells across regions. Asterisk indicates significant proportion of cells exhibit phase precession (ps< 0.002, binomial test). C) Distribution of circular-linear regression slopes identified for neurons exhibiting significant phase precession. Black line indicates mean. D) Distribution of average firing rate of peak firing bins in which phase precession was observed. E) Prevalence of phase precession across the environment. Colors indicate percentage of firing fields in each bin that exhibited precession.

tion procedure, we found that precession was widespread, with 12% (35/292) of neurons exhibiting this phenomenon, which is well above what would be observed by chance ($p < 3 \times 10^{-6}$, binomial test; Fig. 3.3A). Of these 35 neurons, 22 neurons exhibited uni-directional spatial tuning and precession and 10 neurons exhibited bi-directional spatial tuning and precession. The remaining 3 neurons exhibited uni-directional precession in one location and bi-directional precession in another. Notably, we specifically observed significant proportions of spatially modulated cells exhibiting spatial phase precession in the hippocampus and entorhinal cortex (p's< 0.002, binomial test; Fig. 3.3B). Phase precessing neurons exhibited an average circular–linear correlation coefficient of -0.26 ± 0.09, an average slope of -1.36 ± 0.8 radians/VR-units (Fig. 3.3C), and an

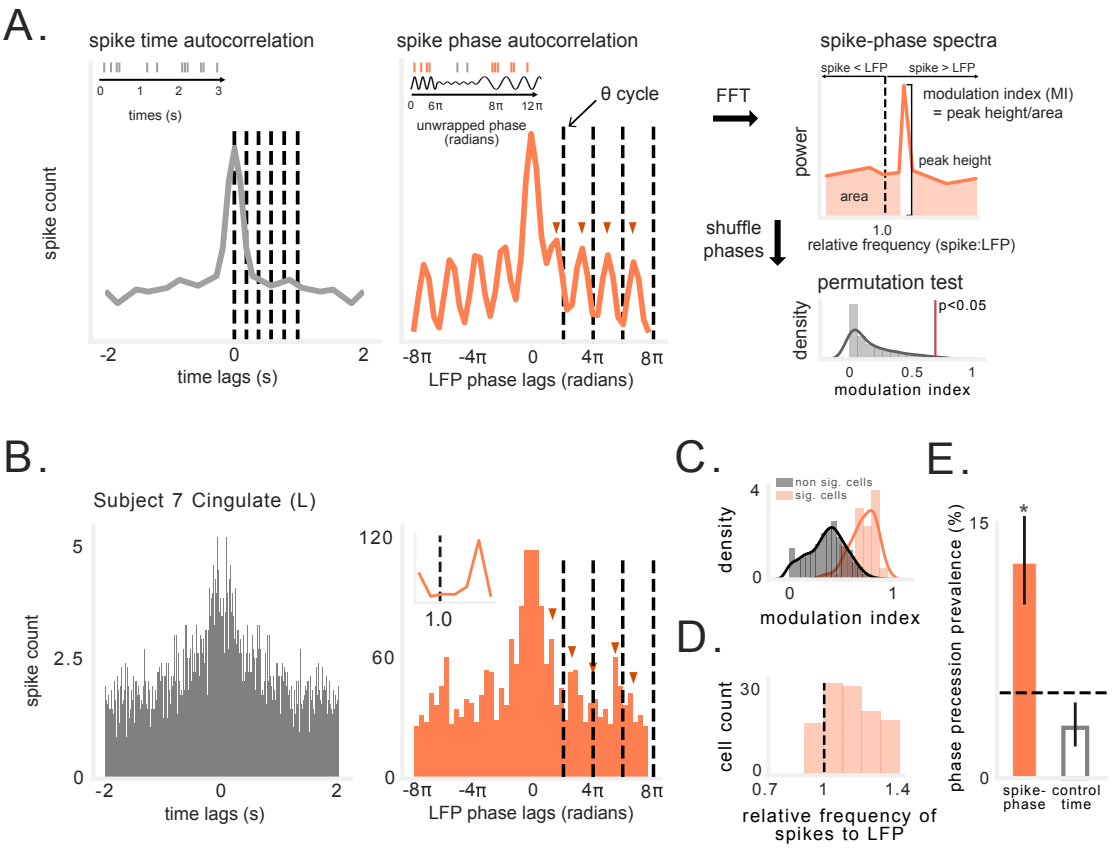

Figure 3.4: **Spike-phase spectra reveals precession-like pattern in non-spatially tuned neurons.** A) Schematic illustrating analysis of rhythmic spiking frequency relative to LFP oscillation (*see Methods*). Left: Autocorrelation of spike times (gray), with dotted lines at 200 ms intervals. Middle: Autocorrelation of unwrapped spike phases. Dotted lines indicate one cycle of ongoing LFP in 2–10 Hz band. Red arrows indicate peaks in autocorrelation, which occur progressively earlier than cycles of ongoing LFP. Fast Right: Fourier transform (FFT) of autocorrelation function yields power spectral density(PSD) showing cell spiking frequency relative to ongoing LFP frequency. The modulation index (MI) is visualized here as the ratio of the spectral peak height to power at all other relative frequencies. This value is compared to a null distribution of MI values generated by shuffling spike phases in each cycle. B) Left: Spike time autocorrelation showing little evidence of theta modulation. Right: Spike phase autocorrelation (orange) showing cell oscillating slightly faster than ongoing LFP (cycles of 2–10 Hz LFP indicated by dotted line). Inset shows spike-phase spectra. C) Modulation index (MI) of spike-phase spectral peaks for significant vs. non-significant neurons. D) Distribution of relative frequencies for neurons exhibiting significant MI. Values to the right of the black line indicate that the rhythmic spiking frequency slightly exceeded the LFP frequency. E) Percentage of non-spatial cells that exhibit precession-like spiking relative to LFP phase, compared to cell's exhibiting precession relative to time in a spiking episode. Black dotted line denotes chance level. Solid black line indicates 95% binomial confidence interval. Asterisk indicates significant proportion of cells ($p < 7 \times 10^{-18}$, binomial test).

average in-field firing rate of 4.9 ± 1.7 Hz (Fig. 3.3D). Phase precessing neurons had spatial firing fields throughout the environment (Fig. 3.3E). To test whether spatial phase precession was consistent across an entire behavioral session, we separately computed the circular–linear correlation coefficient for the first and second halves of the session and found no difference between halves ($p = 0.4$, paired t-test), with significantly negative correlation coefficients in each half (ps< 0.002, one-sample t-test). We found evidence for spatial phase precession in 11/12 of the subjects with spatially modulated neurons. These results thus demonstrate the existence of phase precession as a neural code for spatial position in humans during virtual navigation. The theta-frequency (2–10 Hz) and regions involved (hippocampus, entorhinal cortex) suggest that the phase precession we observed is largely analogous to that documented in rodent place and grid cells.

To be sure that our findings of precession indicated a spatial phase code relative to space, we tested two alternative explanations for our results: that precession was equally prevalent at randomly selected spatial locations (in which the neuron was sufficiently active), or that precession was actually measuring the advance of spike phase according to elapsed time (see *Methods*; Supplementary Fig. S3.4A, C). Neither alternative model identified significant proportions of phase-precessing cells, and these models resulted in the identification of a smaller number of cells as compared to our primary analyses ($\chi^2 = 20.6$, $p < 4 \times 10^{-5}$, chi-squared test; Fig. 3.3A; see also Supplementary Fig. S3.4B, D). These results indicate that human phase precession occurs more strongly at locations that show the highest firing rates, and that phase precession in spatially tuned neurons is more closely tied to location than elapsed time during movement.

3.3.2 Evidence for phase precession without spatial coding.

While phase precession has been observed most readily relative to specific spatial locations, there is also evidence for precession with respect to non-spatial behaviors and stimuli [128, 149, 57, 150, 147], and in regions outside the hippocampal formation [148, 145]. These findings suggest that phase precession could be a more general phenomenon that the brain uses to represent diverse types of consecutive, relevant stimuli/states using different phases of an oscillation. To ex-

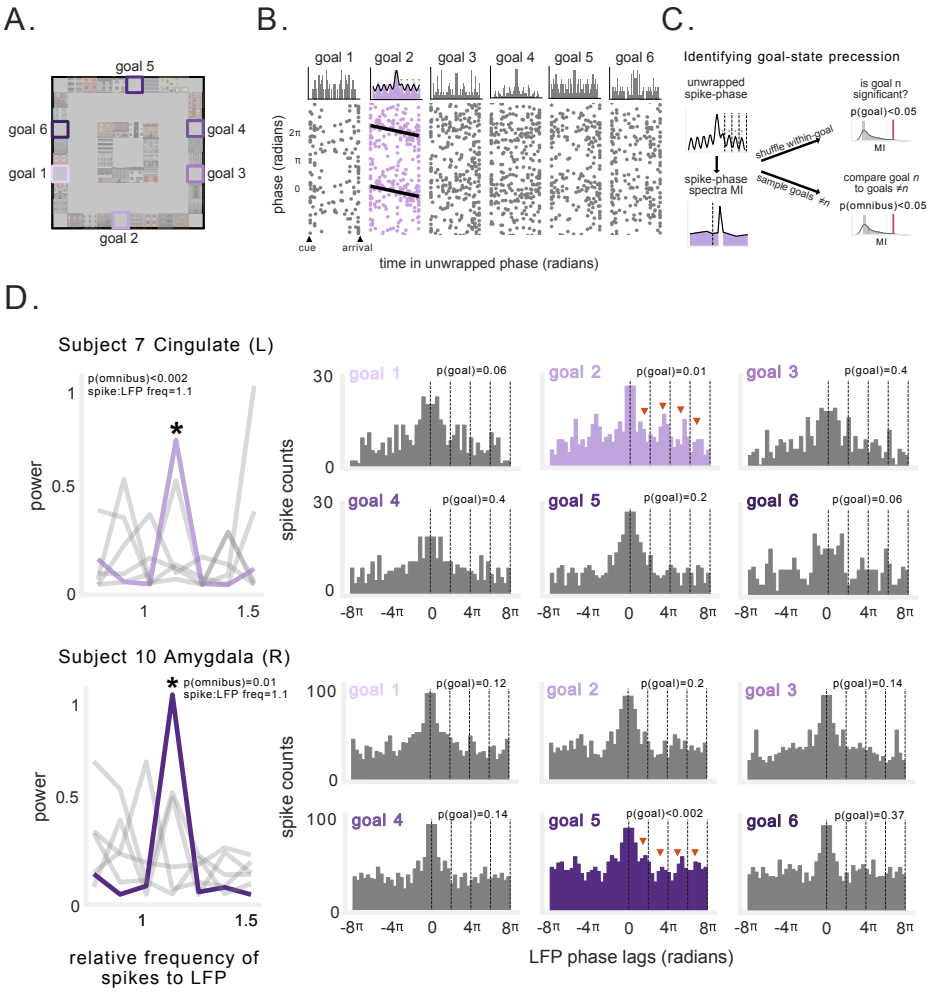

Figure 3.5: **Goal-state phase precession.** A) Schematic of task environment. Labels indicate goal locations. B) Spike-phases during navigation to different goals for example neuron. Top: unwrapped spike-phase autocorrelograms for each goal. Black line indicates fit of decaying-oscillation function. Spiking frequency transiently exceeded LFP frequency only during navigation to goal 2. Bottom: Spike-phase as a function of duration within each goal epoch. Black line indicates circular-linear regression fit. C) Schematic of method for assessing goal-state phase precession. If a neuron exhibited a significant spike-phase spectral peak at relative frequency exceeding 1 (following multiple comparisons correction), and this effect was significantly stronger than that observed during trajectories to other goals, then this neuron was classified as exhibiting goal-state precession (*see Methods*). D) Example neurons exhibiting phase precession during navigation to specific goals. Left: Spike-phase spectra depicting frequency of neuronal spiking relative to ongoing LFP. Asterisk denotes spectral peaks that were significant and significantly different from other spike-phase spectra for other goals. Gray lines denote non-significant goals. Right: Spike-phase autocorelograms during navigation to each goal (significant goal epochs depicted in color). Text indicates the p-value for significance tests described in C).

amine this possibility, we used a broader analytical method to test whether the non-spatially tuned neurons exhibited phase precession without reference to position. To do this, we measured each neuron's rhythmic frequency of spiking in comparison to the local theta oscillation [180, 186]. Identifying a consistent pattern of faster-than-LFP rhythmic spiking would indicate the presence of a precession-like pattern of LFP-coordinated spiking that could bind and compress sequential, non-spatial features of the task — just as spatial phase precession is theorized to do for locations [187, 29].

We identified neurons that showed rhythmic spiking at a frequency faster than the theta oscillation by using a method that has identified this pattern in animals with very stereotyped, 8 Hz theta such as rats [157, 188, 146] and mice [189, 190], as well as animals with human-like theta that appears at a range of frequencies, such as bats [173]. In brief, in this method we first measured the theta phase estimate for each spike from the concurrent 2–10-Hz LFP and "unwrapped" the phase time series so that it increased linearly, like elapsed time. We then measured the spike-phase spectrum, which we defined as the power spectral density of the time series of unwrapped spike phases (*see Methods*). In contrast to conventional spectral analysis that measures the frequency of a signal relative to absolute time, the spike–phase spectra reflects the relative frequency of rhythmic spiking compared to the frequency of concurrent LFP oscillations. If a spike-phase spectra showed a peak at a relative frequency > 1.0 it would indicate that a neuron's rhythmic spiking was faster than the concurrent oscillations in the LFP, and thus this neuron's spiking exhibited precession relative to the LFP (Fig. 3.4A). This method ensures that a consistent relationship between the spiking frequency and LFP frequency can be identified even if the LFP shifts in frequency or amplitude, and even though neuronal spike times alone may not show a clear oscillation (Supplementary Fig. S3.1B), as is the case in humans and bats [173]. We validated this method by applying it to data from rodent CA1 and identifying a consistent > 1.0 relative frequency (Supplementary Fig. S3.1C,D), consistent with the spatial phase precession observed in these neurons [157].

To assess whether precession-like rhythmic spiking was evident for non-spatially tuned cells, we applied this method to the 744 neurons that were active during the task but did not exhibit sig-

nificant spatial tuning. Figure 3.4B depicts an example neuron that we identified with this method that showed significant precession. This analysis found that the rhythmicity of this cell's spiking frequency occurred at a frequency that reliably exceeded the frequency of the LFP (right panel), although no consistent rhythm is apparent from the spike timing alone (left panel). Using this method we found that 12% of non-spatially tuned neurons (90/744) showed a significant relationship between neuronal spiking frequency and LFP frequency (Fig. 3.4C), at a range of relative frequencies > 1.0 (Fig. 3.4D). The number of neurons that showed this phenomenon was significantly more than we expected by chance ($p < 7 \times 10^{-18}$, binomial test; Fig. 3.4E).

We performed a control analysis (Supplementary Fig. S3.4C) to rule out the possibility that these effects could be explained by the absolute spike timing, though this was unlikely given the relative lack of intrinsic rhythmicity in the spike timing (see Supplementary Fig. S3.1B). This analysis confirmed that most of these neurons show phase precession only when spiking is measured relative to the instantaneous ongoing oscillation rather than absolute time [191] (Fig. 3.4E). These results illustrate how the frequency variability of human hippocampal theta [169] may diminish traditional measures of phase precession, and demonstrate the potential for phase precession in neurons that are not spatially tuned. We next sought to test whether this new non-spatial precession pattern might vary behaviorally in relation to non-spatial, higher level features of the task, such as prospective goals.

3.3.3 Evidence for phase precession during trajectories to specific goals.

Having shown that non-spatially tuned neurons can exhibit phase precession, we next tested whether this was a tonic pattern [186] or, alternatively, one that emerged selectively to code for specific stimuli or states. Specifically, recent work has shown that human hippocampal–cortical networks represent goals and their intermediate locations [192]; furthermore we found previously that this task elicits distinctive patterns of rate- and phase- coding for goals [161]. Therefore, we assessed whether phase precession emerged selectively during trajectories to specific goals in service of binding those trajectories for learning and memory.

During each trial of this task, the subject was cued to travel to a randomly selected goal location (Fig. 3.5A). We found that some neurons specifically showed phase precession only during travel to particular goals. Figure 3.5B shows an example of a neuron whose spiking shows phase precession during navigation to goal 2, but not the other goals. This effect is evident in the spike-phase autocorrelogram for that goal, which shows that during travel to goal 2 rhythmic spiking occurs at a frequency that is slightly faster than the ongoing 2–10 Hz LFP. To systematically test for goal-state phase precession, we measured the spike-phase spectrum during trajectories to each goal and compared these spectra between goals, using a permutation procedure and correcting for multiple comparison across goals (Fig. 3.5C, see *Methods*). Figure 3.5D depicts two example neurons from the hippocampus and amygdala of two different subjects (see Supplementary Fig. S3.5 for additional examples). These neurons exhibited rhythmic spiking at faster frequencies than the ongoing LFP while the subjects were en route to specific goals. Critically, this rhythmic spiking was goal-specific and did not appear during trajectories to other goals. These patterns were thus examples of phase precession for a particular goal-state, similar to phase precession in a place field.

We applied this method to the 448 non-spatially tuned neurons that were sufficiently active during each goal, and found a population of neurons exhibiting a significant pattern of faster-than-LFP rhythmic spiking during at least one goal (Fig. 3.6A), across a range of relative frequencies (Fig. 3.6B). Overall, 11% of these neurons (49/448) exhibited significant goal-state precession. We found at least one neuron exhibiting goal-state phase precession in 10/13 subjects. Of the neurons exhibiting goal-state precession, almost all did so for only one of the six goals (Fig. 3.6C). This effect was present at significant levels in anterior cingulate, orbitofrontal cortex, amygdala, and hippocampus, but not parahippocampal gyrus or entorhinal cortex (p's$<$ 0.02, binomial test; Fig. 3.6D).

We performed a series of control analyses that rules out the possibility that our observation of precession for specific goal states was confounded by between-goal differences in LFP power or neuronal firing rate (Fig. 3.6E). Indeed, neither example neuron in Figure 3.5 exhibited increased

firing rates during goals that showed precession, suggesting that goal-state precession was independent of goal-specific firing rate increases [161]. Overall, only 17 of the 49 neurons that showed goal-state precession also showed increased goal-specific firing rate increases (ps< 0.05, one-way ANOVA), and only 2 of 17 of these neurons showed precession and a firing rate increase for the same goal [153] (Fig. 3.6F). Next, we tested whether subject performance on different goals might be responsible for our results, i.e., whether precession might occur when subjects perform more efficient navigation. We measured subject's performance on each goal (*see Methods*) and found no significant difference in navigational performance between goals that elicited precession and those that did not (Supplementary Fig. S3.6A, B). Because differences in theta power, firing rate, and behavior did not account for our results, our findings indicate that non-spatial phase precession selectively occurs during trajectories to specific goals and may also support the representation of non-spatial, sequential features of behavior.

3.4 Discussion

The nature of the neural code is a fundamental question in neuroscience. Our findings show the first evidence that neurons in the human brain spike in rhythm with local network oscillations to represent spatial position and non-spatial events, in addition to the well-established code based on firing rate. Specifically, we demonstrate the existence of phase precession in humans during a virtual spatial memory task. We provide evidence for rodent-like spatial phase precession in human hippocampus and entorhinal cortex, in which spatially tuned neurons spike at earlier phases of theta (2–10 Hz) LFP oscillations as subjects moved through the putative place field center. We also provide evidence for the existence of non-spatial, goal-state phase precession which occurs transiently during trajectories to specific goals. These findings thus extend phase precession beyond rodents, and beyond spatial location, highlighting its potential as a more widespread neuronal mechanism for coordinating spike timing during behavior and cognition.

The spatial phase precession we observed bears important similarities to phase precession in rodents. We found spatial phase precession most predominantly in hippocampus and entorhinal

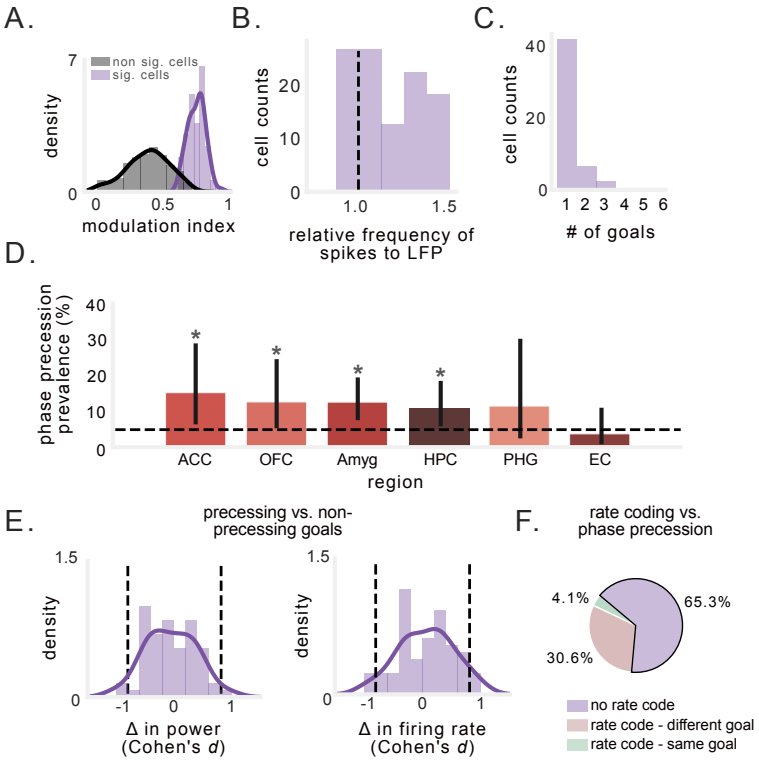

Figure 3.6: **Prevalence and characteristics of goal-state phase precession in neurons that are not spatially tuned.** A) Modulation index (MI) of spike-phase spectral peaks for significant vs. non-significant goals. B) Peak spike-phase PSD frequency for all goals for which a neuron exhibited a significant MI in the spike-phase spectra. Values to the right of the black line indicate that the neuronal frequency slightly exceeded the LFP frequency, indicating precession. C) Number of goals per neuron for which precession was observed. Most neurons exhibited precession during only one goal. D) Percentage of non-spatial cells in each region that exhibited goal-state phase precession. Asterisks indicate significant proportion of cells ($ps< 0.02$, binomial test). E) Distribution of Cohen's d for the difference in 2–10 Hz power (left) and firing rate (right) between trajectories to goals showing precession vs. those that did not. Black dotted line indicate effect size of ±0.8. F) Analysis of overlap between goal-state phase precession and rate coding for goals.

cortex, where place and grid cells, respectively, are canonically found [23, 24, 32, 33]. This suggests that the spatial phase precession we observed may be driven primarily by place- and grid- cells, as it is in rodents. One potential reason why phase precession has not previously been observed in humans is because human theta oscillations often appear at a slower and broader range of frequencies compared to those seen in rodents [168, 167, 169]. We specifically assessed phase precession relative to the broader range of theta frequency (2–10 Hz) fluctuations of the LFP, in line with the recent discoveries of phase precession in bats [173] and marmosets [193] — two animals

with similarly heterogeneous theta oscillations. Our findings are also consistent with findings from rodents, who continue to show phase precession even when LFP theta power and theta-modulated spiking are reduced [194, 145, 195], and have also shown evidence of lower frequency oscillations [196, 197]. Furthermore, phase coding may not depend on regular, high amplitude rhythmicity in neural activity [198]. Instead, shifting LFP frequency can modulate spike-time intervals for synaptic plasticity without affecting the spike-phase [187]. Recent work in rodents has indeed demonstrated that the theta phase code is robust to changes in theta frequency, even as temporal lags between spikes are altered [191]. It is thus likely that the spatial phase precession we observed is analogous to that described in rodents, despite differences in theta range and rhythmicity.

Phase precession has predominantly been observed during place- or grid- cell spiking [199]. However, recent work has discovered the presence of phase precession relative to sound [128, 152], odor [152], time in an episode [149, 57, 150], task progression [147], and REM sleep [149]. These findings highlight the potential generalizability of phase precession to non-spatial domains. In these instances, phase precession may enable the encoding of any successive stimuli or state, with the progression of phases binding a myriad of non-spatial sequences together for learning. By leveraging the idea that any variable may be encoded in spike phase if the frequency of spike rhythmicity exceeds the frequency of the local LFP oscillation [157, 187], we showed that phase precession also occurs with respect to behavioral states other than inhabiting a specific physical location—in this case, exclusively during trajectories to specific goals. The fact that this result is so specific, only showing up for a subset of goals for each neuron, might suggest an ensemble temporal code responsible for encoding all of the goals in the task [200, 201].

The goal-state phase precession we observed was largely independent of rate coding for goals, which has been described previously in human studies [32, 161, 202]. That the presence of rate and phase coding for goals is statistically independent is consistent with observations in rodents that showed that phase precession can appear for specific behavioral states even in the absence of concurrent firing-rate changes [153]. These findings support the theory that phase precession is used by the brain to signal behavioral states independent of firing-rate changes [203, 204]. A

challenge for future work is to understand the specific features of this phenomenon, such as the role of different phases within goal-state precession. One hypothesis is that goal-state precession may help track a person's "episodic" position within a goal-seeking event. This would align with work in rodents showing phase-precession in "episode" or "time" cells when a rodent runs on a treadmill with a goal [57] but not without a goal [205], as well as evidence from human imaging showing that hippocampal and entorhinal cortex population activity correlates with distance to goal [206]. Furthermore, goal-state phase precession may relate to the phase precession observed in ventral striatum "ramp cells" [145], and medial prefrontal cortex neurons in rodents [148]. The former exhibited precession as rodents approached reward locations, and the latter exhibited precession that was clearest when rodents approached the decision point in a maze [148]. Given that we found goal-state phase precession across various brain regions, including frontal cortex, these prior works further support the hypothesis that precession may represent "episodic" position within top-down behavioral states.

It is important to understand the prevalence of phase precession due to its likely theoretical relevance as neuronal mechanism for binding and compressing sequential events. In brief, phase precession organizes spiking at time intervals below the deactivation time constant of NMDA receptors, facilitating synaptic plasticity between neurons that encode events at behavioral timescales [132, 207, 208, 209, 135, 29]. Strengthening associations between consecutively active neurons may be a widely useful mechanism for learning associations. Our findings extend phase precession to the human brain and demonstrate that precession does not necessarily depend on physiological constraints, such as a stationary ~8 Hz theta oscillations [194, 145, 195, 173, 187]. Furthermore, our results show that a consistent difference between spiking and LFP frequency extends beyond place- or grid- field activity and may represent non-spatial mental sequences related to a memory task. This consistent spike–LFP frequency difference has been characterized by oscillatory-interference models as a function of spatial inputs, such as velocity, but may include non-spatial inputs if they increase spiking frequency above the network oscillation [210, 211]. Therefore, our findings demonstrate the potential utility for phase precession in humans, across

diverse brain regions, as a general, domain-free mechanism for temporal compression of specific experiences.

In summary, we have provided evidence for spatial phase precession in the human hippocampus and entorhinal cortex during virtual navigation and shown that it exhibits features similar to those seen in rodents. Further, we also demonstrated the existence of phase precession that is specific to trajectories to particular goals. These findings suggest that phase precession is a general mechanism for temporal coding in the human brain, despite the heterogeneity in theta rhythmicity in human MTL. Furthermore, the discovery of goal-state phase precession extends the potential for phase coding to be physiologically relevant for an array of experiential features, even when the neurons do not show concurrent firing rate changes for those features. Overall, our results suggest that phase precession is an important neural code across species and brain regions, not only for spatial cognition and memory but also for non-spatial features of experience.

3.5 Supplementary Material

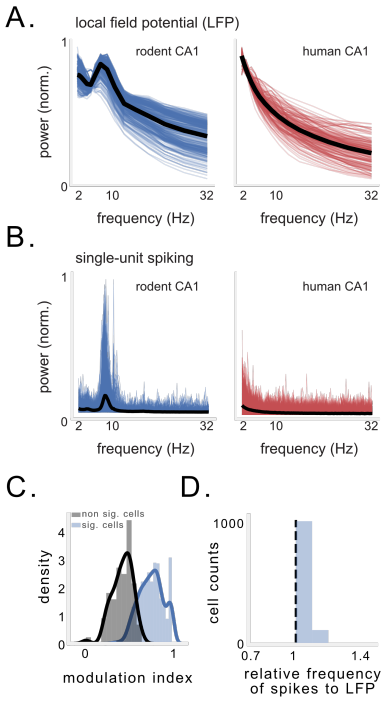

Figure S3.1: **Rodent hippocampal theta oscillations and measurement of precession without position.** Related to Figures 3.1, 3.4. A) Power spectral density of hippocampal LFPs recorded in navigating rodents (blue) and humans (red). Black line denotes average across channels. Rodent hippocampal LFP shows a clear peak in the 5-10 Hz range in almost all channels, while the human LFP does not. B) Power spectral density from single-unit discharge from rodent (blue) and human (red) hippocampus. Black line denotes average across neurons. C) Modulation index (MI) of spike-phase spectral peaks for significant vs. non-significant neurons recorded in rodent CA1. D) Distribution of relative frequencies for neurons exhibiting significant MI in the spike-phase spectra. Values to the right of the black line indicate that the neuronal frequency slightly exceeded the LFP frequency.

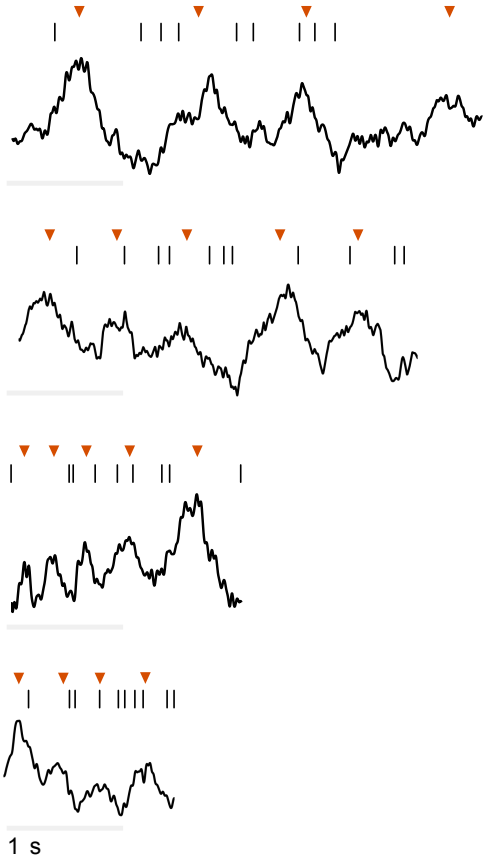

Figure S3.2: **Examples of spatial phase precession during individual passes through a field.** Related to Figure 3.2. Spike times and 1–30-Hz filtered LFP data during individual passes through peak firing bins for four neurons that exhibited significant spatial phase precession. Red arrows denote peaks of individual theta cycles.

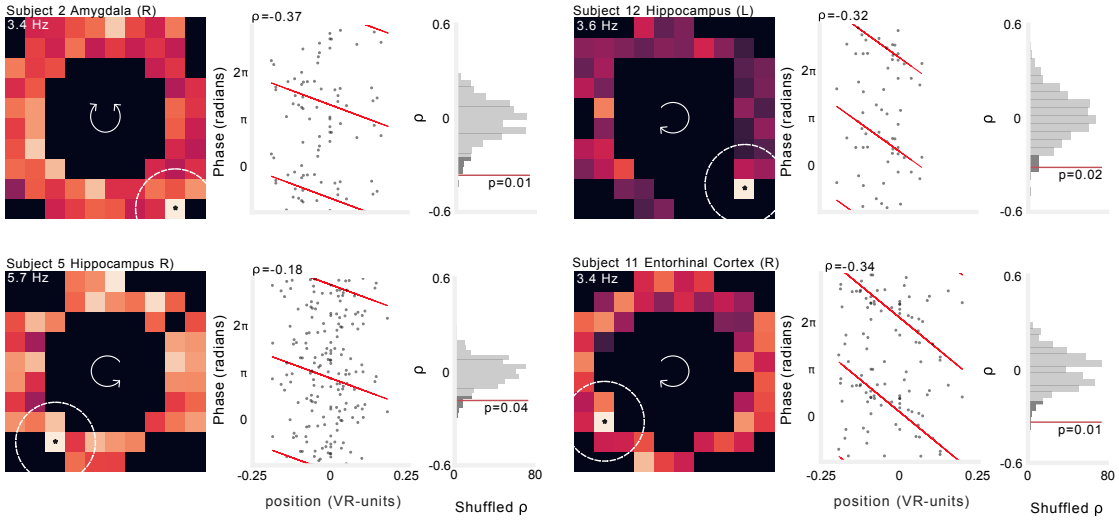

Figure S3.3: **Additional examples of spatial phase precession.** Related to Figure 3.2. The activity of four neurons that show significant spatial phase precession. Left: firing rate heat map. Brighter colors denote higher firing rates. Text label indicates the color scale for the plot with the mean firing rate of the peak firing bin, which is noted with an asterisk. Dotted lines indicate maximum radius around field in which spiking was assessed. Arrows in the center of the heatmap indicate the movement direction for which this plot was computed. Middle: spike phase as a function of location relative to the field center. Spike phases are duplicated vertically to enable visualization of circular–linear regression (red). Text indicates circular-linear regression coefficient (rho). Right: surrogate distribution of circular-linear regression rho-values generated by permutation of spike phases. Red line indicates value of real data. Dark gray shading indicates 95^{th} percentile of surrogate distribution.

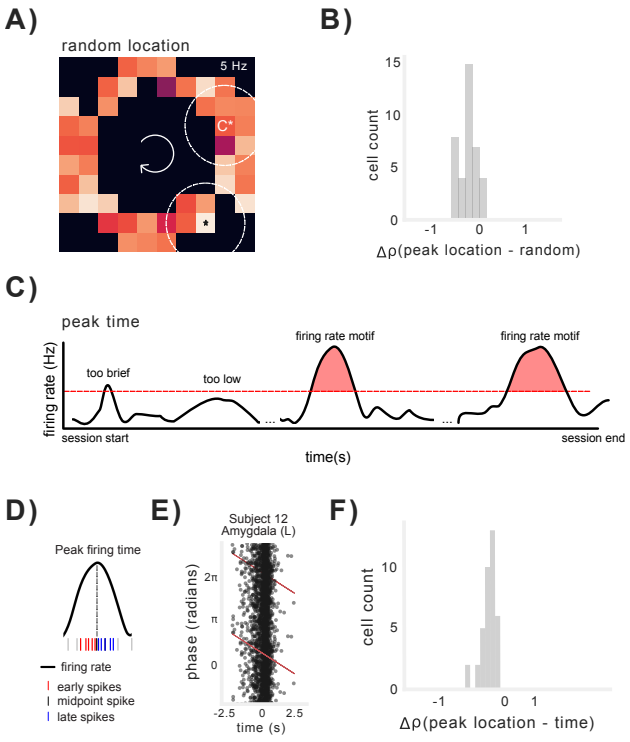

Figure S3.4: **Location- and time- control analyses for spatial phase precession.** Related to Figure 3.3. A) Example of alternate location selected to test whether peak firing bins exhibited significantly greater phase precession than randomly selected locations. B) Distribution of differences in circular-linear correlation coefficients for precession observed in peak firing bin vs. randomly selected location. C) Schematic of method for identifying elevated firing rate. Firing rate had to exceed a firing rate threshold of 1.5 Hz for at least 250 ms in order to be classified as a firing rate "motif". D) Schematic of of method for time-based phase precession within motifs of elevated firing rate. E) Example neuron exhibiting significant phase precession relative to elapsed time within a firing rate motif. F) Distribution of differences in circular-linear correlation coefficients for precession observed in peak firing bin vs. time in firing motifs.

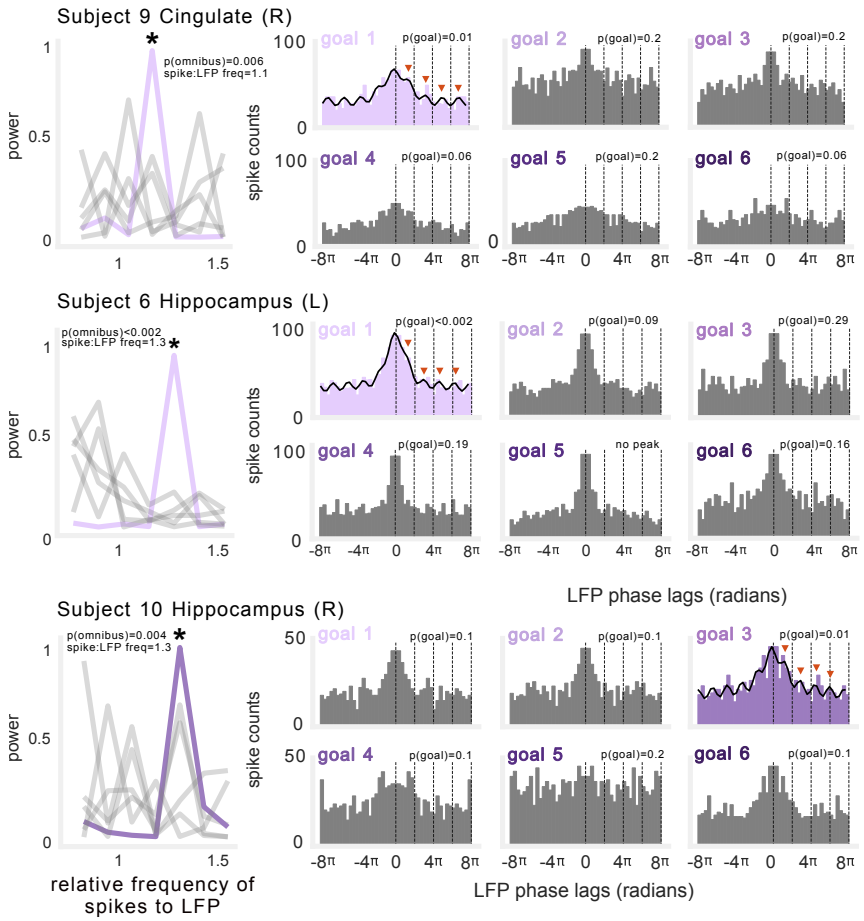

Figure S3.5: **Additional examples of goal-state phase precession.** Related to Figure 3.5. Three example neurons exhibiting phase precession during navigation to specific goals. Left: Power spectral density depicting frequency of neuronal spiking relative to ongoing LFP. Asterisk denotes peaks that were significant and significantly different from other goals. Gray lines denote spike-phase spectra for non-significant goals. Right: Spike-phase autocorelograms during navigation to each goal (significant goal epochs depicted in color). Text indicates the p-value for both significance tests described in Figure 3.5C), and relative frequency of spiking to LFP. Black line indicates fit of decaying-oscillation function added to significant examples shows oscillation in spike-phase autocorrelogram.

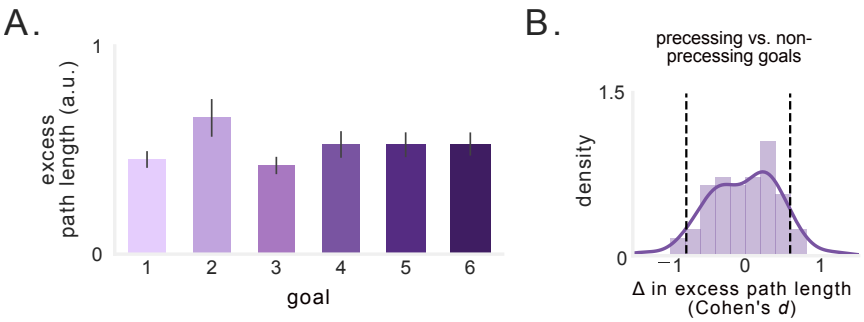

Figure S3.6: **Goal-state phase precession is not a function of a differences in navigation performance.** Related to Figure 3.6. A) Excess path length as a function of goal. B) Distribution of Cohen's d comparing excess path length during trajectories to goals that showed precession vs. those that did not. Black dotted line indicates effect size of ±0.8.

Chapter 4: Gamma oscillations in the human amygdala and hippocampus discriminate emotional features of episodic memory

Salman E. Qasim, Uma Mohan, & Joshua Jacobs
Manuscript in preparation.

The emotional context of an event can determine if and how you remember that experience later. We examined the neuronal circuits underlying the influence of emotional context on memory encoding by analyzing direct recordings of brain activity in the hippocampus and amygdala of epilepsy patients who encoded and recalled lists of words. The emotional features of these words (valence and arousal) were predictive of subsequent recall, and gamma oscillations increased in the hippocampus and amygdala during the successful encoding of highly arousing words, or highly negative words, respectively. These emotional features also elicited distinct patterns of amygdala-hippocampus theta-gamma coupling, particularly for high arousal words. Finally, 50 Hz electrical stimulation in the amygdala impaired memory for neutral words while hippocampal stimulation impaired memory for high arousal words. These findings illustrate the importance of emotional context to episodic memory, and identify a specific role for the amygdala-hippocampus circuit in processing this emotional context during memory encoding.

4.1 Introduction

Episodic memories, memories of personal events and experiences, are almost impossible to untangle from their emotional context. Emotional events comprise some of our most vivid, important, and persistent memories, and their loss to diseases like Alzheimer's illustrate the importance of understanding the neuronal circuits that strengthen memory for events with emotional context [212].

Indeed, the brain region known for its role in emotion processing[213, 214]—the amygdala—is an early target of Alzheimer's disease [215]. The amygdala abuts the anterior portion of the hippocampus, the brain region most strongly associated with declarative memory [216]. This anatomical convergence has been investigated through careful lesion studies, which have shown that the amygdala is also an essential brain region for memory pertaining to events with emotional salience [217]. Furthermore, brain activity in the amygdala is often correlated with emotional memory processes. Research in rodents, for example, has shown that neurons in the amygdala become more active and more synchronized after the animal encounters fearful conditions, indicative of an active neuronal ensemble for fear memory [218]. Recent discoveries of manipulable fear memory engrams have further supported the idea that synchronously active neurons in the amygdala and hippocampus are mechanistically involved in binding emotional context to events for memory [219]. In humans, functional imaging studies have provided evidence for this hypothesis, demonstrating that the amygdala is more active during the encoding of emotional stimuli, in parallel with the MTL system [220]. Stimulation research in humans has shown that direct electrical stimulation of the amygdala can lead to memory improvements for non-neutral stimuli [221].

However, investigating the precise neuronal patterns underlying a potential amygdala-hippocampal circuit for memory is difficult. While animal studies allow for direct brain recordings, researchers are often limited to studying conditioned fear responses as a proxy for emotional context. While human studies enable more direct assessment of emotional stimuli, direct brain recordings are rare. The few that exist have shown that neurons in the human amygdala and hippocampus show rate-and phase- based coding of working memory and high phase-locking to hippocampal theta oscillations, providing evidence that neuronal activity in the amygdala and hippocampus is tied to memory demands and may be coordinated between regions [222, 96, 74, 223]. Critically, one study found that coordination between amygdala and hippocampal LFPs is enhanced during fearful image viewing, suggesting that simply viewing stimuli with emotional content is sufficient to engage the amygdala-hippocampal circuit. These studies did not, however, assess the influence emotional context has on memory processes, and their corresponding neuronal patterns. Overall,

it is not clear what cognitive process the emotional context influences, as emotional features have been theorized to play a role in encoding, storage, and retrieval processes during memory [224]. If emotional context influenced processes relating to memory encoding, we theorized that neuronal activity during the encoding period should reflect subsequent memory success as a function of the valence and arousal of words.

Here, we tested the hypothesis that groups of neurons in the amygdala and hippocampus exhibit correlated firing during the encoding of memories with emotional content, and that increased activity in this amygdala-hippocampal enhances the successful encoding of such memories. We did so by analyzing a dataset of iEEG recordings from epilepsy patients during a verbal free recall task, a test of episodic memory for words. We characterized the emotional features of each word along the two dimensions—arousal and valence—and found that these features were predictive of subsequent memory recall. Furthermore, we show that modulatory effects of emotional context may involve gamma oscillations in the amygala-hippocampal circuit, and particularly theta-gamma coupling between these regions for high arousal words. Finally, we demonstrate that direct electrical stimulation impairs memory for high arousal words, suggesting a causal role for these neuronal patterns in the effects of emotional context on episodic memory.

4.2 Methods

4.2.1 Data recording and participants.

Data was recorded from patients undergoing invasive iEEG monitoring in the course of their treatment for drug-resistant epilepsy. Patients were recruited to participate in a multi-center project, with data collected at Thomas Jefferson University Hospital, Mayo Clinic, Hospital of the University of Pennsylvania, Emory University Hospital, University of Texas Southwestern Medical Center, Dartmouth-Hitchcock Medical Center, Columbia University Medical Center, National Institutes of Health, and University of Washington Medical Center. Experimental protocol was approved by the IRB at each institution and informed consent was obtained from each participant.

Electrodes were implanted in the hippocampus and amygdala using localized, penetrating

depth electrodes (Ad-tech Medical Instruments, WI). Electrodes were spaced 10 mm apart, and data was recorded using either the Nihon Kohden EEG-1200, Natus XLTek EMU 128 or Grass Aura-LTM64. iEEG signals were sampled at either 500, 1,000, or 1,600 Hz and referenced to an intracranial electrode, or a contact on the scalp or mastoid process.

4.2.2 Task

Subjects participated in a free-recall verbal memory task. During this task, a 10 s countdown preceded each list of 12 words, which were presented for 1600 ms each with interstimulus intervals randomly sampled from between 750-1000 ms. Each list was followed by a math distractor task to prevent rehearsal, lasting at least 20 seconds, during which simple math problems were presented until a response was entered or recall began. A visual cue paired with a 800 Hz tone signaled the start of each recall period, and subjects had 30 seconds to verbally recall as many words from the list of 12 words they had just seen, in any order. These vocal responses were recorded and annotated offline to assess recall accuracy. Subjects encoded and recalled 25 lists in each session, and did not see the same list twice across sessions.

Subjects performed one or both versions of this task that differed in the semantic structure of the word lists. The uncategorized version of the task utilizes a word pool of 300 words (`http://memory.psych.upenn.edu/files/wordpools/iEEG_FR_nouns.txt`), constructed by selecting words from the Toronto word pool with intermediate recall performance (after accounting for recall dynamics and clustering effects inherent to free recall) [225]. This word pool was split into lists of 12 words such that the mean pairwise semantic similarity within list was relatively constant across lists. For the categorized free recall task, the word pool was drawn from user-rated semantic categories (using Amazon Mechanical Turk). Words were sequentially presented as categorical pairs (drawn from the same category), and each list consisted of four words drawn from each of three categories. Two pairs drawn from the the same semantic category were never presented consecutively [226].

4.2.3 Characterizing emotional context during encoding

We utilized a publicly available rating-scale, the NRC Lexicon, to quantify the emotional context of the words present in the word pool for each task. We selected this rating scale, as opposed to other commonly used rating scales, because of the higher number of independent raters involved, and the use of split-half reliability testing for all ratings. In sum, 97% of the words tested had ratings in the NRC Lexicon and were analyzed in this study.

For each subject, we quantified the relationship between word valence, arousal, and subsequent recall using an L2-normalized logistic regression classifier (equation [1]), with an inverse regularization parameter $C = 0.0072$. Valence was included as both a linear and polynomial feature due to the hypothesis that low (negative) or high (positive) valence may be equally predictive of recall. Observations were weighted by the frequency of forgotten vs. remembered word counts.

$$Pr(recall = 1) = \frac{1}{1 + exp^{-(\beta_0 + \beta_1 V + \beta_2 A + \beta_3 V^2 + \beta_4 (V \times A))}} \tag{4.1}$$

In equation (1), V = valence, A = arousal. We used leave-one-out cross validation in each one list was held out from each session for testing, and classifier performance was average across all folds. We assessed the performance of each subject's classifier by computing the area under the ROC curve, and compared these AUC values to those generated by randomly shuffling labels for recalled and unrecalled words.

4.2.4 Spectral analysis

All data was band-stop filtered around 60 Hz to minimize line noise, and data were bipolar referenced to eliminate reference channel artifacts and noise [227]. Local field potential data were downsampled to 256 Hz for analyses. We computed spectral power during 2000 ms epochs, with word presentation occurring at $t = 500$ ms. We used a continuous wavelet transform (Morlet wavelets, wave number=5) with 30 log-spaced frequencies between 2 and 128 Hz, and 1000 ms buffer windows to attenuate convolution edge effects. We then averaged power during the encoding

period into two bands: theta (2-10 Hz), and gamma (30-120 Hz). We fit a linear model using the to assess the affects of emotional context and subsequent memory on oscillatory power in each band (z-scored within-subject) equation (2).

$$power \sim \beta_0+\beta_1 V+\beta_2 A+\beta_3 V^2+\beta_4 R+\beta 5M+\beta_6 MA+\beta_7 MV^2+\beta_8 MRA+\beta_9 MRV^2+\beta_{10} MRAV^2 \tag{4.2}$$

In equation (2), M = memory (recalled vs. unrecalled) and R = region (amygdala vs. hippocampus). We used a likelihood ratio test (LRT) to assess the significance of the model after removing interactions and main effects, in order to detemine which factors explained a significant amount of the variance in power.

4.2.5 Phase amplitude coupling

We computed the phase-amplitude coupling (PAC) by using normalized direct estimator of PAC [228]. Briefly, this method is similar to more standard metric characterizing the modulation-index describing the Kullback-Leibler distance between the theta-phase binned distribution and a uniform distribution. However, this method normalizes the gamma amplitude and minimizes the influence of changes in amplitude between signals. To assess whether significant differences existed between PAC in the remembered and forgotten conditions, we used a non-parametric cluster-based permutation test, by generating surrogate data by swapping time blocks.

4.2.6 Stimulation

Stimulation was applied only after a neurologist determined safe amplitudes using an iterative mapping procedure, stepping up stimulation in 0.5 mA increments and monitoring for afterdischarges. The maximum amplitude selected (1.5 mA) fell well below standard safety boundaries for charge density [229]. We applied stimulation in a bipolar configuration, with current passing through a single pair of adjacent electrodes. Stimulation consisted of charge-balance biphasic rect-

angular pulses (width = 300 μs) applied continuously at 50 Hz frequency for 4.6 s while subjects encoded two consecutive words. Then, stimulation was paused for the following two words, and then applied again, for each list of 12 words. Stimulation began 200 ms prior to word presentation and lasted until 200–450 ms after the offset of the second word in the stimulated pair. We applied stimulation during 20/25 of the lists in a session, so subjects were stimulated during encoding for 120 words and not stimulated for 180 words per session.

4.3 Results

4.3.1 Emotional features of a word predicts subsequent episodic recall

We analyzed data from a verbal episodic memory task in which subjects were shown lists of words and asked to memorize them. After each list subjects performed a math distractor task to prevent rehearsal, and then told to recall as many words as possible, in any order. This free recall paradigm has been used to identify memory-related biomarkers in the human brain [230]. We assessed the influence of emotion on recall success by quantifying the valence and arousal of each word based on a publicly available lexicon [231, 232].

Briefly, this lexicon consists of rating made by thousands of participants with high consistency in a split-half reliability test. The words in the free recall task were not chosen based on their emotional associations and exhibited higher valence (0.56±0.15) and lower arousal (0.36±0.16) than the broader lexicon ($ps< 3x10^{-9}$, Wilcoxon rank-sum test, Fig. 4.1A), but these features have been shown to affect successful recall, generally[232, 233], and in this particular dataset [234]. Furthermore, the emotional dimensions of the words in this dataset have also been shown to influence their clustering during memory retrieval [235]. We thus tested whether the valence and arousal of a word could predict that the word would be subsequently recalled, within each of the 157 subjects who performed the task. Overall, classification accuracy using valence and arousal was significantly better than chance (median AUC = 53, Fig. 4.1B). Over the population, negative words and highly arousing words were both remembered more often, and were recalled first more often (Fig. S4.1B). These results suggest that valence and arousal of word stimuli potentially

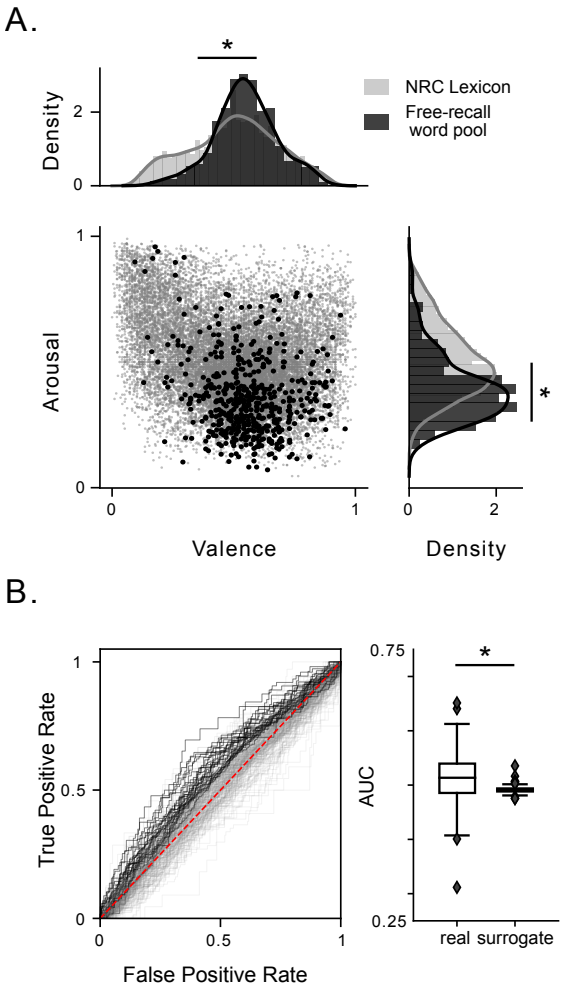

Figure 4.1: **Emotional context predicts subsequent recall.** A) Joint scatter plot and marginal distributions of valence and arousal ratings in the general rating Lexicon (gray) and the word pool for the free recall tasks performed by subjects (black). Asterisks indicate significant difference between the mean ratings for valence and arousal between the word pool and the general lexicon. B) Left, AUC for each within-subject classifier of recall success as a function of word valence and arousal. Black lines indicate classifier performance significantly better than chance. Right, averaged AUC across all subjects, compared to chance-level performance generated by shuffling trial labels. Asterisk indicates significant difference.

influenced memorability in this task, in line with past work.

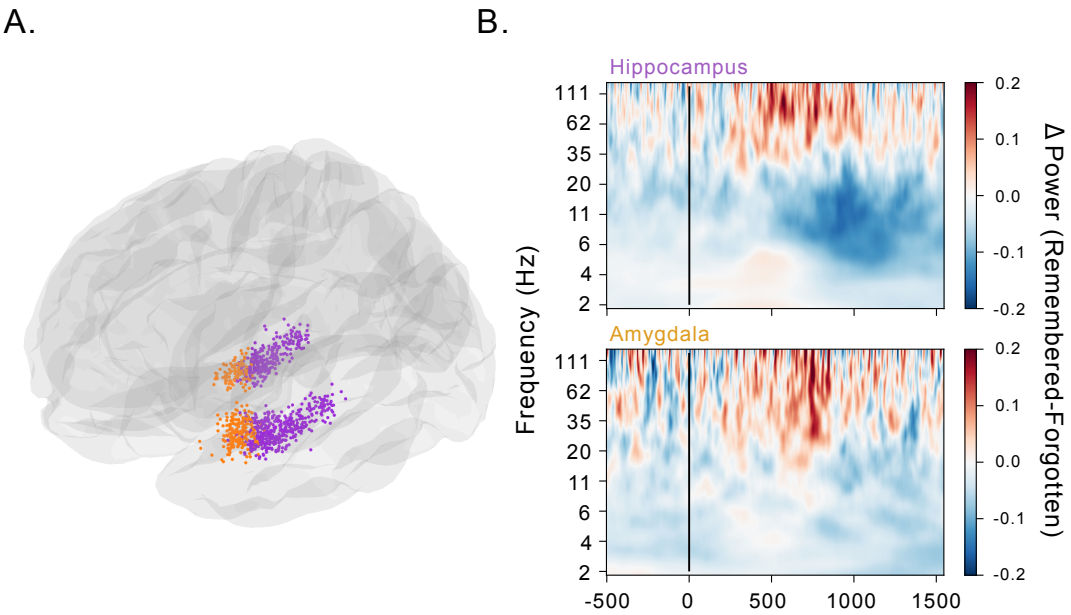

Figure 4.2: **Subsequent memory effect in hippocampus and amygdala.** A) Location of all 1,376 electrodes recorded across all subjects. Purple circles indicate electrodes localized to hippocampus, orange circles indicate electrodes localized to the amygdala. B) Z-scored spectrogram for hippocampal (top) and amygdala (bottom) electrodes showing difference between remembered and forgotten words. Warm colors indicate an increase in power during encoding of remembered words, while cool colors indicate a decrease in power. Vertical black line denotes the onset of word presentation.

4.3.2 Emotional features correspond to distinct neuronal dynamics during memory encoding

We next tested whether the behavioral influence of these emotional dimensions arose from distinct patterns of neuronal activity in the hippocampus and amygdala. We analyzed 965 electrodes in the hippocampus and 411 electrodes in the amygdala of 157 subjects who underwent depth-electrode implantation during treatment of their epilepsy (Fig. 4.2A). First, we assessed the subsequent memory effect (SME), a commonly applied contrast comparing brain activity during encoding for remembered vs. forgotten items [236, 237]. Prior iEEG work has identified a characteristic pattern of high-frequency increases and low-frequency decreases in the medial temporal lobe associated with successfuly recalled words [238, 239, 227, 240]. Over all the hippocampal electrodes, we replicated this pattern, and found a similar pattern present across the amygdala elec-

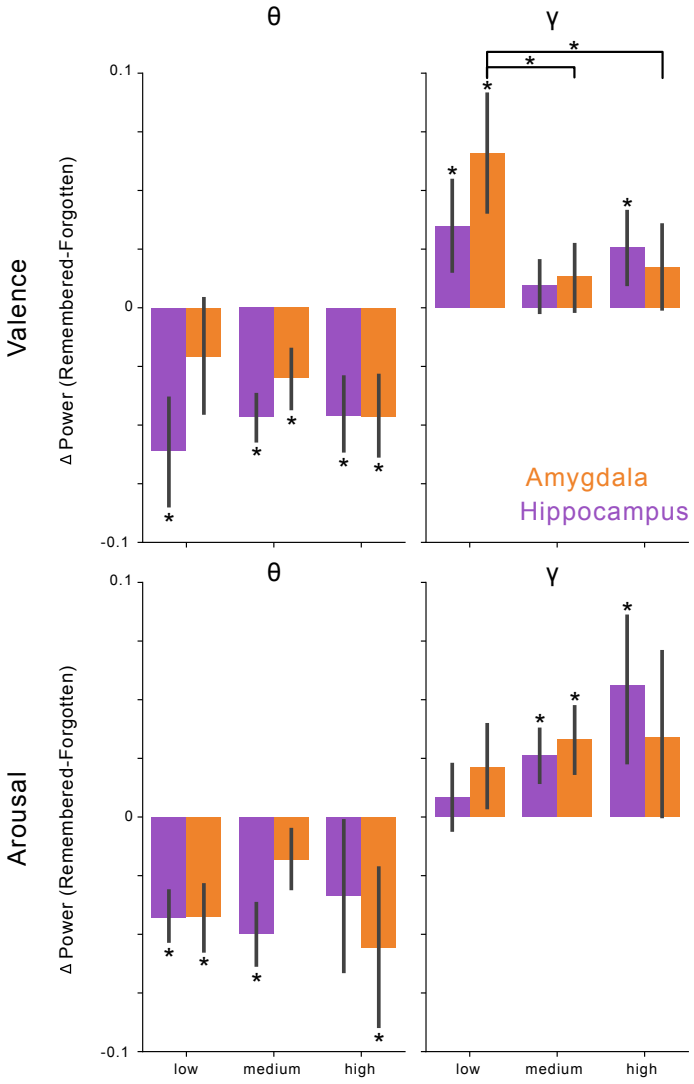

Figure 4.3: **Memory-related power change as a function of frequency, region, and emotional context.** Z-scored power differences (remembered - forgotten) in the theta (2-10 Hz) and gamma (30-120 Hz) bands, plotted as a function of region (hippocampus, amygdala) and emotional features (valence, arousal). Emotional features were binned into terciles spanning the whole range of possible values. Asterisks represent significance for comparison of power between remembered and forgotten items, or between power differences as a function of emotional feature.

trodes (Fig. 4.2B), whereby gamma power seemed to increase while theta power decreased during encoding of subsequently remembered items.

In order to determine the effect of emotional context on these oscillatory dynamics, we modelled theta and gamma power as a function of valence, arousal, memory performance, and brain region, and their interactions. We found a significant effect of memory performance on theta

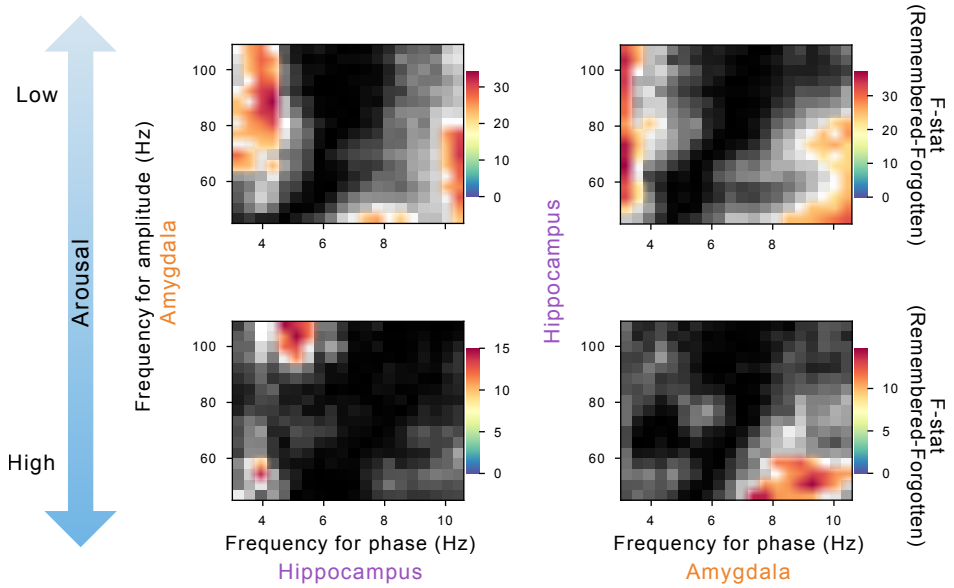

Figure 4.4: **Phase-amplitude coupling during low and high arousal word encoding as a function of subsequent memory.** Heatmaps showing differences in PAC (F-statistic) from cluster permutation test comparing remembered and forgotten items for low arousal (top) and high arousal (bottom) words). Warm colors indicate higher F-statistic values. Non-significant portions were portrayed in grayscale.

power ($\chi_{(12)} = 222.9$, $p < 7x10^{-41}$, likelihood ratio test), indicating that the robust decrease in theta power associated with successful encoding was persistent across both the amygdala and hippocampus, regardless of emotional context (Fig. 4.3). However, gamma power was significantly modulated by the interaction of arousal and memory performance ($\chi_{(7)} = 30.4$, $p < 9x10^{-5}$, likelihood ratio test), such that gamma power increased in both regions with arousal for words that were successfully encoded (Fig. 4.3, bottom right). We also performed individual t-tests comparing subsequent memory effects (SME) for theta and gamma power as a function of valence and arousal (binned in terciles). These results were largely consistent with the outcomes of the full linear mixed model, but also revealed that amygdala gamma was significantly enhanced during memory encoding for negative (low valence) words (Fig. 4.3). This effect was significantly greater than for neutral (medium valence) or positive (high valence) words (ps< 0.007). Overall, the valence and arousal associated with each word elicits gamma oscillations in the human amygdala-hippocampal circuit that may be related to their subsequent recall. Theta oscillations, on the other hand, are consistently weaker during encoding of subsequently recalled words, regardless of its emotional

context.

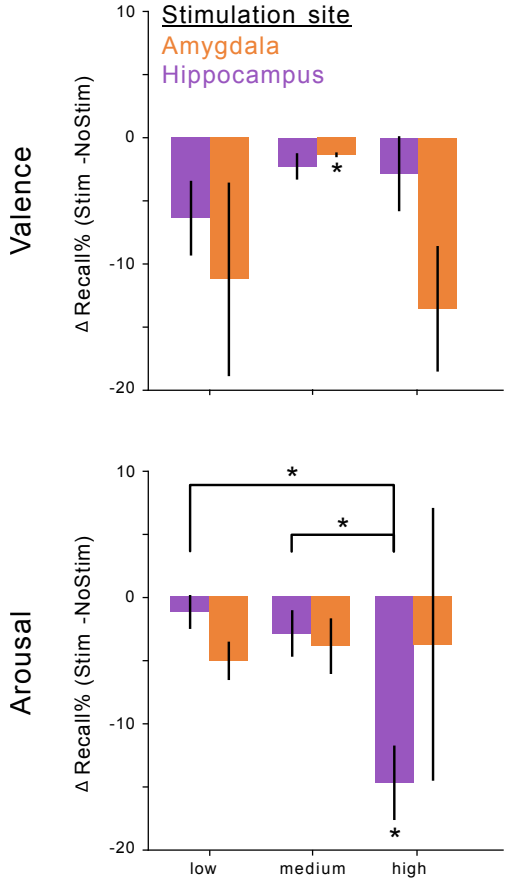

Figure 4.5: **Memory performance as a function of direct brain stimulation.** Difference in percentage of recalled words (stimulation - no stimulation), plotted as a function of region (hippocampus, amygdala) and emotional features (valence, arousal). Colors indicate the site of stimulation. Asterisks indicate either indicate a significant change in recall performance with stimulation, or significant comparisons between the effects of stimulation on recall performance for words with different emotional features.

A subset of subjects (n = 89) analyzed in this study had electrodes in ipsilateral hippocampus and amygdala, enabling us to assess the connectivity between these two regions as a function of memory performance and emotional context. In accordance with recent work in humans showing phase-amplitude coupling (PAC) between amygdala and hippocampus during viewing of salient stimuli [241], we computed PAC between these regions during word encoding. This enabled us to measure how the phase of low-frequency oscillations might modulate the amplitude of the high-frequency oscillations that varied as a function of arousal and memory. During encoding of words associated with low arousal, a similar pattern of bi-directional modulation at both low and high

theta frequencies (4 and 9 Hz, respectively) was significantly more prevalent for words that were subsequently remembered than those that were forgotten (Fig. 4.4). However, for words associated with high arousal, this pattern differed depending on which region was considered to be driving the modulation. When comparing remembered words to forgotten words, low hippocampal theta (5 Hz) modulated high frequency amygdala gamma (100 Hz), while high frequency amygdala theta (9 Hz) modulated low frequency hippocampal gamma (50 Hz) (Fig. 4.4). In contrast, no significant difference between remembered and forgotten words was observed in either direction for negative (low valence) words (Fig. S4.3).

4.3.3 Electrical stimulation of the amygdala-hippocampal circuit selectively disrupts memory

If the emotional context of a stimulus engages the amygdala-hippocampal circuit to enhance memory, than disruption of this circuit should disrupt memory. We thus tested the effect of direct brain stimulation on memory performance, which has been shown to impair memory when applied to MTL regions [92]. We applied direct electric stimulation to this circuit in a subset of the subjects in this study ($n = 16$), as part of a larger study examining the effects of stimulation on memory circuits (see *Methods* for details). Of these sixteen subjects, 13 subjects were stimulated at 14 different sites in the hippocampus, across 36 total sessions. The other 3 subjects were simulated at 4 different sites in the amygdala, across 10 total sessions. In these subjects, 50 Hz stimulation was applied and paused for consecutive pairs of words (Fig. S4.2, see *Methods*). We analyzed how stimulation in the amygdala and hippocampus during the encoding period impacted subsequent recall for words of varying arousal and valence. Figure 4.5 shows that amygdala stimulation caused a small but significant disruption of recall for neutral valence words (t=−6.14, p=0.01). Conversely, hippocampal stimulation significantly disrupted memory for highly arousing words (t=−4.82, p=0.0003), and significantly more than for medium or low arousal words (ps< 0.01). Overall, the disruptive effect of encoding-period stimulation in the hippocampus was conserved, but differed as a function of arousal.

4.4 Discussion

The amygdala is most directly associated with fear-related behaviors in animals, but has also been shown to play an important role in memory [242]. Studies in humans enable us to examine the more diverse role of the amygdala through cognitive experiments that utilize cues with semantic emotional associations. Here, we tested whether such associations affected encoding processes related to episodic memory. By directly recording oscillatory activity in the amygdala and hippocampus as subjects performed an episodic verbal memory task, we found that the emotional associations of encoded words influenced the underlying neuronal dynamics in the amygdala-hippocampal circuit. Specifically, gamma oscillations in the two regions exhibited clear correspondence with the emotional context of a word and its subsequent recall, particularly the associated arousal. Furthermore, distinct patterns of amygdala-hippocampal connectivity were associated with successful recall for words associated with high arousal. Finally, we perturbed these neuronal dynamics (using direct brain stimulation) and impaired memory for words as a function of their arousal. This suggests that the neuronal patterns we observed in this circuit are causally related to episodic memory processes for stimuli with emotional associations.

One advantage of studying the role of emotion in humans is that we are able to utilize stimuli with emotional associations, rather than relying on stimuli that elicit physiological, anxiety-driven behaviors. In this study, we found that word valence (negative, neutral, or positive) and word arousal (low to high) were sufficient to impact subjects' recall performance of those words, replicating similar findings on similar datasets [233, 234]. Prior iEEG research in humans has demonstrated that, during encoding, MTL gamma oscillations are positively correlated with subsequent recall, while theta oscillations are negatively correlated with subsequent recall[238, 227]. More recent work has shown that theta oscillations show similar correlations for semantic and temporal distances in these tasks, demonstrating that semantic associations for words play some role in the oscillatory dynamics relating to memory processes in this task [243]. Because the amygdala is also involved in the processing of valence and arousal we assessed whether oscillatory activity in the

region correlated with subsequent recall [244]. We found that the amygdala shows an overall similar pattern of oscillatory activity to the rest of the MTL during encoding of subsequently recalled items, suggesting its involvement in the broader circuit underlying successful memory.

Critically, we found that theta oscillations decreased fairly uniformly across both the amygdala and hippocampus during encoding for subsequently recalled words, while gamma oscillations increased selectively, depending on region, valence, and arousal. Theta synchrony between the amygdala and hippocampus has been correlated with consolidation and retrieval of fear memories, and anxiety-like behavior in rodents [245, 246]. One future direction of this work is to more closely assess measures of theta synchrony within this circuit (i.e. coherence) to tease out whether this pattern holds in humans. However, because our task involved words with emotional associations, rather than stimuli that elicit emotional responses, such as anxiety, it is possible that theta coherence may play a smaller role in successful encoding and retrieval.

Conversely, our finding that highly arousing words showed PAC for amygdala high-theta and hippocampal low-gamma align with recent work in humans showing elevated hippocampal PAC correlated with subsequent recall [247], and work in rodents demonstrating that amygdala stimulation benefits memory and elicits gamma synchrony in the hippocampus. Furthermore, our observation that amygdala stimulation impaired memory it might then suggest that stimulation interferes with the amygdala-hippocampus theta-gamma coupling associated with successful memory [248]. Other work in humans has also suggested that gamma oscillations and PAC in the amygdala-hippocampal circuit are related to processing stimuli with emotional associations [241]. We identified different patterns of PAC depending on the direction of modulation. Future work will parse whether low and high gamma [249], and low and high theta [169], show functionally different patterns of PAC relating to memory retrieval. Notably, significant PAC was not present during successful encoding of negative (low valence) words. This suggests that are results are not driven by increases in gamma power, but more importantly indicates that arousal, specifically, engages the amygdala-hippocampal circuit during memory encoding. To test this hypothesis further, we analyzed data from a subset of patients who underwent direct brain stimulation in the amygdala and

hippocampus. Indeed, we found that 50 Hz stimulation to the hippocampus specifically impaired subsequent recall for highly arousing words. This manipulation provides more causal evidence that highly arousing words engage the amygdala-hippocampal circuit via theta-gamma coupling, and that this enhances successful memory processes. This also aligns, mechanistically, with deep-brain stimulation findings in movement disorders, showing that direct electrical stimulation in humans disrupts cross-regional theta-gamma PAC [250].

Given that these analyses focus on oscillations and synchrony during the encoding period of the task, one possible mechanism involved is attention. Emotional context, in parallel with cognitive control, drives attention to salient stimuli during memory encoding [251], and that attention, in turn, is thought to lead to improved memory and hippocampal representations for past stimuli [232, 252]. Indeed, gamma oscillations in visual cortex are thought to be involved in the selection of visual inputs for subsequent processing, and theta-gamma modulation, specifically, has been found to correlate with increased visual attention [253, 254]. One possibility, then, is that attention induces bursts of gamma oscillations that represent a form of coordination within and between these regions necessary for selecting the inputs and cell ensembles for encoding an experience into memory [249]. These gamma oscillations may be segregated across different phases of concurrent low-frequency fluctuations [155].

Overall, our findings present substantial evidence that the human amygdala is involved in episodic memory processes for stimuli with emotional associations, even when that emotional context is not relevant to the particular task at hand. Furthermore, we identify specific neuronal substrates, in the form of gamma oscillations and amygdala-hippocampus theta-gamma PAC, that correlate with memory performance as a function of emotional context. Finally, we demonstrate that these signals may be causally related to memory by impairing memory for high arousal words though direct electrical stimulation of the hippocampus. These data suggest an important role for the amygdala in episodic memory in humans.

4.5 Supplementary Material

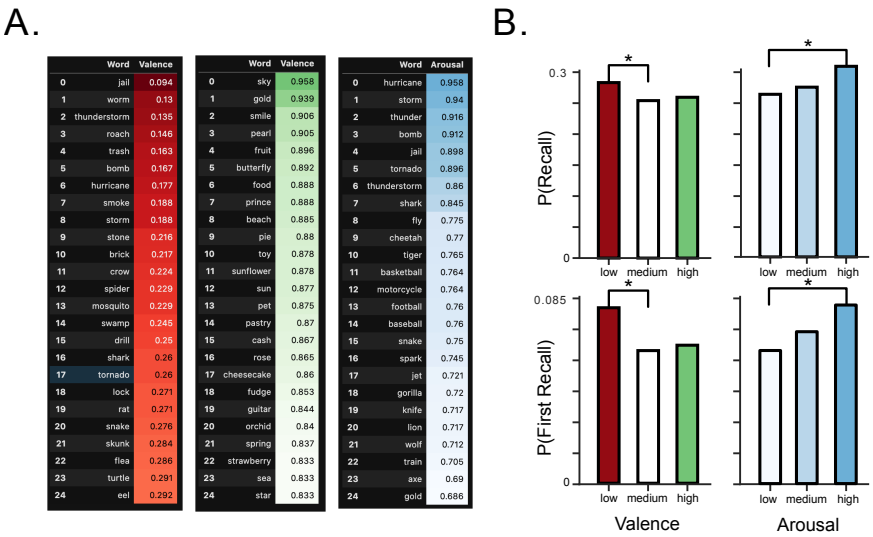

Figure S4.1: **Examples of assigned emotion metrics and effects on recall.** Related to Figure 4.1. A) Lists of the 25 words assigned the most negative (low valence - red), most positive (high valence - green), and most arousing (blue) ratings using the NRC Lexicon. B) Top: Probability of recall as a function of binned valence (left) and arousal (right). Asterisks indicate significant comparisons. Bottom: Probability of first recall as a function of binned valence (left) and arousal (right).

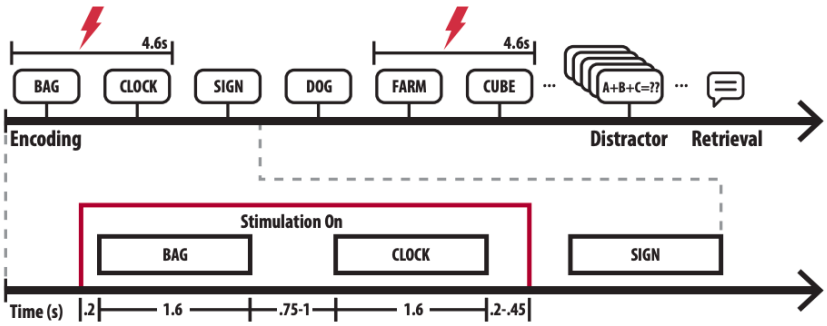

Figure S4.2: **Schematic of stimulation paradigm during free recall tasks.** Related to Figure 4.5. Illustration depicting general task design for stimulation. Words were stimulated in pairs, such that 50 Hz stimulation was applied for the full encoding period spanning the two words. Stimulation was then paused for the next two words. Stimulation was not applied during the math distractor task, or during retrieval.

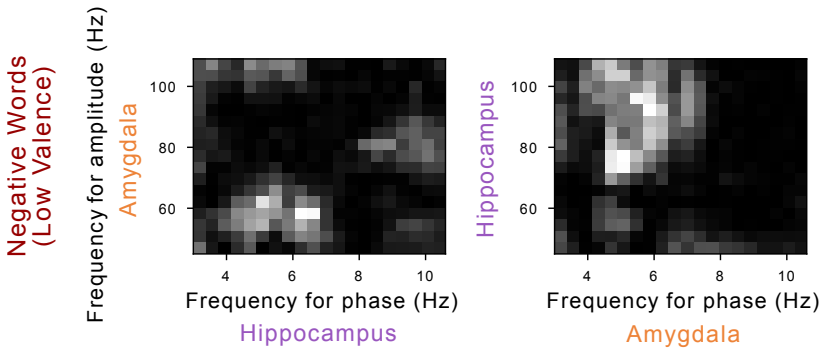

Figure S4.3: **Phase-amplitude coupling during low valence word encoding as a function of subsequent memory.** Related to Figure 4.4. Heatmaps showing differences in PAC (F-statistic) from cluster permutation test comparing remembered and forgotten items for negative (low valence) words). Non-significant portions were portrayed in grayscale.

Chapter 5: General discussion and future directions

My research has demonstrated that important neuronal correlates of space translate from animals to humans, and discovered novel neuronal patterns in humans corresponding to the conjunction of space, memory, and internal features of experience like goals and emotions. Here, I will synthesize across each study to describe how these findings build uniquely on the animal literature to contribute to a broader understanding of the neural systems underlying declarative memory. I will conclude by summarizing the new questions that my work has raised, and the future directions I hope to pursue.

5.1 The conjunctive representations of space and memory in the human brain

Is a cognitive map just a map, representing coordinates in a space? Or does it contain information about what happened within that space? Some of the earliest hypotheses of the brain's spatial representations accorded them a broader function related to memory [23], due to their shared anatomy across rodents and other mammals. Recent work in rodents has strongly supported this approach, demonstrating a potentially causal role between place-cell activity and memory-driven behavior [56]. However, this intuitive hypothesis has been limited in its general value because few studies have been able to generalize the rodent findings on spatial representation to humans and identify their role in memory processes.

In Chapter 2, I sought to answer this question more directly in humans. I recorded single-neuron activity in the human MTL as people performed a spatial memory task, in order to understand whether spatially-tuned neurons in humans reflected memory for past events. I show evidence for memory-trace cells in the human EC whose spiking activity represented the the location a person is trying to remember. The neurons were active near the locations a person *thought*

was associated with a past event, and were also active when people were cued to recall that event but standing outside the environment. As such, I hypothesized that memory-trace cells represent a neuronal code for subjective declarative-memory recall, tying the memory for an event to its spatial context. Furthermore, by illustrating the re-activation of memory-trace cell firing during cue maintenance, I showed that these conjunctive space-memory representations may extend beyond space as a more general marker for memory retrieval. This provides further justification for the general hypothesis that memory processes influence, and are potentially influenced by, spatial representations in the brain, suggesting that the brain's map binds location to the things that happened in those locations. These neurons may represent a neural substrate for declarative memory, as the EC is an early target of Alzheimer's disease [120, 121]. It is possible that loss of memory-trace cells, or alterations in their firing patterns, may underlie some deficit in disorders like Alzheimer's.

Still, many of the neuronal phenomena underlying spatial navigation that hold more general computational value have never been observed in humans. These patterns, like phase precession, are thought to represent mechanisms for organizing events/locations in relation to one another, and in sequences for learning and memory [155, 5]. However, phase precession has largely only been observed in rodents, with only minimal examples in bats[173] and non-human primates [193], partially because of the difference in theta oscillations between species. In Chapter 3 I show, for the first time, that phase precession generalizes to the human MTL. First, by providing clear evidence for spatial phase precession in humans, I show that phase precession is a widespread phenomenon despite the differences in theta oscillations across species. Second, I also show that phase precession generalizes beyond space to potentially encode more abstract sequence progression in specific goal states. Specifically, I found that neurons which did not encode space still showed a pattern of consistent precession-like frequency differences that suggest phase precession plays a role in encoding goal states. By identifying phase precession in humans, in different brain regions than in rodents, and with respect to navigational goal (instead of location), I demonstrate the potential use of phase precession for learning non-spatial sequences for subsequent memory.

These two studies, taken together, provide a strong case for the relationship of neuronal repre-

sentations of space to memory by demonstrating their existence in humans and generalizing them to new domains that are difficult to test in animal models. As such, they also strengthen the broader theoretical argument that any cognitive map, should one exist, is likely to represent a more general form of neural coding that happens to serve spatial representation, but is not exclusive to it. Furthermore, these studies open up avenues of research in both rodents and humans. For example, since "trace cells" have been found in rodents, researchers may pursue clear studies examining their role in memory using careful experimental design and targeted manipulation/lesion/stimulation. Similarly, the methods we used to identify goal-state phase precession may be applied to a wide variety of rodent studies to examine the prevalence of non-spatial, state-dependent phase precession in rodents, even outside of the MTL [255].

Internal context influences memory circuits Episodic memory is imbued with internal, subjective qualities [43]. Two of those qualities are examined in some detail across all three studies: goals and emotions. Goals relate both to a person's cognitive control, and to the reward structure of an event, while emotions refer to the emotional associations and responses involved. I refer to both these features as part of the "internal context" of an event, as opposed to externally observable contexts such as space. Both features are known to impact what the brain remembers, and how it remembers it [256, 257, 258].

Goal-directed behavior has long been known to influence hippocampal neuronal activity. Early work by Jim Ranck (preceding the publication of the first place-cell paper) demonstrated that subsets of hippocampal complex-spike cells discharge during appetitive approach or consumption in a task during which food, milk, and water-rewards were consistently associated with particular locations [259]. This work, and much that followed, has shown that internal states relating to goals, motivations, intentions, and emotions, might play a role in hippocampal processes relating to both space and memory [260, 54, 261]. Both Chapter 2 and Chapter 3 feature some influence of a person's goals on the neuronal activity underlying some basic spatial or memory computation. Memory-trace cells only activate when a person is approaching their current target; goal-state phase

precession only occurs while moving towards one goal and not towards others. These findings converge with a growing body of work demonstrating a role for mid-brain reward circuitry and prefrontal executive control in MTL activity relating to memory and spatial navigation [262, 263].

In Chapter 4, I address this question most directly. Chapter 4 is primarily concerned with the influence of emotional salience on memory encoding. Emotional context is a difficult variable to access in animal models. A majority of the work relies on conditioning paradigms in which a conditioned stimulus leads to memory retrieval measured by a conditioned response. By utilizing fear stimuli (such as shocks), researchers study "fear memories" in animals. But emotion, particularly in humans, spans a wide range of valence and arousal and these factors impact many important elements of human cognition such as attention, learning, and memory[264]. In Chapter 4 we identified the network-level neuronal circuits involved in the encoding of memories with different emotional contexts. We found that gamma oscillations in both the hippocampus and amygdala increased during successful memory encoding for more arousing words, and that bi-directional theta-gamma PAC between these regions also differentiated between memories that were subsequently recalled vs. forgotten. Furthermore, applying electrical stimulation to the hippocampus selectively impaired recall for highly arousing words. However, two open questions remain, that future directions of this work will seek to answer. To assess whether these neuronal dynamics uniquely relate to memory encoding processes, we will analyze these patterns in relation to the retrieval period, when subjects actually performed recall. Significant correlation between encoding and retrieval dynamics would instead suggest that the amygdala-hippocampal circuit is involved more broadly throughout encoding, storage, and retrieval. Second, in order to more carefully assess the neuronal mechanisms involved, we will analyze single-neuron data recorded from the amygdala and hippocampus during this task and measure their rate- and phase- coding with respect to emotional context during encoding and retrieval. Doing so may reveal the underlying neuronal mechanisms involved with the network-level observations described in Chapter 4.

By demonstrating a potential role for the amygdala-hippocampal circuit in memory for words with different levels of arousal and valence, and showing that electrical stimulation disrupted these

memories, Chapter 4 illustrates a wider network for human memory processes integrated with internal context. The amygdala is also a region affected by Alzheimer's, and is often also lesioned in amnesiac patients. In this way, it is possible then that diseases affecting the connectivity between the amygdala and the hippocampus could affect memory for events with emotional context. This latter effect is particularly important for studying potential stimulation treatments for memory disorders, especially as amygdala stimulation has been shown to improve memory under certain valence conditions [221].

5.2 Future directions

5.2.1 Investigating memory independent of space

Spatial context has been a key aspect of understanding memory and has enabled a litany of discoveries in the the neuronal basis of memory. The general hypothesis binding space and memory together in the brain relies on two possible relationships between the two domains: that spatial context is a fundamental feature of events in episodic memory, and/or that spatial representations may be abstracted to represent knowledge for semantic memory. Chapters 2 and 3 focused primarily on the former hypothesis, recapitulating and extending the lessons of decades of rodent research examining the link between spatial context and memory in the brain. However, as I begin to show in Chapter 4, we now possess a broader understanding of these systems and a broader set of experimental tools to examine the brain signals involved in memory more generally in humans, and in relation to non-spatial features of experience. Non-spatial features have already been shown to engage similar brain circuits as spatial features [128], suggesting common mechanisms across domains in service of memory.

Overall, the work in this thesis posits that MTL neuronal representations are important for general "maps" of knowledge and experiences that modulate the neuronal circuits involved in memory [25]. For example, imaging work has begun to show, broadly, that MTL activity is correlated with abstract inferential processes probing knowledge of relational structure [265, 127]. Direct recordings in humans should next record the neuronal patterns identified in this work (spatially-tuned

single neurons, phase precession, local network oscillations) in relation to non-spatial stimuli and tasks. In order to do so, a future aim of my research is to carefully analyze correlated neuronal activity across brain regions thought to be involved in the abstraction of these representational principles beyond space. These regions include prefrontal cortex, amygdala, parahippocampal areas, and temporal lobe—all regions that are often covered by electrodes in epilepsy patients. To investigate the abstraction of these principles, I also aim to design tasks that allow us to measure neuronal activity in these regions while subjects perform tasks requiring higher levels of cognition or training than is possible in animal models, so that we may further tease out the unique aspects of human cognition and memory that emerges from these neuronal patterns.

5.2.2 Technology for invasive measurements of neuronal activity in humans

One primary future direction of research into the neuronal basis of human cognition is to record more neurons simultaneously. Many aspects of cognition we care about may be sparsely coded by a few, distributed neurons, which can be difficult to capture without extensive coverage of the brain area. The hippocampus, in particular, tends to yield fewer active neurons than other regions, such as the amygdala [266, 267]. As such, we are unable to assess the existence of important ensemble-level phenomena, such as theta sequences, a coordination of place-cell firing across a group of place cells, which is thought to represent a critical juncture between space and memory coding [268]. Furthermore, ensemble representations may hold great value for understanding how conjunctive rate codes are represented in the brain for complex, abstract aspects of cognition [269]. A significant amount of research has also demonstrated that ensembles of neurons exhibit emergent coding properties that are absent from individual neurons [270]. Increasing the number of neurons recorded from these regions thus has great scientific value - technological advances in animal electrophysiology have resulted in the ability to simultaneously record upwards of 10,000 neurons in a single animal. However, increasing the number of electrodes is difficult in present stereotactic EEG surgical paradigms, without potentially compromising patient health. Adding microwires along the shank would lead to electrode termination in tissue that may not be resected,

potentially damaging healthy brain tissue. Increasing the diameter of the micro-macro electrode used would lead to larger burr holes, as well as a greater risk of damage to brain tissue and vasculature. Decreasing the size of the electrodes, in order to fit more into the bundle, would increase the risk of breakage. For this reason, few alternative designs have emerged [271, 267]. Future technologies may instead implement mixed designs with microwires emerging from the tip of the electrode as well as along the length of the shaft. Not only would this design increase yield, but the stereotyped organization of wires along the shaft may enable improved spike-sorting utilizing the relative spatial position of the wires.

Another important direction for future research is to better untangle the neuronal circuits involved in human cognition. Currently, this is done primarily through analyzing synchrony between signals recorded at distal locations (as in Chapter 4), but this does not provide direct evidence of a functional connection between regions. However, it is often not an option to record data from other regions we might care about, because recording locations depend on the clinical indications for each patient. Therefore, one solution will be to measure a direct physiological indicator of inter-regional functional communication, particularly neurotransmitter concentrations. One emerging and promising technology that may be integrated with current micro-wire probes is fast-scan cyclic voltammetry (FSCV). FSCV utilizes applied current to detect changes in electrochemical concentrations, and can be used to measure fast fluctuations in important neurochemicals such as dopamine. Dopaminergic terminals in the MTL come from regions like the locus ceruleus and ventral tegmental area—regions in which electrodes are almost never placed [272]. FSCV has been utilized in human deep-brain stimulation cases to measure dopamine in the striatal system, and future work may integrate FSCV with micro-wire recordings for use in epilepsy patients [273]. For example, we show in Chapter 4 that word arousal is tightly related to neural correlates of memory. Arousal is thought to influence human memory via neural activity in the amygdala, and the adrenergic system, which we may be able to track by measuring the concentration of epinephrine/norepinephrine in the amygdala [274]. Furthermore, measuring dopamine in the MTL during goal-directed navigation may help us better understand how goals modulate the cognitive

map, and measuring acetylcholine in concert with LFP data may further untangle how network level rhythms correspond to memory [275, 263]. In this way we may be able to better untangle neural circuits involved in memory.

Conclusion

Overall, my work has examined the electrophysiological basis for spatial cognition and memory in humans. By leveraging direct-brain recordings and carefully designed experimental tasks, I have generalized fundamental electrophysiological findings from animal research and demonstrated how the same signals and brain regions may more broadly be involved with memory. These experiments have produced new findings into the neuronal patterns binding space and memory in the entorhinal cortex, new, widespread patterns of phase-coding for space and goals, and the amygdala-hippocampal circuit involved in episodic memory encoding. Further pursuit of this research should continue to yield valuable insights into how the human brain represents memories.

References

[1] A. Association, *Alzheimer's disease facts and figures*. Chicago, 2020.

[2] N. Burgess, "The hippocampus, space, and viewpoints in episodic memory," *The Quarterly Journal of Experimental Psychology Section A*, vol. 55, no. 4, pp. 1057–1080, 2002.

[3] H. Eichenbaum, "Still searching for the engram," *Learn Behav*, vol. 44, no. 3, pp. 209–22, Sep. 2016.

[4] H. Eichenbaum and N. J. Cohen, "Can we reconcile the declarative memory and spatial navigation views on hippocampal function?" *Neuron*, vol. 83, no. 4, pp. 764–70, 2014.

[5] G. Buzsaki and E. Moser, "Memory, navigation and theta rhythm in the hippocampal-entorhinal system," *Nature Neuroscience*, vol. 16, no. 2, pp. 130–138, 2013.

[6] K. O. Johnson, "Neural coding," *Neuron*, vol. 26, no. 3, pp. 563–6, 2000.

[7] J. L. Cummings, T. Morstorf, and K. Zhong, "Alzheimer's disease drug-development pipeline: Few candidates, frequent failures," *Alzheimers Res Ther*, vol. 6, no. 4, p. 37, 2014.

[8] M. Piccolino, "Luigi galvani's path to animal electricity," *C R Biol*, vol. 329, no. 5-6, pp. 303–18, 2006.

[9] B. P. Bean, "The action potential in mammalian central neurons," *Nat Rev Neurosci*, vol. 8, no. 6, pp. 451–65, 2007.

[10] B. Renshaw, A. Forbes, and B. R. Morison, "Activity of isocortex and hippocampus: Electrical studies with micro-electrodes," *Journal of Neurophysiology*, vol. 3, no. 1, pp. 74–105, 1940. eprint: `https://doi.org/10.1152/jn.1940.3.1.74`.

[11] G. Buzsaki, C. Anastassiou, and C. Koch, "The origin of extracellular fields and currents - eeg, ecog, lfp and spikes," *Nature Reviews Neuroscience*, vol. 13, pp. 407–419, 2012.

[12] H. G. Rey, C. Pedreira, and R. Quian Quiroga, "Past, present and future of spike sorting techniques," *Brain Res Bull*, vol. 119, no. Pt B, pp. 106–17, 2015.

[13] H. Berger, "Über das Elektrenkephalogramm des menschen (On the human electroencephalogram)," *Archiv für Psychiatry und Nervenkrankheiten*, vol. 87, pp. 527–570, 1929.

[14] A. Puce and M. S. Hämäläinen, "A review of issues related to data acquisition and analysis in eeg/meg studies," *Brain Sci*, vol. 7, no. 6, 2017.

[15] G. H. Glover, "Overview of functional magnetic resonance imaging," *Neurosurg Clin N Am*, vol. 22, no. 2, pp. 133–9, vii, 2011.

[16] R. A. Poldrack, C. I. Baker, J. Durnez, K. J. Gorgolewski, P. M. Matthews, M. R. Munafò, T. E. Nichols, J.-B. Poline, E. Vul, and T. Yarkoni, "Scanning the horizon: Towards transparent and reproducible neuroimaging research," *Nat Rev Neurosci*, vol. 18, no. 2, pp. 115–126, Feb. 2017.

[17] A. A. Ward and L. B. Thomas, "The electrical activity of single units in the cerebral cortex of man.," *Electroencephalography and Clinical Neurophysiology*, vol. 7, no. 1, pp. 135–136, 1955.

[18] A. Chari, R. C. Thornton, M. M. Tisdall, and R. C. Scott, "Microelectrode recordings in human epilepsy: A case for clinical translation," *Brain Commun*, vol. 2, no. 2, fcaa082, 2020.

[19] H. Eichenbaum, A. Yonelinas, and C. Ranganath, "The medial temporal lobe and recognition memory," *Annual Review of Neuroscience*, vol. 30, pp. 123–152, 2007.

[20] T. A. Allen and N. J. Fortin, "The evolution of episodic memory," *Proc Natl Acad Sci U S A*, vol. 110 Suppl 2, pp. 10 379–86, 2013.

[21] E. C. Tolman, "Cognitive maps in rats and men," *Psychology Review*, vol. 55, pp. 189–208, 1948.

[22] J. O'Keefe and J. Dostrovsky, "The hippocampus as a spatial map: Preliminary evidence from unit activity in the freely-moving rat," *Brain Research*, vol. 34, pp. 171–175, 1971.

[23] J. O'Keefe, "A review of hippocampal place cells," *Prog Neurobiol*, vol. 13, no. 4, pp. 419–439, 1979.

[24] T. Hafting, M. Fyhn, S. Molden, M.-B. Moser, and E. I. Moser, "Microstructure of a spatial map in the entorhinal cortex.," *Nature*, vol. 436, pp. 801–806, 2005.

[25] T. E. J. Behrens, T. H. Muller, J. C. R. Whittington, S. Mark, A. B. Baram, K. L. Stachenfeld, and Z. Kurth-Nelson, "What is a cognitive map? organizing knowledge for flexible behavior," *Neuron*, vol. 100, no. 2, pp. 490–509, 2018.

[26] E. I. Moser, M.-B. Moser, and B. L. McNaughton, "Spatial representation in the hippocampal formation: A history," *Nat Neurosci*, vol. 20, no. 11, pp. 1448–1464, 2017.

[27] G. Buzsáki, "Theta rhythm of navigation: Link between path integration and landmark navigation, episodic and semantic memory," *Hippocampus*, vol. 15, pp. 827–840, 2005.

[28] J. O'Keefe and M. L. Recce, "Phase relationship between hippocampal place units and the EEG theta rhythm.," *Hippocampus*, vol. 3, pp. 317–30, 1993.

[29] E. T. Reifenstein and R. Kempter, "Synaptic learning rules for sequence learning," *bioRxiv*, 2020. eprint: `https://www.biorxiv.org/content/early/2020/04/15/2020.04.13.039826.full.pdf`.

[30] R. G. Morris, P Garrud, J. N. Rawlins, and J O'Keefe, "Place navigation impaired in rats with hippocampal lesions," *Nature*, vol. 297, no. 5868, pp. 681–3, 1982.

[31] A McGregor, A. J. Hayward, J. M. Pearce, and M. A. Good, "Hippocampal lesions disrupt navigation based on the shape of the environment," *Behav Neurosci*, vol. 118, no. 5, pp. 1011–21, 2004.

[32] A. D. Ekstrom, M. J. Kahana, J. B. Caplan, T. A. Fields, E. A. Isham, E. L. Newman, and I. Fried, "Cellular networks underlying human spatial navigation," *Nature*, vol. 425, pp. 184–187, 2003.

[33] J. Jacobs, C. T. Weidemann, J. F. Miller, A. Solway, J. F. Burke, X. Wei, N. Suthana, M. R. Sperling, A. D. Sharan, I. Fried, and M. J. Kahana, "Direct recordings of grid-like neuronal activity in human spatial navigation," *Nature Neuroscience*, vol. 16, no. 9, pp. 1188–1190, 2013.

[34] J. F. Miller, M. Neufang, A. Solway, A. Brandt, M. Trippel, I. Mader, S. Hefft, M. Merkow, S. M. Polyn, J. Jacobs, M. J. Kahana, and A. Schulze-Bonhage, "Neural activity in human hippocampal formation reveals the spatial context of retrieved memories," *Science*, vol. 342, no. 6162, pp. 1111–1114, 2013.

[35] R. A. Epstein, E. Z. Patai, J. B. Julian, and H. J. Spiers, "The cognitive map in humans: Spatial navigation and beyond," *Nat Neurosci*, vol. 20, no. 11, pp. 1504–1513, Oct. 2017.

[36] T. Hartley, E. Maguire, H. Spiers, and N. Burgess, "The well-worn route and the path less traveled: Distinct neural bases of route following and wayfinding in humans," *Neuron*, vol. 37, no. 5, pp. 877–888, 2003.

[37] G. Iaria, M. Petrides, A. Dagher, B. Pike, and V. Bohbot, "Cognitive strategies dependent on the Hippocampus and Caudate Nucleus in human navigation: Variability and change with practice," *Journal of Neuroscience*, vol. 23, no. 13, pp. 5945–5952, 2003.

[38] N. Suthana, A. D. Ekstrom, S. Moshirvaziri, B. J. Knowlton, and S. Y. Bookheimer, "Human hippocampal ca1 involvement during allocentric encoding of spatial information," *Journal of Neuroscience*, 2009.

[39] L. K. Morgan, S. P. MacEvoy, G. K. Aguirre, and R. A. Epstein, "Distances between real-world locations are represented in the human hippocampus," *Journal of Neuroscience*, vol. 31, no. 4, pp. 1238–1245, 2011.

[40] C. F. Doeller, J. A. King, and N. Burgess, "Parallel striatal and hippocampal systems for landmarks and boundaries in spatial memory," *Proceedings of the National Academy of Sciences, USA*, vol. 105, no. 15, pp. 5915–5920, 2008.

[41] S. Maidenbaum, J. Miller, J. M. Stein, and J. Jacobs, "Grid-like hexadirectional modulation of human entorhinal theta oscillations," *Proc Natl Acad Sci U S A*, vol. 115, no. 42, pp. 10 798–10 803, Oct. 2018.

[42] L. R. Squire, R. E. Clark, and P. J. Bayley, *The Cognitive Neurosciences*, M. S. Gazzaniga, Ed. Cambridge, MA, US: MIT Press, 2004.

[43] E. Tulving, "Episodic memory: From mind to brain.," vol. 53, pp. 1–25, 2002.

[44] B. C. Dickerson and H. Eichenbaum, "The episodic memory system: Neurocircuitry and disorders," *Neuropsychopharmacology*, vol. 35, no. 1, pp. 86–104, 2010.

[45] P GLEES and H. B. GRIFFITH, "Bilateral destruction of the hippocampus (cornu ammonis) in a case of dementia," *Monatsschr Psychiatr Neurol*, vol. 123, no. 4-5, pp. 193–204, 1952.

[46] B. A. Strange, M. P. Witter, E. S. Lein, and E. I. Moser, "Functional organization of the hippocampal longitudinal axis," *Nature Reviews Neuroscience*, vol. 15, no. 10, pp. 655–669, 2014.

[47] A Jeewajee, C Barry, V Douchamps, D Manson, C Lever, and N Burgess, "Theta phase precession of grid and place cell firing in open environments," *Philos Trans R Soc Lond B Biol Sci*, vol. 369, no. 1635, p. 20 120 532, 2014.

[48] S Corkin, D. G. Amaral, R. G. González, K. A. Johnson, and B. T. Hyman, "H. m.'s medial temporal lobe lesion: Findings from magnetic resonance imaging," *J Neurosci*, vol. 17, no. 10, pp. 3964–79, 1997.

[49] L. R. Squire, "Memory and brain systems: 1969-2009," *J Neurosci*, vol. 29, no. 41, pp. 12 711–6, 2009.

[50] R. S. Rosenbaum, S. Köhler, D. L. Schacter, M. Moscovitch, R. Westmacott, S. E. Black, F. Gao, and E. Tulving, "The case of k.c.: Contributions of a memory-impaired person to memory theory," *Neuropsychologia*, vol. 43, no. 7, pp. 989–1021, 2005.

[51] S. J. Babb and J. D. Crystal, "Episodic-like memory in the rat," *Curr Biol*, vol. 16, no. 13, pp. 1317–21, 2006.

[52] A. Johnson and A. Redish, "Dynamic representations in the hippocampus: Implications for navigation and memory," *Computational and Systems Neuroscience (Coysne)*, 2007.

[53] A. Tsao, M.-B. Moser, and E. I. Moser, "Traces of experience in the lateral entorhinal cortex," *Current Biology*, 2013.

[54] E. R. Wood, P. A. Dudchenko, R. J. Robitsek, and H. Eichenbaum, "Hippocampal neurons encode information about different types of memory episodes occurring in the same location," *Neuron*, vol. 27, pp. 623–633, 2000.

[55] D. Dupret, J. O'Neill, B. Pleydell-Bouverie, and J. Csicsvari, "The reorganization and reactivation of hippocampal maps predict spatial memory performance," *Nat Neurosci*, vol. 13, no. 8, pp. 995–1002, 2010.

[56] G. de Lavilléon, M. M. Lacroix, L. Rondi-Reig, and K. Benchenane, "Explicit memory creation during sleep demonstrates a causal role of place cells in navigation," *Nature neuroscience*, vol. 4, 2015.

[57] E. Pastalkova, V. Itskov, A. Amarasingham, and G. Buzsáki, "Internally generated cell assembly sequences in the rat hippocampus," *Science*, vol. 321, pp. 1322 –1327, 2008.

[58] C. MacDonald, K. Lepage, U. Eden, and H. Eichenbaum, "Hippocampal "time cells" bridge the gap in memory for discontiguous events," *Neuron*, vol. 71, no. 4, pp. 737–749, 2011.

[59] A. Tsao, J. Sugar, L. Lu, C. Wang, J. J. Knierim, M.-B. Moser, and E. I. Moser, "Integrating time from experience in the lateral entorhinal cortex," *Nature*, vol. 561, no. 7721, pp. 57–62, Sep. 2018.

[60] J. Spaniol, P. S. Davidson, A. S. Kim, H. Han, M. Moscovitch, and C. L. Grady, "Event-related fmri studies of episodic encoding and retrieval: Meta-analyses using activation likelihood estimation," *Neuropsychologia*, vol. 47, no. 8, pp. 1765–1779, 2009.

[61] B. A. Kirchhoff, A. D. Wagner, A. Maril, and C. E. Stern, "Prefrontal-temporal circuitry for episodic encoding and subsequent memory," *Journal of Neuroscience*, vol. 20, no. 16, pp. 6173–6180, 2000.

[62] L. Davachi and A. D. Wagner, "Hippocampal contributions to episodic encoding: Insights from relational and item-based learning," *J Neurophysiol*, vol. 88, no. 2, pp. 982–90, 2002.

[63] M. Uncapher and M. Rugg, "Effects of divided attention on fMRI correlates of memory encoding," *Journal of cognitive neuroscience*, vol. 17, no. 12, pp. 1923–1935, 2005.

[64] M. J. Chadwick, D. Hassabis, N. Weiskopf, and E. A. Maguire, "Decoding individual episodic memory traces in the human hippocampus," *Current Biology*, vol. 20, no. 6, pp. 544–547, 2010.

[65] J. Rissman, T. E. Chow, N. Reggente, and A. D. Wagner, "Decoding fmri signatures of real-world autobiographical memory retrieval," *J Cogn Neurosci*, vol. 28, no. 4, pp. 604–20, 2016.

[66] D. M. Nielson, T. A. Smith, V. Sreekumar, S. Dennis, and P. B. Sederberg, "Human hippocampus represents space and time during retrieval of real-world memories," *Proceedings of the National Academy of Sciences*, vol. 112, no. 35, pp. 11 078–11 083, 2015.

[67] M. Crespo-García, M. Zeiller, C. Leupold, G. Kreiselmeyer, S. Rampp, H. M. Hamer, and S. S. Dalal, "Slow-theta power decreases during item-place encoding predict spatial accuracy of subsequent context recall," *NeuroImage*, 2016.

[68] P. H. Crandall, R. Walter, and R. W. Rand, "Clinical applications of studies on stereotactically implanted electrodes in temporal-lobe epilepsy.," *Journal of Neurosurgery*, vol. 20, pp. 827–840, 1963.

[69] E. Halgren, T. L. Babb, and P. H. Crandall, "Activity of human hippocampal formation and amygdala neurons during memory testing," *Electroencephalography and Clinical Neurophysiology*, vol. 45, pp. 585–601, 1978.

[70] G. Heit, M. E. Smith, and E. Halgren, "Neuronal activity in the human medial temporal lobe during recognition memory," *Brain*, vol. 113, pp. 1093–1112, 1990.

[71] H. Gelbard-Sagiv, R. Mukamel, M. Harel, R. Malach, and I. Fried, "Internally generated reactivation of single neurons in human hippocampus during free recall," *Science*, vol. 3, pp. 96–101, 2008.

[72] J. F. Miller, I. Fried, N. Suthana, and J. Jacobs, "Repeating spatial activations in human entorhinal cortex," *Current Biology*, 2015.

[73] U. Rutishauser, I. Ross, A. Mamelak, and E. Schuman, "Human memory strength is predicted by theta-frequency phase-locking of single neurons," *Nature*, vol. 464, no. 7290, pp. 903–907, 2010.

[74] J. Kamiński, A. Brzezicka, A. N. Mamelak, and U. Rutishauser, "Combined phase-rate coding by persistently active neurons as a mechanism for maintaining multiple items in working memory in humans," *Neuron*, vol. 106, no. 2, 256–264.e3, 2020.

[75] W. B. Scoville and B. Milner, "Loss of recent memory after bilateral hippocampal lesions," *Journal of Neurology, Neurosurgreery, and Psychiatry*, vol. 20, pp. 11–21, 1957.

[76] L. R. Squire, B. Knowlton, and G. Musen, "The structure and organization of memory," *Annual Review of Psychology*, vol. 44, pp. 453–495, 1993.

[77] J. O'Keefe and L. Nadel, *The hippocampus as a cognitive map*. New York: Oxford University Press, 1978.

[78] S. Leutgeb, J. K. Leutgeb, A. Treves, M.-B. Moser, and E. I. Moser, "Distinct ensemble codes in hippocampal areas ca3 and ca1," *Science*, vol. 305, no. 5688, pp. 1295–1298, 2004.

[79] L. Colgin, E. Moser, and M. Moser, "Understanding memory through hippocampal remapping," *Trends in Neurosciences*, vol. 31, no. 9, pp. 469–477, 2008.

[80] E. J. Markus, Y. L. Qin, B. Leonard, W. E. Skaggs, B. L. McNaughton, and C. A. Barnes, "Interactions between location and task affect the spatial and directional firing of hippocampal neurons," *Journal of Neuroscience*, vol. 15, no. 11, p. 7079, 1995.

[81] J. L. Gauthier and D. W. Tank, "A dedicated population for reward coding in the hippocampus," *Neuron*, vol. 99, no. 1, 179–193.e7, 2018.

[82] J. Sugar and M.-B. Moser, "Episodic memory: Neuronal codes for what, where, and when," *Hippocampus*, 2019.

[83] V. Brun, M. Otnæss, S. Molden, H. Steffenach, M. Witter, M. Moser, and E. Moser, "Place cells and place recognition maintained by direct entorhinal-hippocampal circuitry," *Science*, vol. 296, no. 5576, p. 2243, 2002.

[84] O. Y. Chao, J. P. Huston, J.-S. Li, A.-L. Wang, and M. A. de Souza Silva, "The medial prefrontal cortex-lateral entorhinal cortex circuit is essential for episodic-like memory and associative object-recognition," *Hippocampus*, vol. 26, no. 5, pp. 633–45, 2016.

[85] J. J. Knierim, J. P. Neunuebel, and S. S. Deshmukh, "Functional correlates of the lateral and medial entorhinal cortex: Objects, path integration and local-global reference frames," *Philos Trans R Soc Lond B Biol Sci*, vol. 369, no. 1635, p. 20 130 369, 2014.

[86] L. Kunz, T. N. Schröder, H. Lee, C. Montag, B. Lachmann, R. Sariyska, M. Reuter, R. Stirnberg, T. Stöcker, P. C. Messing-Floeter, *et al.*, "Reduced grid-cell–like representations in adults at genetic risk for alzheimer's disease," *Science*, vol. 350, no. 6259, pp. 430–433, 2015.

[87] W. N. Butler, K. Hardcastle, and L. M. Giocomo, "Remembered reward locations restructure entorhinal spatial maps," *Science*, vol. 363, no. 6434, pp. 1447–1452, 2019. eprint: `http://science.sciencemag.org/content/363/6434/1447.full.pdf`.

[88] I. Fried, C. Wilson, N. Maidment, J. J. Engel, E. Behnke, T. Fields, K. MacDonald, J. Morrow, and L. Ackerson, "Cerebral microdialysis combined with single-neuron and electroencephalographic recording in neurosurgical patients," *Journal of Neurosurgery*, vol. 91, pp. 697–705, 1999.

[89] J. Niediek, J. Boström, C. E. Elger, and F. Mormann, "Reliable analysis of single-unit recordings from the human brain under noisy conditions: Tracking neurons over hours," *PLoS One*, vol. 11, no. 12, e0166598, 2016.

[90] D. Hill, S. Mehta, and D. Kleinfeld, "Quality metrics to accompany spike sorting of extracellular signals," *Journal of Neuroscience*, vol. 31, no. 24, pp. 8699–8705, 2011.

[91] A. B. Valdez, E. N. Hickman, D. M. Treiman, K. A. Smith, and P. N. Steinmetz, "A statistical method for predicting seizure onset zones from human single-neuron recordings," *J Neural Eng*, vol. 10, no. 1, p. 016 001, 2013.

[92] J. Jacobs, J. Miller, S. A. Lee, T. Coffey, A. J. Watrous, M. R Sperling, A. Sharan, G. Worrell, B. Berry, B. Lega, B. Jobst, K. Davis, R. E. Gross, S. A. Sheth, Y. Ezzyat, S. R. Das, J. Stein, R. Gorniak, M. J. Kahana, and D. S. Rizzuto, "Direct electrical stimulation of the human entorhinal region and hippocampus impairs memory," *Neuron*, vol. 92, no. 5, pp. 1–8, 2016.

[93] H. Wang, J. W. Suh, S. R. Das, J. B. Pluta, C. Craige, P. Yushkevich, *et al.*, "Multi-atlas segmentation with joint label fusion," *Pattern Analysis and Machine Intelligence, IEEE Transactions on*, vol. 35, no. 3, pp. 611–623, 2013.

[94] P. A. Yushkevich, J. B. Pluta, H. Wang, L. Xie, S.-L. Ding, E. C. Gertje, L. Mancuso, D. Kliot, S. R. Das, and D. A. Wolk, "Automated volumetry and regional thickness analysis of hippocampal subfields and medial temporal cortical structures in mild cognitive impairment," *Human Brain Mapping*, vol. 36, no. 1, pp. 258–287, 2015.

[95] B. B. Avants, C. L. Epstein, M. Grossman, and J. C. Gee, "Symmetric diffeomorphic image registration with cross-correlation: Evaluating automated labeling of elderly and neurodegenerative brain," *Medical Image Analysis*, vol. 12, no. 1, pp. 26–41, 2008.

[96] J. Kamiński, S. Sullivan, J. M. Chung, I. B. Ross, A. N. Mamelak, and U. Rutishauser, "Persistently active neurons in human medial frontal and medial temporal lobe support working memory," *Nat Neurosci*, vol. 20, no. 4, pp. 590–601, Apr. 2017.

[97] S. Hollup, S. Molden, J. Donnett, M. Moser, and E. Moser, "Accumulation of hippocampal place fields at the goal location in an annular watermaze task," *Journal of Neuroscience*, vol. 21, no. 5, pp. 1635–1644, 2001.

[98] M Fyhn, S Molden, M. Witter, E. Moser, and M. Moser, "Spatial representation in the entorhinal cortex," *Science*, vol. 305, pp. 1258–1264, 2004.

[99] C. B. Alme, C. Miao, K. Jezek, A. Treves, E. I. Moser, and M.-B. Moser, "Place cells in the hippocampus: Eleven maps for eleven rooms," *Proc Natl Acad Sci U S A*, vol. 111, no. 52, pp. 18 428–35, 2014.

[100] R. Robitsek, J. White, and H Eichenbaum, "Place cell activation predicts subsequent memory," *Behavioural brain research*, 2013.

[101] K. H. Mauritz and S. P. Wise, "Premotor cortex of the rhesus monkey: Neuronal activity in anticipation of predictable environmental events," *Exp Brain Res*, vol. 61, no. 2, pp. 229–44, 1986.

[102] J. P. Lachaux, D Rudrauf, and P Kahane, "Intracranial EEG and human brain mapping," *Journal of Physiology-Paris*, vol. 97, no. 4–6, pp. 613–628, 2003.

[103] N. Wilming, P. König, S. König, and E. A. Buffalo, "Entorhinal cortex receptive fields are modulated by spatial attention, even without movement," *Elife*, vol. 7, 2018.

[104] P. W. Holland and R. E. Welsch, "Robust regression using iteratively reweighted least-squares," *Communications in Statistics: Theory and Methods*, vol. A6, pp. 813 –827, 1977.

[105] B. J. Kraus, M. P. Brandon, R. J. Robinson, M. A. Connerney, M. E. Hasselmo, and H. Eichenbaum, "During running in place, grid cells integrate elapsed time and distance run," *Neuron*, vol. 88, no. 3, pp. 578–589, 2015.

[106] E. Kropff, J. E. Carmichael, M.-B. Moser, and E. I. Moser, "Speed cells in the medial entorhinal cortex," *Nature*, vol. 523, no. 7561, pp. 419–24, 2015.

[107] K. Sakai and Y. Miyashita, "Neural organization for the long-term memory of paired associates," vol. 354, pp. 152–155, 1991.

[108] J O'Keefe and A Speakman, "Single unit activity in the rat hippocampus during a spatial memory task," *Exp Brain Res*, vol. 68, no. 1, pp. 1–27, 1987.

[109] W. E. Skaggs, B. L. McNaughton, K. M. Gothard, and E. J. Markus, "An information-theoretic approach to deciphering the hippocampal code," in *Advances in neural information processing systems*, S. J. Hanson, J. D. Cowan, and C. L. Giles, Eds., vol. 5, San Mateo, CA: Morgan Kaufmann, 1993, pp. 1030–1037.

[110] K. L. Stachenfeld, M. M. Botvinick, and S. J. Gershman, "The hippocampus as a predictive map," *Nat Neurosci*, vol. 20, no. 11, pp. 1643–1653, 2017.

[111] A. Sarel, A. Finkelstein, L. Las, and N. Ulanovsky, "Vectorial representation of spatial goals in the hippocampus of bats," *Science*, vol. 355, no. 6321, pp. 176–180, Jan. 2017.

[112] J. Theeuwes, A. F. Kramer, and D. E. Irwin, "Attention on our mind: The role of spatial attention in visual working memory," *Acta Psychol (Amst)*, vol. 137, no. 2, pp. 248–51, 2011.

[113] N. Kriegeskorte, "Pattern-information analysis: From stimulus decoding to computational-model testing," *Neuroimage*, vol. 56, no. 2, pp. 411–21, 2011.

[114] R. U. Muller and J. L. Kubie, "The effects of changes in the environment on the spatial firing of hippocampal complex-spike cells," vol. 7, no. 7, pp. 1951–1968, 1987.

[115] S. Leutgeb, J. K. Leutgeb, C. A. Barnes, E. I. Moser, B. L. McNaughton, and M.-B. Moser, "Independent codes for spatial and episodic memory in hippocampal neuronal ensembles," *Science*, vol. 309, no. 5734, pp. 619–623, 2005.

[116] S. N. Burke, A. P. Maurer, S. Nematollahi, A. R. Uprety, J. L. Wallace, and C. A. Barnes, "The influence of objects on place field expression and size in distal hippocampal ca1," *Hippocampus*, vol. 21, no. 7, pp. 783–801, 2011.

[117] W. A. Suzuki, E. K. Miller, and R. Desimone, "Object and place memory in the macaque entorhinal cortex," vol. 78, pp. 1062–1081, 1997.

[118] A. P. Weible, D. C. Rowland, R. Pang, and C. Kentros, "Neural correlates of novel object and novel location recognition behavior in the mouse anterior cingulate cortex," *J Neurophysiol*, vol. 102, no. 4, pp. 2055–68, 2009.

[119] A. Goyal, J. Miller, A. J. Watrous, S. A. Lee, T. Coffey, M. Sperling, A. Sharan, G. Worrell, B. Brent, B. Lega, *et al.*, "The medial temporal lobe organizes memory across time and space: Causal evidence from brain stimulation," *bioRxiv*, p. 215 806, 2017.

[120] H Braak and E Braak, "Neuropathological stageing of alzheimer-related changes," *Acta Neuropathol*, vol. 82, no. 4, pp. 239–59, 1991.

[121] T. Gomez-Isla, J. Price, D. McKeel Jr, J. Morris, J. Growdon, and B. Hyman, "Profound Loss of Layer II Entorhinal Cortex Neurons Occurs in Very Mild Alzheimer's Disease," *Journal of Neuroscience*, vol. 16, no. 14, p. 4491, 1996.

[122] H. I. L. Jacobs, T. Hedden, A. P. Schultz, J. Sepulcre, R. D. Perea, R. E. Amariglio, K. V. Papp, D. M. Rentz, R. A. Sperling, and K. A. Johnson, "Structural tract alterations predict downstream tau accumulation in amyloid-positive older individuals," *Nat Neurosci*, vol. 21, no. 3, pp. 424–431, 2018.

[123] A. Maass, S. N. Lockhart, T. M. Harrison, R. K. Bell, T. Mellinger, K. Swinnerton, S. L. Baker, G. D. Rabinovici, and W. J. Jagust, "Entorhinal tau pathology, episodic memory decline, and neurodegeneration in aging," *J Neurosci*, vol. 38, no. 3, pp. 530–543, 2018.

[124] H. Fu, G. A. Rodriguez, M. Herman, S. Emrani, E. Nahmani, G. Barrett, H. Y. Figueroa, E. Goldberg, S. A. Hussaini, and K. E. Duff, "Tau pathology induces excitatory neuron loss, grid cell dysfunction, and spatial memory deficits reminiscent of early alzheimer's disease," *Neuron*, vol. 93, no. 3, 533–541.e5, 2017.

[125] C. F. Doeller, C. Barry, and N. Burgess, "Evidence for grid cells in a human memory network," *Nature*, vol. 463, no. 7281, pp. 657–661, 2010.

[126] C. N. Boccara, M. Nardin, F. Stella, J. O'Neill, and J. Csicsvari, "The entorhinal cognitive map is attracted to goals," *Science*, vol. 363, no. 6434, pp. 1443–1447, 2019. eprint: `http://science.sciencemag.org/content/363/6434/1443.full.pdf`.

[127] A. O. Constantinescu, J. X. O'Reilly, and T. E. J. Behrens, "Organizing conceptual knowledge in humans with a gridlike code," *Science*, vol. 352, pp. 1464–1468, 2016.

[128] D. Aronov, R. Nevers, and D. W. Tank, "Mapping of a non-spatial dimension by the hippocampal–entorhinal circuit," *Nature*, vol. 543, no. 7647, p. 719, 2017.

[129] N. Burgess, E. Maguire, and J. O'Keefe, "The human hippocampus and spatial and episodic memory," *Neuron*, vol. 35, pp. 625–641, 2002.

[130] D. O. Hebb, *Organization of Behavior*. New York: Wiley, 1949.

[131] D. M. MacKay and W. S. McCulloch, "The limiting information capacity of a neuronal link," *The bulletin of mathematical biophysics*, vol. 14, no. 2, pp. 127–135, 1952.

[132] Y. J. Greenstein, C Pavlides, and J Winson, "Long-term potentiation in the dentate gyrus is preferentially induced at theta rhythm periodicity," *Brain Res*, vol. 438, no. 1-2, pp. 331–4, 1988.

[133] J. J. Hopfield, "Pattern recognition computation using action potential timing for stimulus representation," *Nature*, vol. 376, no. 6535, pp. 33–6, 1995.

[134] H. Markram, J. Lübke, M. Frotscher, and B. Sakmann, "Regulation of synaptic efficacy by coincidence of postsynaptic aps and epsps," *Science*, vol. 275, no. 5297, pp. 213–215, 1997.

[135] G Bi and M Poo, "Synaptic modification by correlated activity: Hebb's postulate revisited," *Annu Rev Neurosci*, vol. 24, pp. 139–66, 2001.

[136] A. Bragin, G. Jando, Z. Nadasdy, J. Hetke, K. Wise, and G. Buzsáki, "Gamma (40-100 Hz) oscillation in the hippocampus of the behaving rat," *Journal of Neuroscience*, vol. 15, pp. 47–60, 1995.

[137] J. J. Chrobak and G. Buzsáki, "Gamma oscillations in the entorhinal cortex of the freely behaving rat," vol. 18, no. 1, pp. 388–298, 1998.

[138] J. R. Manning, J. Jacobs, I. Fried, and M. J. Kahana, "Broadband shifts in local field potential power spectra are correlated with single-neuron spiking in humans," *Journal of Neuroscience*, vol. 29, no. 43, pp. 13 613–13 620, 2009.

[139] R. T. Canolty, K. Ganguly, S. W. Kennerley, C. F. Cadieu, K. Koepsell, J. D. Wallis, and J. M. Carmena, "Oscillatory phase coupling coordinates anatomically dispersed functional cell assemblies," *Proc Natl Acad Sci U S A*, vol. 107, no. 40, pp. 17 356–61, 2010.

[140] S. Zanos, T. P. Zanos, V. Z. Marmarelis, G. A. Ojemann, and E. E. Fetz, "Relationships between spike-free local field potentials and spike timing in human temporal cortex," *J Neurophysiol*, vol. 107, no. 7, pp. 1808–21, 2012.

[141] M. Siegel, M. Warden, and E. Miller, "Phase-dependent neuronal coding of objects in short-term memory," *Proceedings of the National Academy of Sciences, USA*, vol. 106, no. 50, p. 21 341, 2009.

[142] E. T. Reifenstein, R. Kempter, S. Schreiber, M. B. Stemmler, and A. V. M. Herz, "Grid cells in rat entorhinal cortex encode physical space with independent firing fields and phase precession at the single-trial level," *Proc Natl Acad Sci U S A*, vol. 109, no. 16, pp. 6301–6, 2012.

[143] J. Lisman and M. A. Idiart, "Storage of 7 ± 2 short-term memories in oscillatory subcycles," *Science*, vol. 267, pp. 1512–1515, 1995.

[144] W. E. Skaggs, B. L. McNaughton, M. A. Wilson, and C. A. Barnes, "Theta phase precession in hippocampal neuronal populations and the compression of temporal sequences," *Hippocampus*, vol. 6, pp. 149–172, 1996.

[145] M. A. A. van der Meer and A. D. Redish, "Theta phase precession in rat ventral striatum links place and reward information," *J Neurosci*, vol. 31, no. 8, pp. 2843–54, 2011.

[146] S. M. Kim, S. Ganguli, and L. M. Frank, "Spatial information outflow from the hippocampal circuit: Distributed spatial coding and phase precession in the subiculum," *J Neurosci*, vol. 32, no. 34, pp. 11 539–58, 2012.

[147] D. Tingley, A. S. Alexander, L. K. Quinn, A. A. Chiba, and D. Nitz, "Multiplexed oscillations and phase rate coding in the basal forebrain," *Sci Adv*, vol. 4, no. 8, eaar3230, Aug. 2018.

[148] M. W. Jones and M. A. Wilson, "Phase precession of medial prefrontal cortical activity relative to the hippocampal theta rhythm," *Hippocampus*, vol. 15, pp. 867–873, 2005.

[149] K. D. Harris, D. A. Henze, H. Hirase, X. Leinekugel, D. G., A. Czurko, and G Buzsáki, "Spike train dynamics predicts theta-related phase precession in hippocampal pyramidal cells," *Nature*, vol. 417, pp. 738–741, 2002.

[150] P.-P. Lenck-Santini, A. A. Fenton, and R. U. Muller, "Discharge properties of hippocampal neurons during performance of a jump avoidance task," *Journal of Neuroscience*, 2008.

[151] M. Takahashi, H. Nishida, A. D. Redish, and J. Lauwereyns, "Theta phase shift in spike timing and modulation of gamma oscillation: A dynamic code for spatial alternation during fixation in rat hippocampal area ca1," *J Neurophysiol*, vol. 111, no. 8, pp. 1601–14, 2014.

[152] S. Terada, Y. Sakurai, H. Nakahara, and S. Fujisawa, "Temporal and rate coding for discrete event sequences in the hippocampus," *Neuron*, vol. 94, no. 6, 1248–1262.e4, 2017.

[153] N. T. M. Robinson, J. B. Priestley, J. W. Rueckemann, A. D. Garcia, V. A. Smeglin, F. A. Marino, and H. Eichenbaum, "Medial entorhinal cortex selectively supports temporal coding by hippocampal neurons," *Neuron*, vol. 94, no. 3, 677–688.e6, 2017.

[154] N. Burgess, M. Recce, and J. O'Keefe, "A model of hippocampal function," *Neural Networks*, vol. 7, no. 6, pp. 1065 –1081, 1994, Models of Neurodynamics and Behavior.

[155] J. Lisman, "The theta/gamma discrete phase code occurring during the hippocampal phase precession may be a more general brain coding scheme," *Hippocampus*, vol. 15, pp. 913–922, 2005.

[156] J. Jaramillo and R. Kempter, "Phase precession: A neural code underlying episodic memory?" *Curr Opin Neurobiol*, vol. 43, pp. 130–138, Apr. 2017.

[157] K Mizuseki, A. Sirota, and G. Buzsáki, "Theta oscillations provide temporal windows for local circuit computation in the entorhinal-hippocampal loop," *Neuron*, vol. 64, pp. 267–280, 2009.

[158] K Mizuseki, A. Sirota, E. Pastalkova, and G. Buzsáki, "Multi-unit recordings from the rat hippocampus made during open field foraging.,"

[159] ——, "Multiple single unit recordings from different rat hippocampal and entorhinal regions while the animals were performing multiple behavioral tasks. crcns.org.,"

[160] J. Jacobs, M. J. Kahana, A. D. Ekstrom, and I. Fried, "Brain oscillations control timing of single-neuron activity in humans," *Journal of Neuroscience*, vol. 27, no. 14, pp. 3839–3844, 2007.

[161] A. J. Watrous, J. Miller, S. E. Qasim, I. Fried, and J. Jacobs, "Phase-tuned neuronal firing encodes human contextual representations for navigational goals," *eLife*, vol. 7, e32554, 2018.

[162] S. Russell and P. Norvig, *Artificial Intelligence: A Modern Approach*, 3rd ed. Prentice Hall, 2010.

[163] P. Virtanen, R. Gommers, T. E. Oliphant, M. Haberland, T. Reddy, D. Cournapeau, E. Burovski, P. Peterson, W. Weckesser, J. Bright, S. J. van der Walt, M. Brett, J. Wilson, K. J. Millman, N. Mayorov, A. R. J. Nelson, E. Jones, R. Kern, E. Larson, C. J. Carey, bibinitperiodI. Polat, Y. Feng, E. W. Moore, J. VanderPlas, D. Laxalde, J. Perktold, R. Cimrman, I. Henriksen, E. A. Quintero, C. R. Harris, A. M. Archibald, A. H. Ribeiro, F. Pedregosa, P. van Mulbregt, and SciPy 1.0 Contributors, "Scipy 1.0: Fundamental algorithms for scientific computing in python," *Nat Methods*, vol. 17, no. 3, pp. 261–272, Mar. 2020.

[164] S. Seabold and J. Perktold, "Statsmodels: Econometric and statistical modeling with python," in *9th Python in Science Conference*, 2010.

[165] J. D. Hunter, "Matplotlib: A 2d graphics environment," *Computing in Science & Engineering*, vol. 9, no. 3, pp. 90–95, 2007.

[166] M. Haller, T. Donoghue, E. Peterson, P. Varma, P. Sebastian, R. Gao, T. Noto, R. T. Knight, A. Shestyuk, and B. Voytek, "Parameterizing neural power spectra," *bioRxiv*, 2018. eprint: `https://www.biorxiv.org/content/early/2018/04/11/299859.full.pdf`.

[167] A. J. Watrous, D. J. Lee, A. Izadi, G. G. Gurkoff, K. Shahlaie, and A. D. Ekstrom, "A comparative study of human and rat hippocampal low-frequency oscillations during spatial navigation," *Hippocampus*, 2013.

[168] J. Jacobs, "Hippocampal theta oscillations are slower in humans than in rodents: Implications for models of spatial navigation and memory," *Philosophical Transactions of the Royal Society B: Biological Sciences*, vol. 369, no. 1635, p. 20 130 304, 2014.

[169] A. Goyal, J. Miller, S. E. Qasim, A. J. Watrous, H. Zhang, J. M. Stein, C. S. Inman, R. E. Gross, J. T. Willie, B. Lega, J.-J. Lin, A. Sharan, C. Wu, M. R. Sperling, S. A. Sheth, G. M. McKhann, E. H. Smith, C. Schevon, and J. Jacobs, "Functionally distinct high and low theta oscillations in the human hippocampus," *Nat Commun*, vol. 11, no. 1, p. 2469, 2020.

[170] N. Ulanovsky and C. Moss, "Hippocampal cellular and network activity in freely moving echolocating bats," *Nature*, pp. 224–233, 2007.

[171] M. Stewart and S. E. Fox, "Hippocampal theta activities in monkeys," *Brain Res.*, vol. 538, pp. 59–63, 1991.

[172] M. J. Jutras, P. Fries, and E. A. Buffalo, "Oscillatory activity in the monkey hippocampus during visual exploration and memory formation," *Proceedings of the National Academy of Sciences, USA*, 2013.

[173] T. Eliav, M. Geva-Sagiv, M. M. Yartsev, A. Finkelstein, A. Rubin, L. Las, and N. Ulanovsky, "Nonoscillatory phase coding and synchronization in the bat hippocampal formation," *Cell*, vol. 175, no. 4, 1119–1130.e15, Nov. 2018.

[174] A. Siapas, E. Lubenov, and M. Wilson, "Prefrontal phase locking to hippocampal theta oscillations," *Neuron*, vol. 46, pp. 141–151, 2005.

[175] S. Cole and B. Voytek, "Cycle-by-cycle analysis of neural oscillations," *J Neurophysiol*, vol. 122, no. 2, pp. 849–861, Aug. 2019.

[176] J. Huxter, T. Senior, K. Allen, and J. Csicsvari, "Theta phase–specific codes for two-dimensional position, trajectory and heading in the hippocampus," *Nature Neuroscience*, vol. 11, no. 5, pp. 587–594, 2008.

[177] R. Kempter, C. Leibold, G. Buzsáki, K. Diba, and R. Schmidt, "Quantifying circular–linear associations: Hippocampal phase precession," *Journal of Neuroscience Methods*, vol. 207, no. 1, pp. 113–124, 2012.

[178] P. Ravassard, A. Kees, B. Willers, D. Ho, D. Aharoni, J. Cushman, Z. M. Aghajan, and M. R. Mehta, "Multisensory control of hippocampal spatiotemporal selectivity," *Science*, vol. 340, no. 6138, pp. 1342–1346, 2013.

[179] Z. M. Aghajan, L. Acharya, J. J. Moore, J. D. Cushman, C. Vuong, and M. R. Mehta, "Impaired spatial selectivity and intact phase precession in two-dimensional virtual reality," *Nature neuroscience*, 2014.

[180] C. Geisler, D. Robbe, M. Zugaro, A. Sirota, and G. Buzsaki, "Hippocampal place cell assemblies are speed-controlled oscillators," *Proceedings of the National Academy of Sciences, USA*, vol. 104, no. 19, p. 8149, 2007.

[181] Y. Benjamini and Y. Hochberg, "Controlling the False Discovery Rate: A practical and powerful approach to multiple testing," *Journal of Royal Statistical Society, Series B*, vol. 57, pp. 289–300, 1995.

[182] J. Jacobs and M. J. Kahana, "Direct brain recordings fuel advances in cognitive electrophysiology," *Trends in Cognitive Sciences*, vol. 14, no. 4, pp. 162–171, 2010.

[183] B. C. Souza and A. B. L. Tort, "Asymmetry of the temporal code for space by hippocampal place cells," *Sci Rep*, vol. 7, no. 1, p. 8507, Aug. 2017.

[184] E. Reifenstein, M. Stemmler, A. V. M. Herz, R. Kempter, and S. Schreiber, "Movement dependence and layer specificity of entorhinal phase precession in two-dimensional environments," *PLoS One*, vol. 9, no. 6, e100638, 2014.

[185] N. I. Fisher, *Statistical Analysis of Circular Data*. Cambridge, England: Cambridge University Press, 1993.

[186] C. Harvey, F. Collman, D. Dombeck, and D. Tank, "Intracellular dynamics of hippocampal place cells during virtual navigation," *Nature*, vol. 461, pp. 941–946, 2009.

[187] D. Bush and N. Burgess, "Advantages and detection of phase coding in the absence of rhythmicity," *Hippocampus*, 2020.

[188] C. Geisler, K. Diba, E. Pastalkova, K. Mizuseki, S. Royer, and G. Buzsáki, "Temporal delays among place cells determine the frequency of population theta oscillations in the hippocampus," *Proceedings of the National Academy of Sciences, USA*, vol. 107, no. 17, pp. 7957–7962, 2010.

[189] S. J. Middleton, E. M. Kneller, S. Chen, I. Ogiwara, M. Montal, K. Yamakawa, and T. J. McHugh, "Altered hippocampal replay is associated with memory impairment in mice heterozygous for the scn2a gene," *Nat Neurosci*, vol. 21, no. 7, pp. 996–1003, Jul. 2018.

[190] R. Bourboulou, G. Marti, F.-X. Michon, E. El Feghaly, M. Nouguier, D. Robbe, J. Koenig, and J. Epsztein, "Dynamic control of hippocampal spatial coding resolution by local visual cues," *Elife*, vol. 8, Mar. 2019.

[191] P. C. Petersen and G. Buzsáki, "Cooling of medial septum reveals theta phase lag coordination of hippocampal cell assemblies," *Neuron*, 2020.

[192] T. I. Brown, V. A. Carr, K. F. LaRocque, S. E. Favila, A. M. Gordon, B. Bowles, J. N. Bailenson, and A. D. Wagner, "Prospective representation of navigational goals in the human hippocampus," *Science*, vol. 352, no. 6291, pp. 1323–6, 2016.

[193] H. S. Courellis, S. U. Nummela, M. Metke, G. W. Diehl, R. Bussell, G. Cauwenberghs, and C. T. Miller, "Spatial encoding in primate hippocampus during free navigation," *PLoS Biol*, vol. 17, no. 12, e3000546, Dec. 2019.

[194] S. Royer, A. Sirota, J. Patel, and G. Buzsáki, "Distinct representations and theta dynamics in dorsal and ventral hippocampus," *The Journal of neuroscience*, vol. 30, no. 5, pp. 1777–1787, 2010.

[195] M. I. Schlesiger, C. C. Cannova, B. L. Boublil, J. B. Hales, E. A. Mankin, M. P. Brandon, J. K. Leutgeb, C. Leibold, and S. Leutgeb, "The medial entorhinal cortex is necessary for temporal organization of hippocampal neuronal activity," *Nat Neurosci*, vol. 18, no. 8, pp. 1123–32, 2015.

[196] K. Safaryan and M. R. Mehta, "Enhanced hippocampal theta rhythmicity and emergence of eta oscillation in virtual reality," *bioRxiv*, 2020. eprint: `https://www.biorxiv.org/content/early/2020/06/30/2020.06.29.178186.full.pdf`.

[197] N. W. Schultheiss, M. Schlecht, M. Jayachandran, D. R. Brooks, J. L. McGlothan, T. R. Guilarte, and T. A. Allen, "Awake delta and theta-rhythmic hippocampal network modes during intermittent locomotor behaviors in the rat," *Behav Neurosci*, 2020.

[198] M. R. Mehta, A. K. Lee, and M. A. Wilson, "Role of experience and oscillations in transforming a rate code into a temporal code.," *Nature*, vol. 417, no. 6890, pp. 741–746, 2002.

[199] E. Moser, E. Kropff, and M. Moser, "Place cells, grid cells, and the brain's spatial representation system," *Annu Rev Neurosci*, vol. 31, pp. 69–89, 2008.

[200] A. M. Wikenheiser and A. D. Redish, "Hippocampal theta sequences reflect current goals," *Nat Neurosci*, vol. 18, no. 2, pp. 289–94, 2015.

[201] L. Meshulam, J. L. Gauthier, C. D. Brody, D. W. Tank, and W. Bialek, "Collective behavior of place and non-place neurons in the hippocampal network," *Neuron*, vol. 96, no. 5, 1178–1191.e4, 2017.

[202] S. E. Qasim, J. Miller, C. S. Inman, R. E. Gross, J. T. Willie, B. Lega, J.-J. Lin, A. Sharan, C. Wu, M. R. Sperling, S. A. Sheth, G. M. McKhann, E. H. Smith, C. Schevon, J. M. Stein, and J. Jacobs, "Memory retrieval modulates spatial tuning of single neurons in the human entorhinal cortex," *Nat Neurosci*, vol. 22, no. 12, pp. 2078–2086, Dec. 2019.

[203] J. Huxter, N Burgess, and J. O'Keefe, "Independent rate and temporal coding in hippocampal pyramidal cells," *Nature*, vol. 425, pp. 828–832, 2003.

[204] J. O'Keefe and N. Burgess, "Dual phase and rate coding in hippocampal place cells: Theoretical significance and relationship to entorhinal grid cells," *Hippocampus*, vol. 15, no. 7, pp. 853–866, 2005.

[205] H Hirase, A Czurkó, J Csicsvari, and G Buzsáki, "Firing rate and theta-phase coding by hippocampal pyramidal neurons during 'space clamping'," *Eur J Neurosci*, vol. 11, no. 12, pp. 4373–80, 1999.

[206] L. R. Howard, A. H. Javadi, Y. Yu, R. D. Mill, L. C. Morrison, R. Knight, M. M. Loftus, L. Staskute, and H. J. Spiers, "The hippocampus and entorhinal cortex encode the path and euclidean distances to goals during navigation," *Current Biology*, vol. 24, no. 12, pp. 1331–1340, 2014.

[207] D Debanne, B. H. Gähwiler, and S. M. Thompson, "Long-term synaptic plasticity between pairs of individual ca3 pyramidal cells in rat hippocampal slice cultures," *J Physiol*, vol. 507 (Pt 1), pp. 237–47, 1998.

[208] D Debanne, N. C. Guérineau, B. H. Gähwiler, and S. M. Thompson, "Physiology and pharmacology of unitary synaptic connections between pairs of cells in areas ca3 and ca1 of rat hippocampal slice cultures," *J Neurophysiol*, vol. 73, no. 3, pp. 1282–94, 1995.

[209] O. Jensen and J. E. Lisman, "Position reconstruction from an ensemble of hippocampal place cells: Contribution of theta phase coding," *J. Neurophysiol.*, vol. 83, pp. 2602–2609, 2000.

[210] N. Burgess, C. Barry, J. O'Keefe, and U. London, "An oscillatory interference model of grid cell firing," *Hippocampus*, vol. 17, no. 9, pp. 801–12, 2007.

[211] M. E. Hasselmo, "Grid cell mechanisms and function: Contributions of entorhinal persistent spiking and phase resetting," *Hippocampus*, vol. 18, no. 12, pp. 1213–1229, 2008.

[212] D. Reisberg and P. Hertel, *Memory and emotion*. Oxford: Oxford University Press, 2004, ISBN: 0195158563 (alk. paper).

[213] H Klüver and P. C. Bucy, "Preliminary analysis of functions of the temporal lobes in monkeys.," *J Neuropsychiatry Clin Neurosci*, vol. 9, no. 4, pp. 606–20, 1939.

[214] L WEISKRANTZ, "Behavioral changes associated with ablation of the amygdaloid complex in monkeys," *J Comp Physiol Psychol*, vol. 49, no. 4, pp. 381–91, 1956.

[215] S. P. Poulin, R. Dautoff, J. C. Morris, L. F. Barrett, B. C. Dickerson, and Alzheimer's Disease Neuroimaging Initiative, "Amygdala atrophy is prominent in early alzheimer's disease and relates to symptom severity," *Psychiatry Res*, vol. 194, no. 1, pp. 7–13, 2011.

[216] E. Tulving and H. J. Markowitsch, "Episodic and declarative memory: Role of the hippocampus," *Hippocampus*, vol. 8, pp. 198–204, 1998.

[217] R Adolphs, L Cahill, R Schul, and R Babinsky, "Impaired declarative memory for emotional material following bilateral amygdala damage in humans," *Learn Mem*, vol. 4, no. 3, pp. 291–300, 1997.

[218] J. G. Pelletier, E. Likhtik, M. Filali, and D. Paré, "Lasting increases in basolateral amygdala activity after emotional arousal: Implications for facilitated consolidation of emotional memories," *Learn Mem*, vol. 12, no. 2, pp. 96–102, 2005.

[219] S. A. Josselyn and S. Tonegawa, "Memory engrams: Recalling the past and imagining the future," *Science*, vol. 367, no. 6473, Jan. 2020.

[220] F. Dolcos, K. LaBar, and R. Cabeza, "Interaction between the amygdala and the medial temporal lobe memory system predicts better memory for emotional events," *Neuron*, vol. 42, no. 5, pp. 855–863, 2004.

[221] C. S. Inman, J. R. Manns, K. R. Bijanki, D. I. Bass, S. Hamann, D. L. Drane, R. E. Fasano, C. K. Kovach, R. E. Gross, and J. T. Willie, "Direct electrical stimulation of the amygdala enhances declarative memory in humans," *Proc Natl Acad Sci U S A*, vol. 115, no. 1, pp. 98–103, Jan. 2018.

[222] U. Rutishauser, E. Schuman, and A. Mamelak, "Activity of human hippocampal and amygdala neurons during retrieval of declarative memories.," *Proceedings of the National Academy of Sciences, USA*, vol. 105, no. 1, pp. 329–34, 2008.

[223] D. R. Schonhaut, A. G. Ramayya, E. A. Solomon, N. A. Herweg, I. Fried, and M. J. Kahana, "Single neurons throughout human memory regions phase-lock to hippocampal theta," *bioRxiv*, 2020. eprint: `https://www.biorxiv.org/content/early/2020/07/01/2020.06.30.180174.full.pdf`.

[224] H. J. Bowen, S. M. Kark, and E. A. Kensinger, "Never forget: Negative emotional valence enhances recapitulation," *Psychon Bull Rev*, vol. 25, no. 3, pp. 870–891, Jun. 2018.

[225] M. Friendly, P. E. Franklin, D. Hoffman, and D. C. Rubin, "The Toronto Word Pool: Norms for imagery, concreteness, orthographic variables, and grammatical usage for 1,080 words," *Behavior Research Methods and Instrumentation*, vol. 14, pp. 375–399, 1982.

[226] C. T. Weidemann, J. E. Kragel, B. C. Lega, G. A. Worrell, M. R. Sperling, A. D. Sharan, B. C. Jobst, F. Khadjevand, K. A. Davis, P. A. Wanda, A. Kadel, D. S. Rizzuto, and M. J. Kahana, "Neural activity reveals interactions between episodic and semantic memory systems during retrieval," *Journal of Experimental Psychology: General*, in press.

[227] J. F. Burke, N. M. Long, K. A. Zaghloul, A. D. Sharan, M. R. Sperling, and M. J. Kahana, "Human intracranial high-frequency activity maps episodic memory formation in space and time.," *NeuroImage*, vol. 85, pp. 834–843, 2014.

[228] T. E. Özkurt and A. Schnitzler, "A critical note on the definition of phase-amplitude cross-frequency coupling," *J Neurosci Methods*, vol. 201, no. 2, pp. 438–43, 2011.

[229] R. V. Shannon, "A model of safe levels for electrical stimulation," *Biomedical Engineering, IEEE Transactions on*, vol. 39, no. 4, pp. 424–426, 1992.

[230] Y. Ezzyat and D. S. Rizzuto, "Direct brain stimulation during episodic memory," *Current Opinion in Biomedical Engineering*, vol. 8, pp. 78–83, 2018.

[231] J. Posner, J. A. Russell, and B. S. Peterson, "The circumplex model of affect: An integrative approach to affective neuroscience, cognitive development, and psychopathology," *Dev Psychopathol*, vol. 17, no. 3, pp. 715–34, 2005.

[232] K. S. LaBar and R. Cabeza, "Cognitive neuroscience of emotional memory," *Nature Reviews Neuroscience*, vol. 7, no. 1, pp. 54–64, 2006.

[233] C. R. Madan, "Exploring word memorability: How well do different word properties explain item free-recall probability?" *Psychon Bull Rev*, 2020.

[234] A. Aka, T. D. Phan, and M. J. Kahana, "Predicting recall of words and lists," *J Exp Psychol Learn Mem Cogn*, 2020.

[235] N. M. Long, M. S. Danoff, and M. J. Kahana, "Recall dynamics reveal the retrieval of emotional context," *Psychonomic Bulletin and Review*, vol. 22, no. 5, pp. 1328–1333, 2015.

[236] K. A. Paller and A. D. Wagner, "Observing the transformation of experience into memory," *Trends in Cognitive Sciences*, vol. 6, no. 2, pp. 93–102, 2002.

[237] S. Prince, S. Daselaar, and R. Cabeza, "Neural Correlates of Relational Memory: Successful Encoding and Retrieval of Semantic and Perceptual Associations," *Journal of Neuroscience*, vol. 25, no. 5, pp. 1203–1210, 2005.

[238] P. B. Sederberg, A. Schulze-Bonhage, J. R. Madsen, E. B. Bromfield, D. C. McCarthy, A. Brandt, M. S. Tully, and M. J. Kahana, "Hippocampal and neocortical gamma oscillations predict memory formation in humans," *Cerebral Cortex*, vol. 17, no. 5, pp. 1190–1196, 2007.

[239] B. Lega, J. Jacobs, and M. Kahana, "Human hippocampal theta oscillations and the formation of episodic memories," *Hippocampus*, vol. 22, no. 4, pp. 748–761, 2012.

[240] N. M. Long, J. F. Burke, and M. J. Kahana, "Subsequent memory effect in intracranial and scalp EEG," *NeuroImage*, vol. 84, pp. 488–494, 2014.

[241] J. Zheng, K. L. Anderson, S. L. Leal, A. Shestyuk, G. Gulsen, L. Mnatsakanyan, S. Vadera, F. P. K. Hsu, M. A. Yassa, R. T. Knight, and J. J. Lin, "Amygdala-hippocampal dynamics during salient information processing," *Nat Commun*, vol. 8, p. 14 413, Feb. 2017.

[242] J. L. McGaugh, L Cahill, and B Roozendaal, "Involvement of the amygdala in memory storage: Interaction with other brain systems," *Proc Natl Acad Sci U S A*, vol. 93, no. 24, pp. 13 508–14, 1996.

[243] E. A. Solomon, B. C. Lega, M. R. Sperling, and M. J. Kahana, "Hippocampal theta codes for distances in semantic and temporal spaces," *Proc Natl Acad Sci U S A*, vol. 116, no. 48, pp. 24 343–24 352, Nov. 2019.

[244] S. Hamann and H. Mao, "Positive and negative emotional verbal stimuli elicit activity in the left amygdala," *Neuroreport*, vol. 13, no. 1, pp. 15–9, 2002.

[245] T. Seidenbecher, T. Laxmi, O. Stork, and H. Pape, "Amygdalar and hippocampal theta rhythm synchronization during fear memory retrieval," *Science*, vol. 301, no. 5634, p. 846, 2003.

[246] R. T. Narayanan, T. Seidenbecher, S. Sangha, O. Stork, and H.-C. Pape, "Theta resynchronization during reconsolidation of remote contextual fear memory," *Neuroreport*, vol. 18, no. 11, pp. 1107–11, 2007.

[247] B. Lega, J. F. Burke, J. Jacobs, and M. J. Kahana, "Slow theta-to-gamma phase amplitude coupling in human hippocampus supports the formation of new episodic memories," *Cerebral Cortex*, vol. 26, no. 1, pp. 268–278, 2015.

[248] D. I. Bass and J. R. Manns, "Memory-enhancing amygdala stimulation elicits gamma synchrony in the hippocampus," *Behav Neurosci*, vol. 129, no. 3, pp. 244–56, 2015.

[249] L. L. Colgin and E. I. Moser, "Gamma oscillations in the hippocampus," *Physiology (Bethesda)*, vol. 25, no. 5, pp. 319–29, 2010.

[250] C. de Hemptinne, N. C. Swann, J. L. Ostrem, E. S. Ryapolova-Webb, M. San Luciano, N. B. Galifianakis, and P. A. Starr, "Therapeutic deep brain stimulation reduces cortical phase-amplitude coupling in parkinson's disease," *Nat Neurosci*, vol. 18, no. 5, pp. 779–86, 2015.

[251] L. Pessoa, S. Kastner, and L. G. Ungerleider, "Attentional control of the processing of neural and emotional stimuli," *Brain Res Cogn Brain Res*, vol. 15, no. 1, pp. 31–45, 2002.

[252] I. A. Muzzio, L. Levita, J. Kulkarni, J. Monaco, C. Kentros, M. Stead, L. F. Abbott, and E. R. Kandel, "Attention enhances the retrieval and stability of visuospatial and olfactory representations in the dorsal hippocampus," *PLoS Biol*, vol. 7, no. 6, e1000140, 2009.

[253] P. Fries, J. H. Reynolds, A. E. Rorie, and R. Desimone, "Modulation of oscillatory neuronal synchronization by selective visual attention," *Science*, vol. 291, no. 5508, pp. 1560–1563, 2001.

[254] A. N. Landau, H. M. Schreyer, S. van Pelt, and P. Fries, "Distributed attention is implemented through theta-rhythmic gamma modulation," *Curr Biol*, vol. 25, no. 17, pp. 2332–7, 2015.

[255] S. Malhotra, R. W. A. Cross, and M. A. A. van der Meer, "Theta phase precession beyond the hippocampus," *Rev Neurosci*, vol. 23, no. 1, pp. 39–65, 2012.

[256] M. Aly and N. B. Turk-Browne, "Attention promotes episodic encoding by stabilizing hippocampal representations," *Proceedings of the National Academy of Sciences*, 2016.

[257] M. Aly and N. B. Turk-Browne, "How hippocampal memory shapes, and is shaped by, attention.," pp. 369–403, 2017.

[258] E. A. Phelps, "Human emotion and memory: Interactions of the amygdala and hippocampal complex," *Curr Opin Neurobiol*, vol. 14, no. 2, pp. 198–202, 2004.

[259] J. B. Ranck Jr, "Studies on single neurons in dorsal hippocampal formation and septum in unrestrained rats. i. behavioral correlates and firing repertoires," *Exp Neurol*, vol. 41, no. 2, pp. 461–531, 1973.

[260] A. L. Markowska, D. S. Olton, and B. Givens, "Cholinergic manipulations in the medial septal area: Age-related effects on working memory and hippocampal electrophysiology.," vol. 15, no. 3, pp. 2063–2073, 1995.

[261] P. J. Kennedy and M. L. Shapiro, "Motivational states activate distinct hippocampal representations to guide goal-directed behaviors," *Proc Natl Acad Sci U S A*, vol. 106, no. 26, pp. 10 805–10, 2009.

[262] H. Eichenbaum, "On the integration of space, time, and memory," *Neuron*, vol. 95, no. 5, pp. 1007–1018, 2017.

[263] A. M. Kaufman, T. Geiller, and A. Losonczy, "A role for the locus coeruleus in hippocampal ca1 place cell reorganization during spatial reward learning," *Neuron*, vol. 105, no. 6, 1018–1026.e4, Mar. 2020.

[264] C. M. Tyng, H. U. Amin, M. N. M. Saad, and A. S. Malik, "The influences of emotion on learning and memory," *Front Psychol*, vol. 8, p. 1454, 2017.

[265] M. M. Garvert, R. J. Dolan, and T. E. J. Behrens, "A map of abstract relational knowledge in the human hippocampal–entorhinal cortex," *eLife*, vol. 6, e17086, 2017.

[266] A. A. Carlson, U. Rutishauser, and A. N. Mamelak, "Safety and utility of hybrid depth electrodes for seizure localization and single-unit neuronal recording," *Stereotact Funct Neurosurg*, vol. 96, no. 5, pp. 311–319, 2018.

[267] E. Despouy, J. Curot, L. Reddy, L. G. Nowak, M. Deudon, J.-C. Sol, J.-A. Lotterie, M. Denuelle, A. Maziz, C. Bergaud, S. J. Thorpe, L. Valton, and E. J. Barbeau, "Recording local field potential and neuronal activity with tetrodes in epileptic patients," *Journal of Neuroscience Methods*, vol. 341, p. 108 759, 2020.

[268] C. Drieu and M. Zugaro, "Hippocampal sequences during exploration: Mechanisms and functions," *Front Cell Neurosci*, vol. 13, p. 232, 2019.

[269] J. Minxha, R. Adolphs, S. Fusi, A. N. Mamelak, and U. Rutishauser, "Flexible recruitment of memory-based choice representations by the human medial frontal cortex," *Science*, vol. 368, no. 6498, Jun. 2020.

[270] F. Stefanini, L. Kushnir, J. C. Jimenez, J. H. Jennings, N. I. Woods, G. D. Stuber, M. A. Kheirbek, R. Hen, and S. Fusi, "A distributed neural code in the dentate gyrus and in ca1," *Neuron*, vol. 107, no. 4, 703–716.e4, Aug. 2020.

[271] Z. Nadasdy, T. P. Nguyen, Á. Török, J. Y. Shen, D. E. Briggs, P. N. Modur, and R. J. Buchanan, "Context-dependent spatially periodic activity in the human entorhinal cortex," *Proceedings of the National Academy of Sciences*, p. 201 701 352, 2017.

[272] C. G. McNamara and D. Dupret, "Two sources of dopamine for the hippocampus," *Trends Neurosci*, vol. 40, no. 7, pp. 383–384, Jul. 2017.

[273] D. Bang, K. T. Kishida, T. Lohrenz, J. P. White, A. W. Laxton, S. B. Tatter, S. M. Fleming, and P. R. Montague, "Sub-second dopamine and serotonin signaling in human striatum during perceptual decision-making," *Neuron*, 2020.

[274] T. Sharot and E. A. Phelps, "How arousal modulates memory: Disentangling the effects of attention and retention," *Cogn Affect Behav Neurosci*, vol. 4, no. 3, pp. 294–306, 2004.

[275] J. E. Lisman and O. Jensen, "The theta-gamma neural code," *Neuron*, vol. 77, no. 6, pp. 1002–1016, 2013.